Jordanian Journal of Computers and Information Technology

December 2015 VOLUME 01 NUMBER 01 ISSN 2413 - 9351

JJCIT

PAGES	PAPERS
1 - 14	ENHANCED RADIATION PATTERNS OF A WIDE-BAND STRIP-FED DIELECTRIC RESONATOR ANTENNA Asem Al-Zoubi
15 - 30	USING FORMAL METHODS FOR TEST CASE GENERATION ACCORDING TO TRANSITION-BASED COVERAGE CRITERIA Ahmad A. Saifan and Wafa Bani Mustafa
31 - 40	OPTIMIZING AND THINNING PLANAR ARRAY USING CHEBYSHEV DISTRIBUTION AND IMPROVED PARTICLE SWARM OPTIMIZATION Noor S. Alshdaifat and Mohammed H. Bataineh
41 - 50	A HYBRID APPROACH FOR INDEXING AND SEARCHING THE HOLY QURAN Monther Tarawneh and Emad Al-Shawakfa
51 - 66	COMPREHENSIVE INVESTIGATION MODELING FOR SEMICONDUCTOR OPTICAL AMPLIFIER (SOA) Esra A. Alquda and Aser M. Matarneh

www.jjcit.org jjcit@psut.edu.jo

An International Peer-Reviewed Scientific Journal
Financed by Scientific Research Support Fund

Jordanian Journal of Computers and Information Technology (JJCIT)

The Jordanian Journal of Computer and Information Technology (JJCIT) is an international journal that publishes original, high-quality and cutting edge research papers on all aspects and technologies in ICT fields.

JJCIT is hosted by Princess Sumaya University for Technology (PSUT) and supported by the Scientific Research Support Fund in Jordan.

AIMS AND SCOPE

The JJCIT aims to publish the most current developments in the form of original articles and review articles in all areas of Telecommunications, Computer Engineering and Information Technology and make them available to researchers worldwide.

The JJCIT focuses on topics including, but not limited to: Computer Engineering & Communication Networks, Computer Science & Information Systems and Information Technology and Applications.

INDEXING

JJCIT is indexed in:

- ScopeMed: www.scopemed.org
- Index Scholar: www.indexscholar.com

EDITORIAL BOARD SUPPORT TEAM

JJCIT ADDRESS

WEBSITE: www.jjcit.org

EMAIL: jjcit@psut.edu.jo

ADDRESS: Princess Sumaya University for Technology, Khalil Saket Street, Al-Jubaiha.

B.O. BOX: 1438 Amman 11941 Jordan.

TELEPHONE: +962-6-5359949.

FAX: +962-6-7295534.

EDITOR'S NOTE

It is a great honor for me to head the Editorial Board of the Jordanian Journal of Computers and Information Technology (JJCIT). The Editorial Board consists of a group of distinguished colleagues who have a well-recognized research record.

This issue is the first published by JJCIT. We have started our first call for papers in May 2015. The submitted manuscripts have undergone a strict review process in which, at least, three specialized reviewers with well-recognized research track in the subject area reviewed each manuscript. While we received 19 manuscripts, just five papers were accepted and are published in this issue.

I would like to sincerely thank all authors who submitted their latest research work to JJCIT. I also would like to thank all the reviewers of the Journal for their efforts to ensure a very high quality review process while keeping a reasonable timelines for submitting their reviews and recommendations. It is through their voluntarily work that the high standard of this Journal is established and maintained.

I hope to receive from all potential authors, readers and researchers their opinions, suggestions and comments at (jjcit@psut.edu.jo). My colleagues in the Editorial Board and I are very willing to adopt new ideas and thoughts that may be sent to us to improve the content quality and journal presentation.

Editor-in-Chief

Ahmad Hiasat

Jordanian Journal of Computers and Information Technology (JJCIT), Vol. 1, No. 1, December 2015.

ENHANCED RADIATION PATTERNS OF A WIDE-BAND STRIP-FED DIELECTRIC RESONATOR ANTENNA

Asem Al-Zoubi

Department of Communications Engineering,
Yarmouk University,
Irbid, Jordan.
asem@yu.edu.jo

(Received: 06-Sep.-2015, Revised: 03-Oct.-2015, Accepted: 10-Oct.-2015)

ABSTRACT

A simple wide-band rectangular dielectric resonator antenna (DRA) is designed for the X-band and Ku-band applications. The DRA is excited by a vertical strip placed on the middle of the DRA's wide side wall through a coaxial probe attached to a finite size ground plane. Good agreement between measured and simulated results is obtained. The measured 10 dB return loss bandwidth of the antenna is about 7.8 GHz (62%). The simulated gain of the antenna is 6.1 dBi at 12 GHz. The antenna excites undesired modes that perturb the radiation patterns and increase the cross-polarization level. The dielectric resonator is wrapped by a conducting strip to suppress some modes and improve the radiation characteristics of the antenna. Adding the strip reduces the cross-polarization level and improves the co-polarization radiation pattern.

KEYWORDS

Wide-band antenna, Dielectric resonator antenna, Strip-fed antenna, Low cross-polarization.

1. INTRODUCTION

Dielectric resonator antennas (DRAs) have recently been investigated and found to be efficient radiators. The DRAs have the potential to provide significant advantages in terms of size reduction, improved bandwidth, higher power handling capability, and increased efficiency in comparison with the microstrip antennas [1]-[6]. Different DRA shapes, such as cylindrical, rectangular, hemispherical, elliptical, pyramidal and triangular, have been presented in the literature [7]-[12]. The rectangular-shaped DRAs offer practical advantages over cylindrical and hemispherical ones because they are easier to fabricate and have more design flexibility. In order to excite the DRA [13], different techniques have been used, such as probe feeding, in which the probe can be placed adjacent to the DRA [14]; an aperture-coupled dielectric resonator antenna using a strip-line feed [15]; an aperture-fed DRA using a dielectric image guide [16]; and direct coupling using a dielectric image guide [17]. These coupling mechanisms can have a significant impact on the resonant frequency and Q factor. Many methods have been proposed in recent years to achieve a wide-band DRA. One method was to use stacked antennas of different sizes and/or dielectric materials [18], but this increases the size and cost of the antenna. Another approach was to use specially shaped DRAs [7], but these are not easy to fabricate.

Recently, a strip-fed rectangular dielectric resonator antenna was studied [19]. The feeding mechanism—a conformal conducting strip mounted on the surface of the DRA—allows the entire electric current to flow on the DRA surface, and thus its energy coupling is more efficient

than the probe-feed. The obtained 10 dB return loss bandwidth was 43%, and the center frequency was about 4 GHz. Here, we present a strip-fed dielectric resonator antenna design that operates at the X-band and Ku-band. In order to improve the co-polarization radiation patterns at high frequencies and to reduce the cross-polarization, a conducting strip is wrapped around the DRA [20]-[22]. The proposed antenna is fabricated, and the return loss and radiation patterns are measured and compared to the simulated results. In the simulation, the Ansoft HFSS commercial software is used [23]. The proposed antenna geometry is shown in Section 2, while the results and discussion are provided in Section 3. Cross-polarization reduction is studied in Section 4, which is followed by the conclusion.

2. ANTENNA GEOMETRY

The rectangular-shaped DRAs offer more design flexibility than other shapes. For a given resonant frequency, two aspect ratios of the rectangular DRA (height/length and width/length) can be chosen independently. Since the bandwidth of the DRA also depends on the aspect ratio(s), a rectangular-shaped DRA provides more flexibility in terms of bandwidth control. Referring to the DRA and the coordinate system shown in Figure 1, the modes—based on magnetic conducting walls [24]-[26]—with the lowest order indices are TE^{x}_{111}, TE^{y}_{111}, and TE^{z}_{111}. If the dimensions of the DRA are such that $2c > a > b$, the modes (in order of increasing resonant frequency) are TE^{x}_{111}, TE^{y}_{111}, and TE^{z}_{111}. The feeding strip is placed in the middle of the DRA side wall in the y-z plane. With this feeding, the fundamental mode is the TE^{y}_{111}, and the bandwidth is wide because of the excitation of higher order modes.

The geometry of the proposed antenna and the coordinate system are shown in Figure 1 (a), and the fabricated antenna is shown in Figure 1 (b). The rectangular DRA dimensions are calculated using the theory in [17] so that the resonant frequency is approximately 8.4 GHz, following optimization using HFSS software, and the optimized parameters are a = 11.2 mm, b = 5 mm, and c = 9.5 mm, with a dielectric constant of 10.2. The feeding strip has dimensions L_s = 4 mm and W_s = 2 mm. The feeding strip is placed in the center of the DRA's wide side wall. These values are also obtained through a parametric study of the length and width using HFSS. The ground-plane dimensions are $a_g = b_g$ = 90 mm (2.7 λ_0 × 2.7 λ_0 at 10 GHz).

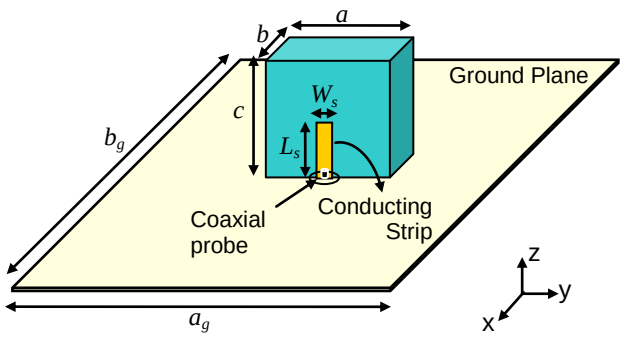

(a)

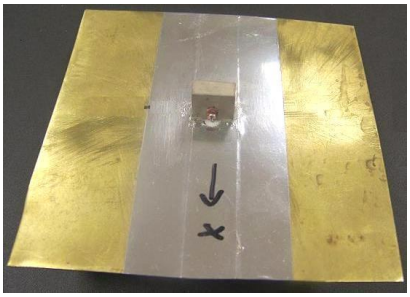

(b)

Figure 1. (a) configuration of the proposed antenna, and (b) photo of the fabricated antenna.

3. RESULTS AND DISCUSSION

The antenna is simulated and measured. The reflection coefficients of the antenna are shown in Figure 2. As shown in the figure, the measured and simulated -10 dB reflection coefficient level bandwidths are 7.75 GHz (62%) and 7.5 GHz (57%), respectively, but the simulated reflection coefficient is poor at around 15 GHz. The upper and lower frequencies in the band are 16.35 GHz and 8.6 GHz, respectively, for the measured reflection coefficient, while for the simulated reflection coefficient the upper and lower frequencies are 16.9 GHz and 9.4 GHz, respectively. The maximum error between the measured and simulated results is 8%. The difference between the measured and simulated results is due to the fabrication errors, the soldering, and the adhesive glue used; these factors affect the measured results. The co-polarization radiation patterns at different frequencies within the band are shown in Figure 3. There is good agreement between the simulated and measured results. Also, in the radiation pattern at 12 GHz, there is a null at about 55°. This may be due to the radiation of the feeding strip. The cross-polarization at different frequencies is shown in Figure 4. As shown in the figure, the maximum cross-polarization level is 10 dB below the co-polarization level, and there is good agreement between the measured and simulated cross-polarization radiation patterns. The measured gain of the antenna is compared to the simulated one at different frequencies, as shown in Figure 5, and there is acceptable agreement between them. The figure also shows the maximum gain of the antenna and its corresponding direction.

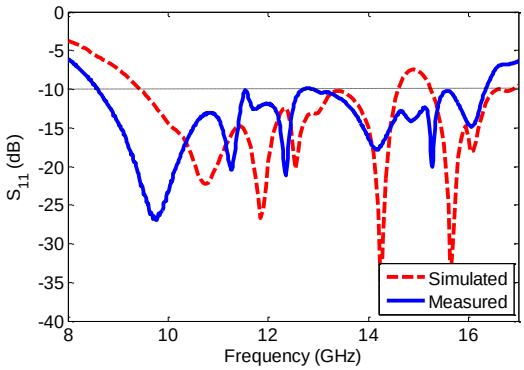

Figure 2. The reflection coefficient of the proposed antenna.

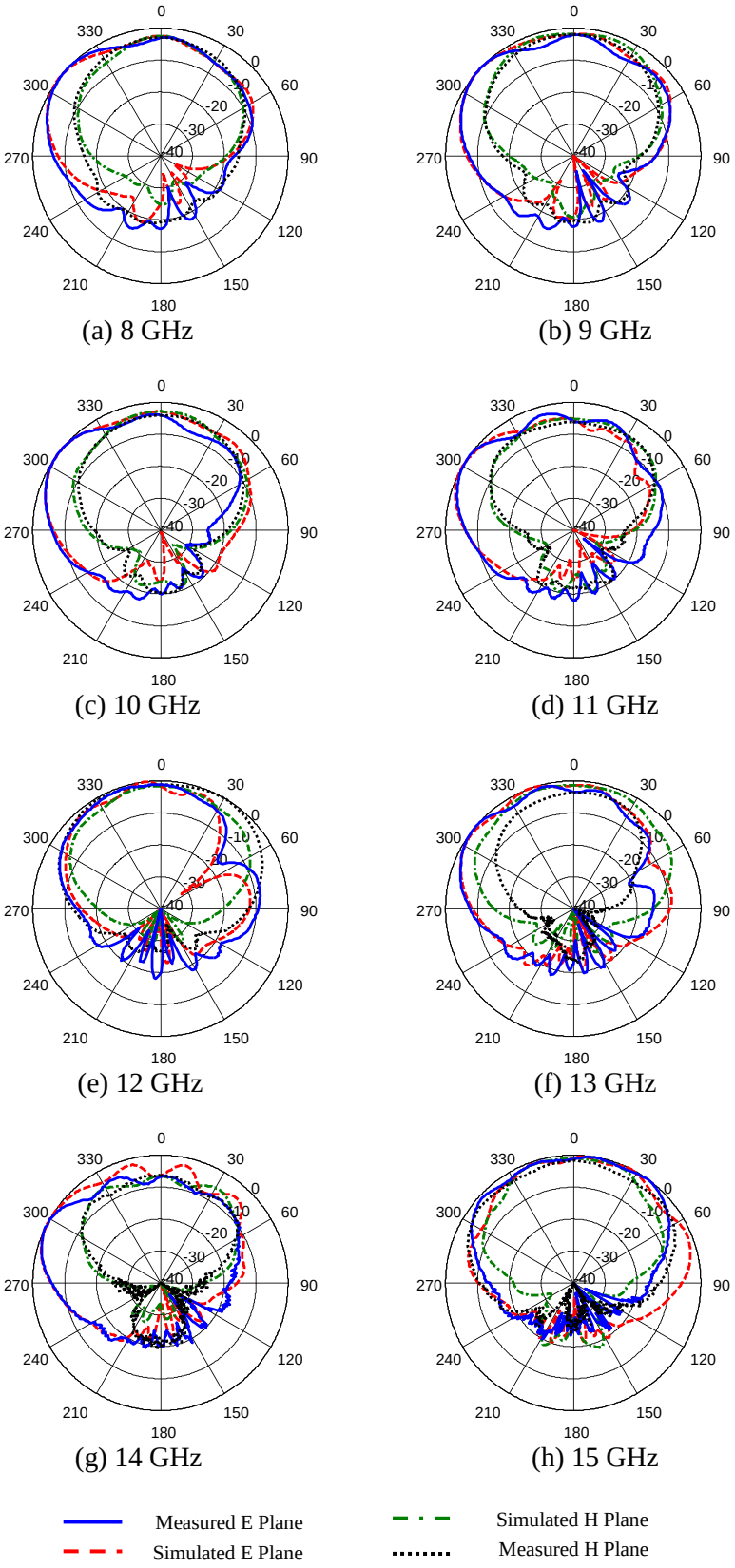

Figure 3. Co-polarization radiation patterns of the proposed antenna at different frequencies.

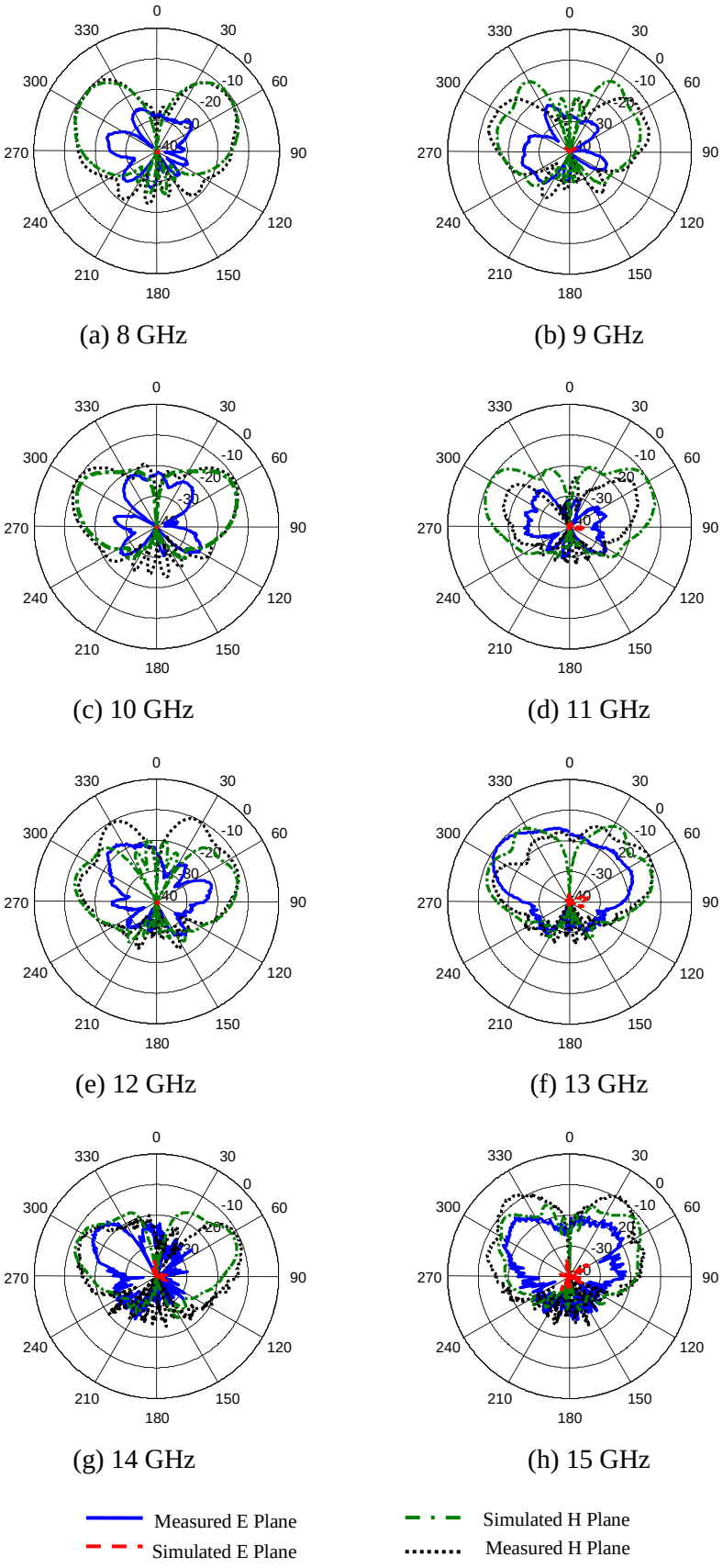

Figure 4. X-polarization radiation patterns of the antenna at different frequencies.

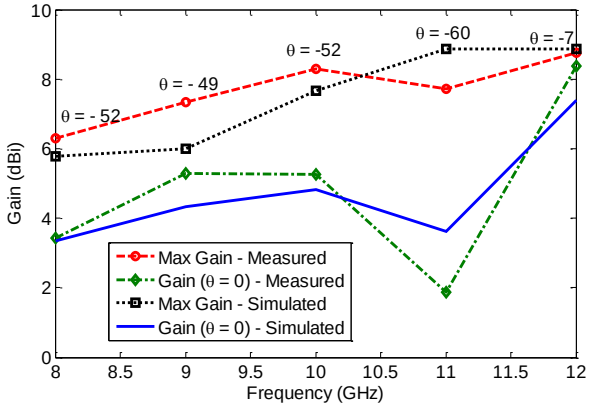

Figure 5. Simulated and measured gain of the antenna at different frequencies.

The simulated radiated power of the antenna is shown in Figure 6. High radiation efficiency is achieved over the entire band. There is a drop in efficiency at 15 GHz; which is due to the mismatch at this frequency, as seen in Figure 2.

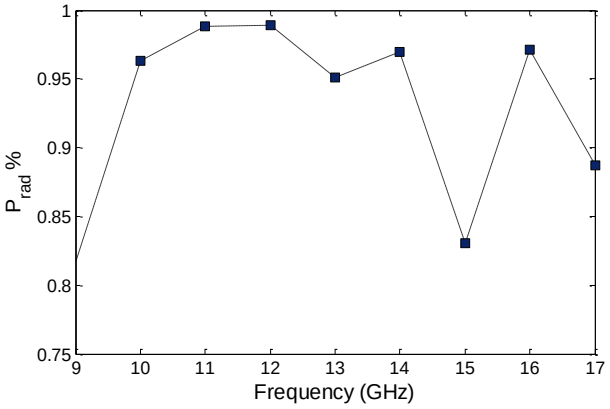

Figure 6. Simulated radiated power of the antenna.

Figure 7 shows the electric field lines for some modes excited by the DRA within the band. These modes are obtained using the Eignmode solution in the HFSS software.

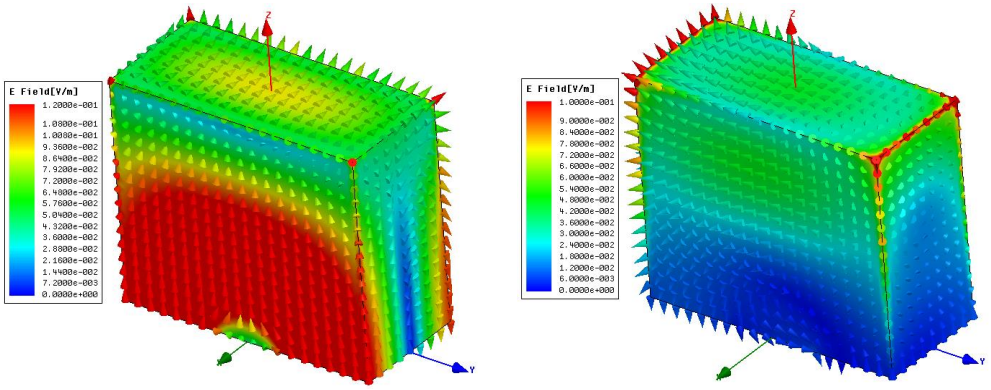

(a) Mode 1 (9.2 GHz) (b) Mode 2 (9.35 GHz)

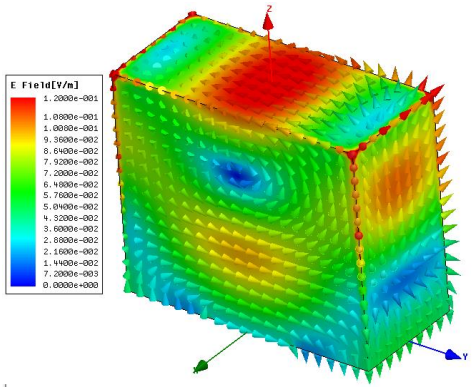

(c) Mode 3 (9.9 GHz)

Figure 7. Electric field lines on the DRA for different modes.

4. CROSS-POLARIZATION SUPPRESSION

In order to reduce the cross-polarization and improve the radiation patterns at high frequencies, a strip is wrapped around the DRA, as shown in Figure 8. This is like placing a shorting wall at the centre of the DRA in the y-z plane, as it has little effect on the co-polarization radiation patterns and it suppresses some of the high-order modes, and thus cross-polarization level is improved [17]. The strip will have no effect if the electric field is perpendicular to the strip (or the sheet), but it will disturb or eliminate the modes with electric field vectors parallel to the strip. The antenna was fabricated and tested. Comparison between the simulated and measured reflection coefficients is shown in Figure 9. The measured and simulated 10 dB return loss bandwidths are 7.83 GHz (62.4%) and 6.79 GHz (53.5%), respectively. The upper and lower frequencies in the band are 16.47 GHz and 8.64 GHz, respectively, for the measured reflection coefficient, while for the simulated reflection coefficient the upper and lower frequencies are 16.09 GHz and 9.3 GHz, respectively. The maximum error between the measured and simulated results is 7.1%. The co-polarization radiation patterns at different frequencies are shown in Figure 10. A good agreement is noted between the simulated and measured results, the axial symmetry in the radiation patterns is improved, and there is no null in the radiation pattern at 12 GHz. The cross-polarization radiation patterns are shown in Figure 11. The maximum cross-polarization level is around -20 dB at 10 GHz; thus, adding the strip reduces the cross-polarization level and improves the co-polarization radiation pattern.

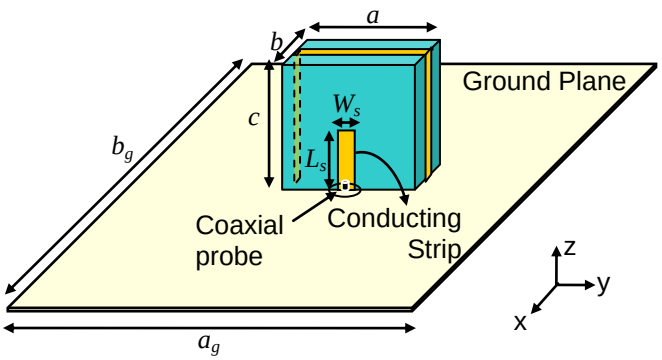

Figure 8. Configuration of the antenna with a strip wrapped around the DRA.

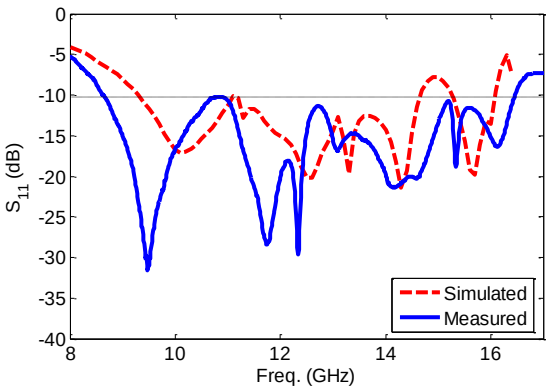

Figure 9. The return loss of the antenna with a strip around the DRA.

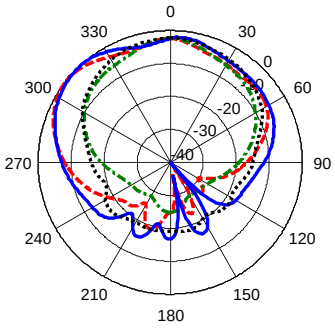

(a) 8 GHz

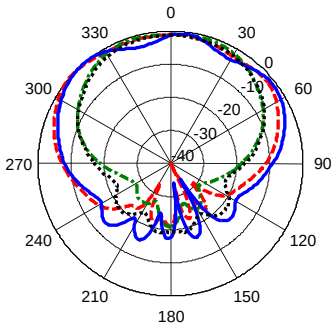

(b) 9 GHz

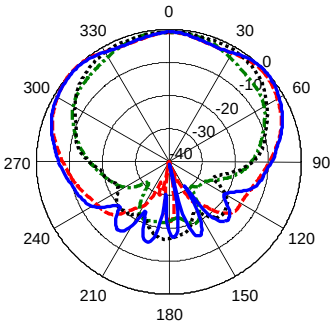

(c) 10 GHz

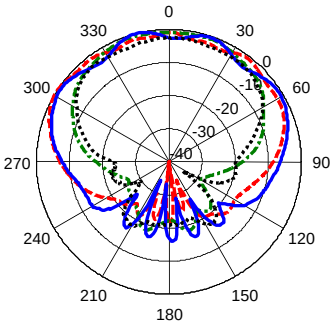

(d) 11 GHz

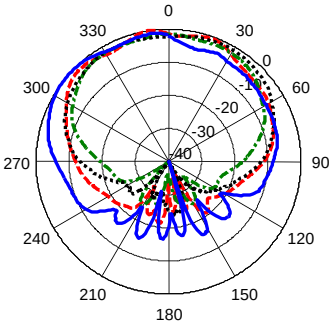

(e) 12 GHz

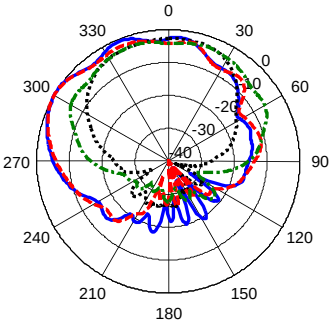

(f) 13 GHz

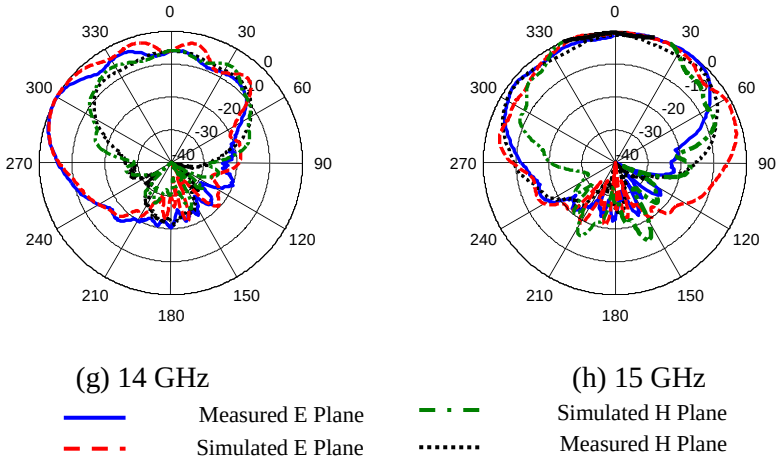

(g) 14 GHz (h) 15 GHz

Figure 10. Co-polarization Radiation patterns of the antenna with a strip around the DRA at different frequencies.

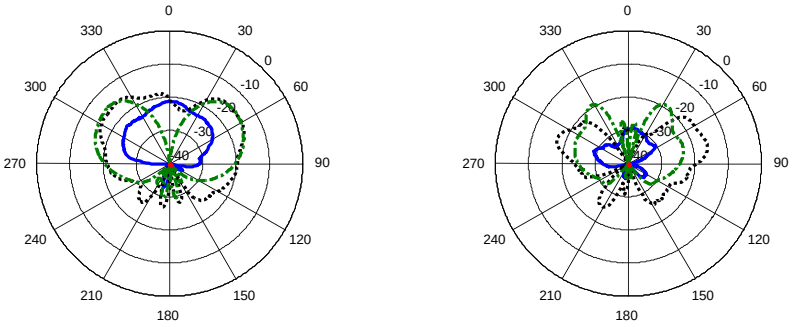

(a) 8 GHz (b) 9 GHz

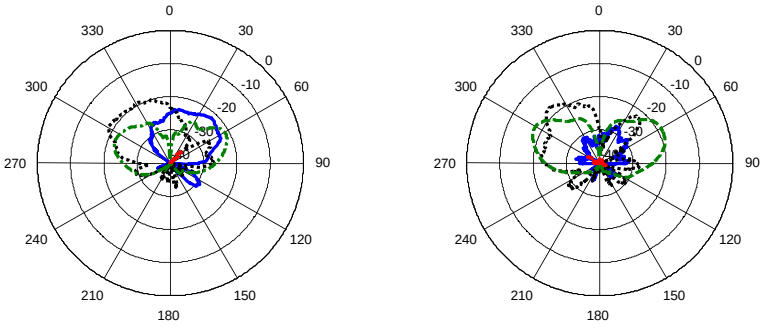

(c) 10 GHz (d) 11 GHz

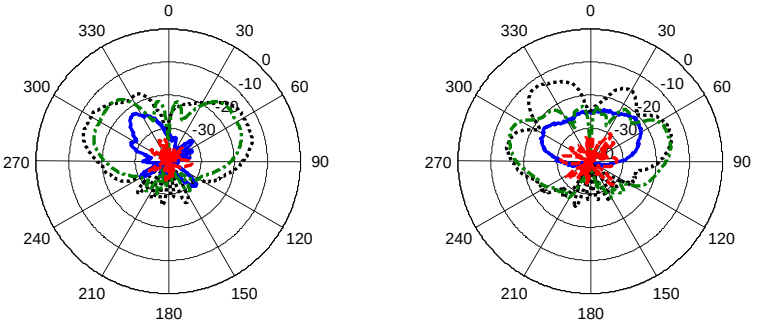

(e) 12 GHz (f) 13 GHz

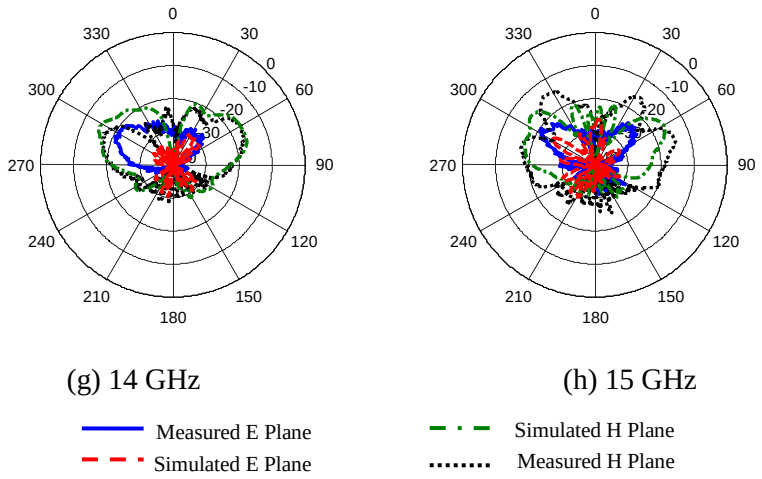

Figure 11. X-polarization Radiation patterns of the antenna with strip around the DRA at different frequencies.

The measured gain of the antenna is compared to the simulated one at different frequencies as shown in Figure 10, showing a very good agreement between them. The figure shows also the maximum gain of the antenna and its direction. It is noticed that in this case the maximum gain and the gain at θ = 0 are close to each other, this is because adding the strip around the DRA makes the radiation pattern more uniform than the case when there is no strip. The electric field lines for the modes are shown in Figure 14.

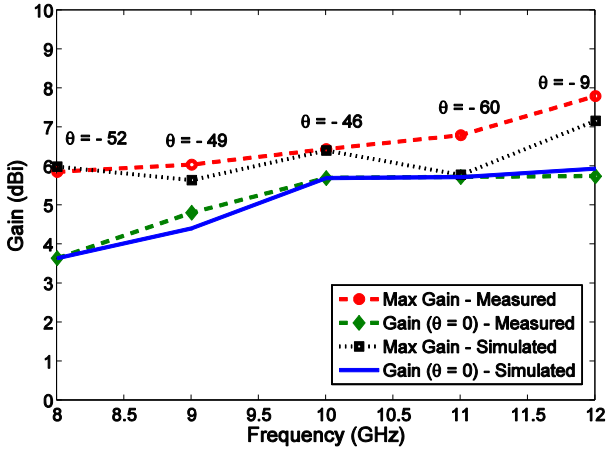

Figure 12. Simulated and measured gain of the antenna with a strip around the DRA at different frequencies.

Jordanian Journal of Computers and Information Technology (JJCIT), Vol. 1, No. 1, December 2015.

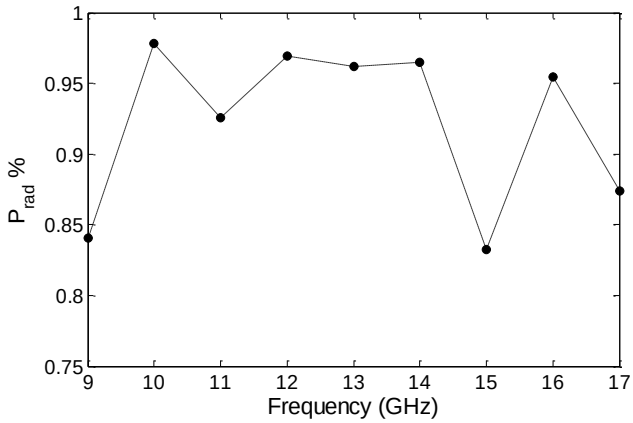

Figure 13. Simulated radiated power of the antenna with a strip around the DRA.

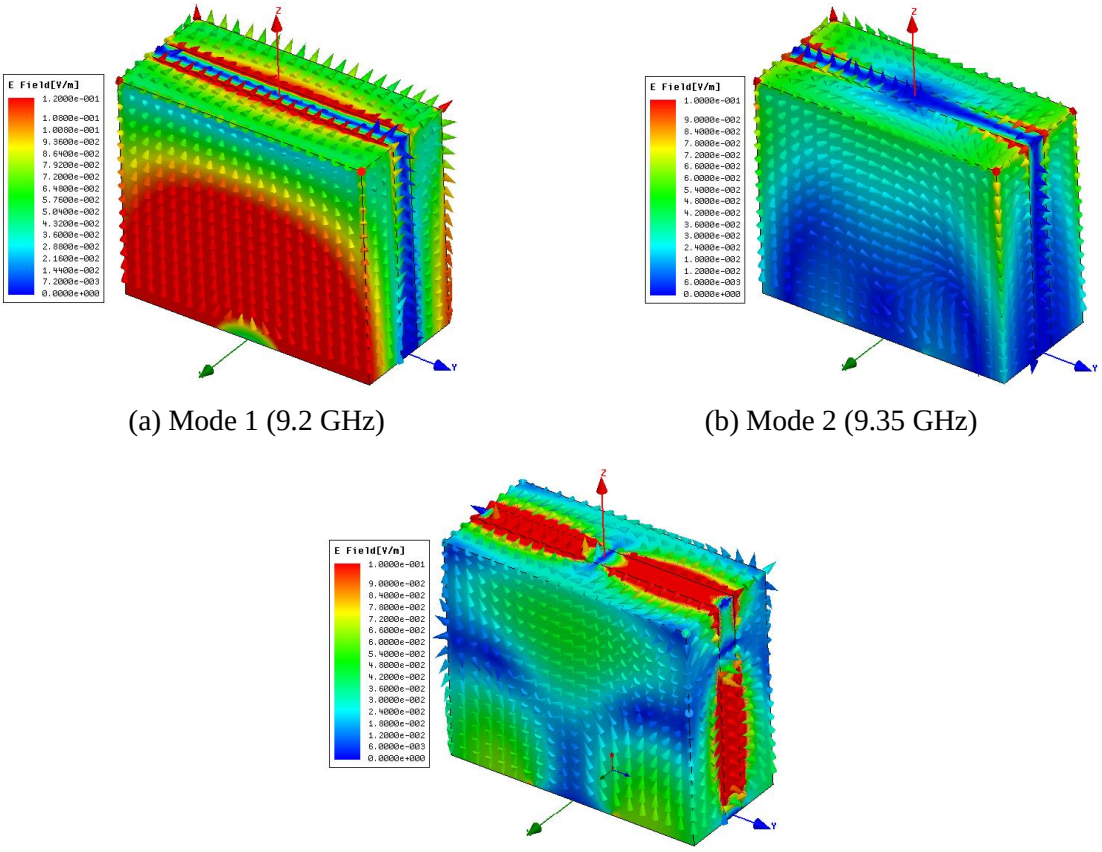

(a) Mode 1 (9.2 GHz)

(b) Mode 2 (9.35 GHz)

(c) Mode 3 (9.9 GHz)

Figure 14. Electric field lines on the DRA with the strip for different modes.

5. CONCLUSIONS

A strip fed rectangular dielectric resonator antenna on a finite size ground plane was designed and fabricated which operates in the X-band and Ku-band frequency ranges. A good agreement between the simulated and measured return loss and radiation patterns was achieved. In order to reduce the cross-polarization level and improve the co-polarization radiations patterns, a strip conductor was wrapped around the DRA, the measured and simulated results for this case were in good agreement. The measured 10 dB return loss bandwidth of the antenna is about 7.8 GHz (62%). The simulated gain of the antenna is 6.1 dBi at 12 GHz.

ACKNOWLEDGEMENTS

Special thanks to Dr. Ahmed Kishk, Department of Electrical and Computer Engineering, Concordia University, Canada for his valuable help.

REFERENCES

[1] A. A. Kishk, "Dielectric Resonator Antenna, a Candidate for Radar Applications," Proceedings of 2003 IEEE radar conference, pp. 258-264, May 2003.

[2] J. Shin, A. A. Kishk and A. W. Glisson, "Analysis of Rectangular Dielectric Resonator Antennas Excited Through a Slot Over a Finite Ground Plane," IEEE AP-S International Symposium, vol. 4, pp. 2076-2079, July 2000.

[3] I. A. Eshrah, A. A. Kishk, A. B. Yakovlev and A. W. Glisson, "Theory and Implementation of Dielectric Resonator Antenna Excited by a Waveguide Slot," IEEE Transaction on Antennas and Propagation, vol. 44, no. 53, pp. 483-494, Jan. 2005.

[4] K. M. Luk and K. W. Leung, Dielectric Resonator Antennas. England: Research Studies Pr Ltd., 2004.

[5] T. A. Denidni and Z. Weng, "Rectangular Dielectric Resonator Antenna for Ultra-Wide Band Applications," IET Electronics Letters, vol. 45, no. 24, pp.1210 -1212, Nov. 2009.

[6] T. A. Denidni Z. Weng and M. Niroo Jazi, "Z-shaped Dielectric Resonator Antenna for Ultra Wide Band Applications," IEEE Transaction on Antennas and Propagation, vol. 58, no. 12, pp. 4059 - 4062, Dec. 2010.

[7] A. A. Kishk, "Tetrahedron and Triangular Dielectric Resonator Antenna with Wideband Performance," IEEE Antennas and Propagation Society International Symposium, vol. 4, pp. 462-465, June 2002.

[8] G. Zhou, A. A. Kishk and A. W. Glisson, "Input Impedance of a Spherical Dielectric Resonator Antenna Excited by a Coaxial Probe," IEEE Antennas and Propagation Society International Symposium, vol. II, pp. 1038-1041, 1993.

[9] S. L. Steven Yang, Ricky Chair, A. A. Kishk, K. F. Lee and K. M. Luk, "Aperture Feed Elliptical Dielectric Resonator Antenna for Circularly Polarized Applications," 22nd Annual Review of Progress in Applied Computational Electromagnetics, Miami, FL, pp. 94-100, 12-16 March 2006.

[10] S. L. Steven Yang, Ricky Chair, A. A. Kishk, K. F. Lee and K. M. Luk, "Study on Sequential Feeding Networks for Sub-Arrays of Circularly Polarized Elliptical Dielectric Resonator Antenna," IEEE Transactions on Antennas and Propagation, vol. 55, no. 2, pp. 321-333, Feb. 2007.

[11] S. L. Steven Yang, Ricky Chair, A. A. Kishk, K. F. Lee and K. M. Luk, "Single Feed Elliptical Dielectric Resonator Antennas for Circularly Polarized Applications," Microwave and Optical Technology Letters, vol. 48, issue 11, pp. 2340-2345, November 2006.

[12] A. Tadjalli, A. R. Sebak, T. A. Denidni and A. A. Kishk, "Spheroidal Dielectric Resonator Antenna," URSI Digist, 2004 USNC/URSI National Radio Science Meeting, pp. 184, 2004.

[13] R. Chair, A. A. Kishk and K. F. Lee, "Comparative Study on Different Feeding Techniques for Dual Polarized Dielectric Resonator Antennas," IEEE Antennas and Propagation Society International Symposium, pp. 2495 – 2498, July 2006.

[14] Y. Zhang, A. A. Kishk, A. B. Yakovlev and A. W. Glisson, "FDTD Analysis of a Probe-Fed Dielectric Resonator Antenna in Rectangular Waveguide," Applied Computational Electromagnetics Society Journal, vol. 21, no. 1, pp. 37-44, 2006.

[15] K. W. Leung, M. L. Poon, W. C. Wong, K. M. Luk and K. N. Yung, "Aperture-Coupled Dielectric Resonator Antenna Using a Strip-Line Feed," Microwave and Optical Technology Letters, vol. 24, issue 2, pp. 120-121, Dec. 1999.

[16] Asem S. Al-Zoubi, Ahmed A. Kishk and Allen W. Glisson, "Aperture Coupled Rectangular Dielectric Resonator Antenna Array Fed by Dielectric Image Guide," IEEE Transactions on Antennas and Propagation, vol. 57, no. 8, pp. 2252-2259, Aug. 2009.

[17] Asem S. Al-Zoubi, Ahmed A. Kishk and Allen W. Glisson, "A Linear Rectangular Dielectric Resonator Antenna Array Fed by Dielectric Image Guide with Low Cross Polarization," IEEE Transactions on Antennas and Propagation, vol. 58, no. 3, March 2010.

[18] A. A. Kishk, X. Zhang, A. W. Glisson and D. Kajfez, "Numerical Analysis of Stacked Dielectric Resonator Antennas Excited by a Coaxial Probe for Wideband Applications," IEEE Transactions on Antennas and Propagation, vol. 51, no. 8, pp. 1996–2006, Aug. 2003.

[19] B. Li and K W. Leung, "Strip-Fed Rectangular Dielectric Resonator Antennas with/without a Parasitic Patch," IEEE Transactions on Antennas and Propagation, vol. 53, issue 7, pp. 2200-2207, July 2005.

[20] M. T. K. Tam and R. D. Murch, "Half Volume Dielectric Resonator Antenna Designs," Electronics Letters, vol. 33, no. 23, November 1997.

[21] A. S. Al-Zoubi, Rectangular Dielectric Resonator Antennas Fed By Dielectric Image Guides, Ph.D. Dissertation, Department of Electrical Engineering, University of Mississippi, 2008.

[22] Asem Al-Zoubi and Ahmed Kishk, "Wide Band Strip-Fed Rectangular Dielectric Resonator Antenna," 3rd European Conference on Antennas and Propagation, Berlin, Germany, March 2009.

[23] HFSS: High Frequency Structure Simulator Based on Finite Element Method, v. 11.0.2, Ansoft Corporation, 2007.

[24] Y. M. Antar, D. Cheng, G. Seguin, B. Henny and M. Keller, "Modified Waveguide Model (MWGM) for Rectangular Dielectric Resonator Antenna (DRA)," Microwave and Optical Technology Letters, vol. 19, no. 2, Oct. 1998.

[25] R. K. Mongia and A. Ittipiboon, "Theoretical and Experimental Investigations on Rectangular Dielectric Resonator Antennas," IEEE Transactions on Antennas and Propagation, vol. 45, no. 9, pp. 1348-1356, Sept. 1997.

[26] R. K. Mongia, A. Ittipiboon, M. Cuhaci and D. Roscoe, "Radiation Q-Factor of Rectangular Dielectric Resonator Antennas: Theory and Experiment," Proc. of IEEE Antennas and Propagation Society International Symposium, pp. 764-767, July 1994.

ملخص البحث:

يعرض هذا البحث تصميماً لهوائي بسيط عريض النطاق ذي مرنان عازل، مستطيل الشكل، مصمم للعمل في تطبيقات النطاقين X وKu. تتم تغذية الهوائي عن طريق شريط رأسي موضوع في منتصف الجدار الجانبي العريض للهوائي، بحيث يتصل الشريط بالسلك الداخلي للكبل المحوري؛ في حين يتصل السلك الخارجي للكبل بالقاعدة الموصلة محدودة المساحة.

تم الحصول على توافق جيد بين نتائج القياس العملي ونتائج المحاكاة. و كان عرض النطاق الترددي المقاس للهوائي (٧,٨) غيغاهيرتز عند فقد ارتداد مقداره (١٠) ديسيبل؛ أي (٦٢%). أما كسب الهوائي المحسوب عن طريق المحاكاة فبلغ (٦,١) ديسيبل عند تردد مقداره (١٢) غيغاهيرتز. والجدير بالذكر أنّ الهوائي يبثّ أمواجاً غير مرغوب فيها تشوش أنماط الإشعاع وتزيد من مستوى الاستقطاب المتقاطع. لذا، تمّ لفّ شريط موصل حول الهوائي لكبت الأمواج غير المرغوب فيها و تحسين خصائص الإشعاع للهوائي. و قد أدت إضافة الشريط الموصل إلى خفض مستوى الاستقطاب المتقاطع و تحسين نمط إشعاع الاستقطاب المتماثل.

Jordanian Journal of Computers and Information Technology (JJCIT), Vol. 1, No. 1, December 2015.

USING FORMAL METHODS FOR TEST CASE GENERATION ACCORDING TO TRANSITION-BASED COVERAGE CRITERIA

Ahmad A. Saifan[1] and Wafa Bani Mustafa[2]

Computer Information Systems Department, Faculty of IT, Yarmouk University, Irbid, Jordan.
ahmads@yu.edu.jo[1], w_banimustafa@yahoo.com[2]

(Received: 15-Sep.-2015, Revised: 01-Nov.-2015, Accepted: 08-Nov.-2015)

ABSTRACT

Formal methods play an important role in increasing the quality, reliability, robustness and effectiveness of the software. Also, the uses of formal methods, especially in safety-critical systems, help in the early detection of software errors and failures which will reduce the cost and effort involved in software testing.

The aim of this paper is to prove the role and effectiveness of formal specification for the cruise control system (CCS) as a case study. A CCS formal model is built using Perfect formal specification language, and its correctness is validated using the Perfect Developer toolset. We develop a software testing tool in order to generate test cases using three different algorithms. These test cases are evaluated to improve their coverage and effectiveness. The results show that random test case generation with full restriction algorithm is the best in its coverage results; the average of the path coverage is 77.78% and the average of the state coverage is 100%. Finally, our experimental results show that Perfect formal specification language is appropriate to specify CCS which is one of the most safety-critical software systems, so the process of detecting all future possible cases becomes easier.

KEYWORDS

Formal method, Perfect developer, Test case generation, Cruise control system (CCS).

1. INTRODUCTION

Generally, the role of software has become increasingly important and is being used in many critical applications, such as aircraft flight control systems, medical device systems and nuclear systems. Such systems are called safety-critical systems, the most important property of which is dependability, which reflects the extent to which users or customers trust the software system. It also reflects the degree of user confidence that the system will not fail when operated. A failure in these systems may cause significant damage, severe economic consequences or even loss of life. Thus, the reliability, safety and correctness of these systems are important issues, and testing them is a challenging task. Tim [23] shows that the formal method is a technique that is used to reduce the cost of testing safety-critical systems by examining the behaviour of these systems in the early stages of development. One way to reduce the cost and effort of software testing is to depend on formal methods, mainly for safety-critical software, because it provides many different techniques to describe precisely and accurately the system specifications [21].

In recent years, there has been an increased tendency to use formal specification and verification methods and tools, defined by Tim [23] as "the use of ideas and techniques from mathematics and formal logic to specify and reason about computing systems to increase design assurance

and eliminate defects". In addition, they are mainly used to provide a standard software development process.

Formal methods, tools and techniques have an important advantage in that they develop formal system specifications that facilitate and provide comprehensive system analysis, design and implementation as described by Mery and Singh [17]. Mery and Singh [17] adjusted the software development life cycle - from the requirements analysis to code generation - to develop safety critical systems using formal techniques. Formal methods provide an importantly disciplined approach for complex safety-critical systems with many different formal specification languages such as Z- [12], VDM [6], B [16], SCR [20] and Perfect Developer [7]. The formal method used in our work is Perfect Developer.

In this paper, we use the Perfect language as the formal language in order to model and test a real safety-critical system; a cruise control system (CCS). The CCS must be able to maintain the current speed of the car and accelerate it upon the request of the driver. It must also measure the current car speed and display the same to the driver.

In this paper, we present our framework on test case generation using a formal method. Application of the approach starts by building the formal model for the cruise control system using Perfect formal specification language. We verify the formal model in order to check completeness, consistency and validity of the model using the Perfect Developer toolset. Next, we build a C# tool to read the Perfect Developer formal model and produce the state-based specification graph or the FSM graph in order to automatically create test cases from the model according to a transition-based coverage criterion. We evaluate the coverage to test the system's performance and effectiveness. Moreover, we use test case reduction techniques in order to reduce the redundant test cases that will be generated by a set of testing algorithms.

2. RELATED WORK

2.1 Testing Critical Software Systems

According to You and Rayadurgam [25], the failure of software systems can cause significant damage to the software or its environment, severe economic consequences or even loss of life. There are many examples of safety-critical systems, such as aircraft flight control systems, medical device systems, nuclear systems and automobile cruise control systems.

The most important property of the safety-critical system is its dependability, which is shown by the extent to which users or customers trust the software system. Moreover, this will reflect the degree of user confidence in the system's ability not to fail when operated.

Many different formal specification languages and formal verification automated tools have been used to express and verify the formal specification of automobile cruise control systems. For example, Atlee and Gannon [3], Heitmeyer *et al*. [10] and Bultan and Heitmeyer [4] used the SCR-style (Software Cost Reduction) to specify and verify the safety property of the CCS. A formal cruise control B specification is discussed by Krupp *et al*. [13] in which an adaptive cruise control B model and RAVEN model checker are presented. The model is used to improve the confidence and understand ability of the system's behaviour. Another approach presented by Iliasov *et al*. [11], in which the system's dependability is characterized by rigorous design and fault tolerance, is represented by structuring the formal specification in an abstract way in the notion of an operation mode that depends on a state-based formalism approach called (Event-B) to refine the system modes. To check the effectiveness and safety requirements, Yasmeen *et al*. [24] conducted an experimental analysis which simulated a number of indications of safety critical systems. Mishra *et al*. [18] proposed a model-based testing auto-review tool, which was used to partially automate the process of verifying safety-critical systems. You and Rayadurgam [25] proposed a constrained random testing framework on a safety-critical embedded system. They used the constraints to narrow the possible test cases and cover most of the system's

Jordanian Journal of Computers and Information Technology (JJCIT), Vol. 1, No. 1, December 2015.

behaviour. A similar approach to ours was discussed by Nilsson *et al.* [26]. They proposed correct-by-construction control software for Adaptive Cruise Control (ACC) system that is guaranteed to satisfy the formal specification in Linear Temporal Logic (LTL). They formalized the ACC using a hybrid dynamical system model with two modes: the no lead car and the lead car. Then, they constructed two controllers as a solution for the two modes, with the first solution based on continuous state space and the other based on a finite-state abstraction. The two controllers were tested by running a simulation in Simulink and on a vehicle simulation package called CarSim. However, our work depends on the Perfect language for the formalization which is easier than LTL, since the syntax in Perfect language is close to the programming languages. Moreover, according to Zhao [27], with the use of LTL "experiences show that specifications of even moderate-sized systems are too complex".

2.2 Testing Coverage Criteria

Coverage criteria on software systems can be defined as the set of conditions and rules that impose a set of test requirements on a software test. Ammann and Offutt [2] mentioned that test requirements in software testing are a specific set of elements of software artefacts that the software test cases must satisfy or cover.

Categories of coverage criteria include structural coverage, data-flow coverage, decision coverage, call graph coverage and transition-based coverage. In the framework for our cruise control system, a transition-based coverage criterion is used. For transition-based coverage, every precondition in the software's formal specification should be tested at least once so that each transition must be taken as a test requirement.

Several coverage criteria are used in the literature for testing systems. For example, Offutt *et al.* [20] introduced a technique for state-based specifications to generate test cases for cruise control systems. Their technique depends on an SCR formal specification model that represents the cruise control functionality and the coverage criteria that are: transition coverage, full predicate coverage, transition-pair coverage, complete sequence and structural coverage for state-based decision testing.

An experimental study conducted by Fraser and Gargantini [9] addressed the problem of test case generation, optimization and the performance of model checkers. In their study, they depended on explicit state model checkers that use a DFS algorithm. A cruise control system was studied, with its SRC formal specification being put into the model checker and test cases generated according to condition-based and structural coverage criteria.

Liu [14] used VDL-formal specification language notations in order to automatically generate a test prediction to analyze the results from their proposed decompositional approach for automatic test case generation. The results indicated that the researcher's approach was effective in terms of branch coverage, path coverage and statement coverage. In addition, his test case generation algorithm was effective in detecting the defective test cases for his system.

Liu and Nakajima [15] aimed to improve formal specification completeness and feasibility by introducing a new method that depends on verifying completeness and feasibility in the form of pre-conditions and post-conditions. This method uses single formal specification operations to choose the automated teller machine (ATM) system. SOFL formal specification language was used to build the ATM specifications. Appropriate test case generation criteria were used to build a question checklist from the ATM SOFL specifications in the test case generation process.

The proposed method improved the ATM operation's completeness and feasibility through its ability to formally define those characteristics. Furthermore, the generated test cases covered every aspect of the ATM defined specifications, so that it added the advantage of detecting errors in the system and reducing the cost of testing the system.

Another usage for SOFL formal specification language was presented in Chen's [6] research in which he addressed the problem of specification-based testing and test case generation for concurrent software systems.

Test cases were generated to cover the produced specification suggestions according to appropriate coverage criteria related to concurrent software systems. Each one of the generated test cases was executed several times in order to traverse program paths. The proposed approach was applied to an online shipping system and proved its usability for concurrent software systems.

Tian *et al*. [22] realized the problem of automatic test case generation from the pre- and post-conditional formal specifications (PROMELA formal specification language) by obtaining the benefits from connecting specification-based testing and the usage of model checkers (Spin model checker).

Nakatsugawa *et al*. [19] aimed to facilitate formal specification readability by discussing a new specification-based testing framework for interface specifications.

As with our approach, several others have been used to automatically generate test cases from a graph using graph coverage technique, such as: [28]-[30].

Gotlieb *et al.* [28] presented two different algorithms in order to automatically generate functional tests for synchronous executable BPEL processes. The first algorithm, STRUCRUNS, was used to generate test cases covering lengthy feasible paths up to a given length. The second algorithm, RANDOMRUNS, was derived from the desired number of test cases covering a random selection of feasible paths limited by a predetermined length.

Yan *et al.* [29] implemented a prototype that is used to automatically generate test data based on a constraint solving technique. In their approach, they transformed the procedure into a constraint system using static single assignment. Then, the constraint system was solved to check whether at least one feasible path through the selected point existed. Finally, test cases were generated corresponding to one of these paths.

Jehan *et al.* [30] proposed an approach that is used to automatically generate BPEL test cases that handle concurrent features. In their approach, they represented the BPEL program in an extended control graph. After that, they generated all the sequential test paths from XCFG before combining all the sequential test paths into concurrent test paths. Finally, they used the BoNus solver to solve the constraints of the test paths and then generate feasible test cases.

Utting and Legeard [31] in their book "Practical Model-based Testing: A Tools Approach" presented a commercial tool called LTG/UML which is a model-based testing tool that can be used to automatically generate test cases from a UML state machine using different coverage criteria. The tool has been demonstrated on examples and case studies from a variety of software domains, including embedded software and information systems.

3. PERFECT DEVELOPER

Many formal methods have been used to model safety-critical systems in the literature, such as Event-B Abrial [1], Z-formal specification [12], VDM [6], B-specifications [16], SCR specification [20] and a number of other formal languages. Most formal methods only involve the specification of the system; however, some continue the development process until a running code is obtained. However, according to Crocker [7], those formal methods take a long time to produce the running program. In this paper, Perfect Developer is used as a formal method and starts its process by describing the system, verifying a formal specification, refining it to the code within the same notation using a set of algorithms, verifying the refinement by checking its correctness and completeness and translating it into a set of high-level programming languages such as C++, Java and Ada.

Perfect Developer (PD) is an automated tool developed by Escher Technology to verify the Perfect specification software system. Perfect is an expressive language that describes system specification in an object-oriented model style using object-oriented terms and concepts such as classes, functions and constant variables. Perfect, like many object-oriented languages such as Java and C++, supports object concepts, such as encapsulation and inheritance, through object classes and message passing.

Perfect language has the ability to describe software system behaviours without any details of how the behaviour will be performed. It also includes certain design principles, including design by contract, which is the main structural rule or principle which Perfect depends on; it uses the contract to define the input-output relationships for class methods. The contract has two main parts; pre-conditions and post-conditions. The pre-conditions determine what must be true for the call feature, while the post-conditions determine what is guaranteed to be true at the termination of a successful Perfect feature as presented by Carter and Monahan [5].

An investigation was undertaken by Crocker and Carlton [8] to see if the automated reasoning using Perfect developer for the embedded software has the ability to provide the same degree of success in verification of a handwritten C code. The study made use of two small C programs with their specification annotations. As a result, they found that automated reasoning can discharge a very high proportion of verification conditions that arise from specification and software refinement. The number of test cases required was reduced.

4. METHODOLOGY

Our framework consists of seven phases shown in Figure 1. We first understand the cruise control requirements and then write the informal specification description for our system. The main reason for writing the informal specifications is to reflect its different states and transitions and the different conditions that enforce each transition in the system. In the second step, we develop the cruise control formal model, using Perfect formal specification language depending on the informal description of our system. The third step reflects the formal model verification using Perfect developer. After that, we manually extract the CCS formal model adjacency matrix, and then develop a C# tool to read our verified model and extract the different system paths and states in order to generate test cases using a set of proposed algorithms. The evaluation process for our generated test cases is discussed in phase seven. Moreover, we analyze the effectiveness of each algorithm used in the process of the test case generation. We will now discuss each of these steps in detail.

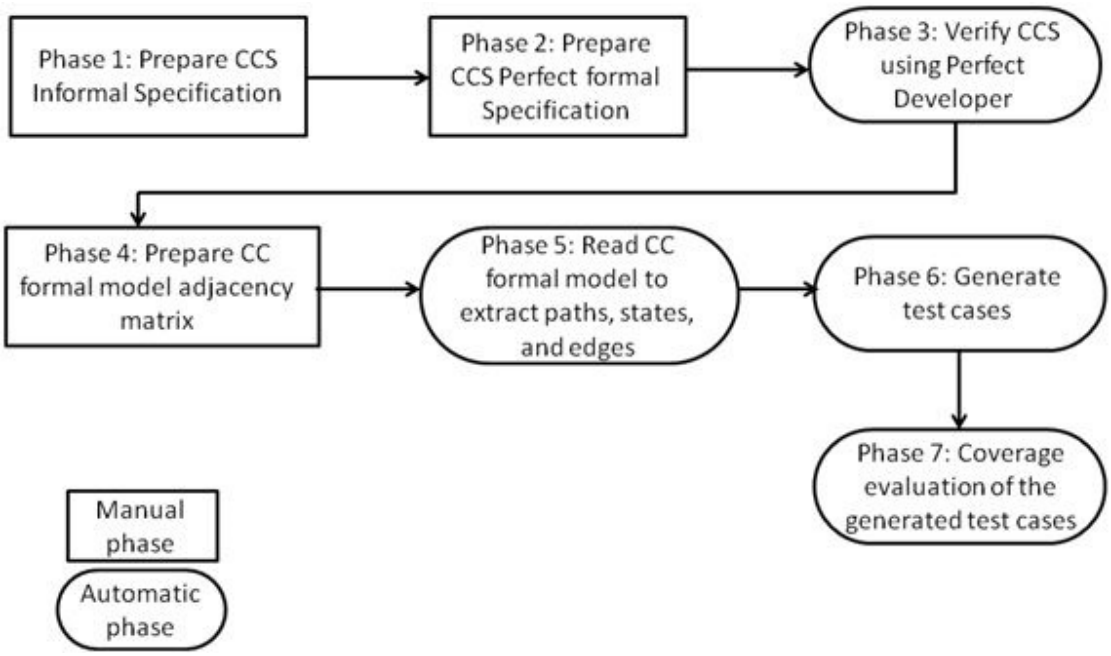

Figure 1. A framework for test case generation using the formal method.

4.1 Informal Specifications of Cruise Control System

The cruise control system (CCS) is a safety-critical system that can be described by a set of behaviours, modes, states and transition variable state quantifiers. Such quantifiers are the ignition switch, cruise control button, automobile speed and cruise control target speed.

CCS transition modes that occur between the system and the driver are started by the initial state when the system ignition is “OFF”. The current speed is at zero and the cruise state is “OFF”. When the driver switches the ignition to “ON”, then the CC state can be “ON” or “OFF” depending on whether the driver wants to switch on the CC button or not. When the CC is switched to “ON” and the driver starts driving, then the cruise state can be “active”, “cruising” or “standby”. The main role of the CCS is to maintain the automobile’s speed as close as possible to the target speed. The target speed is determined by the driver when the CCS is “ON” and the target speed can be increased or decreased by the driver.

The automobile’s actual speed should not exceed a restricted limit and should also not exceed the target speed, so that the driver has an allowance interval that defines how much the actual speed could deviate from the target speed. Where the difference between the two speeds is acceptable, the CC will maintain the current speed. If the driver’s current speed exceeds the target speed, then the CCS will take measures to maintain the target speed.

The CCS states can be affected by a set of factors like: pressing the brake, accelerator and the “ON” / “OFF” button for the CC. In addition, various failures could affect the CCS states, such as a low battery; some of these faults are handled by returning the control to the driver to take certain measures. As a result, the CC could be activated (the state will be changed from “standby” to “active”) or the driver could drive without activating the CC. Figure 2 describes the CCS finite state machine diagram.

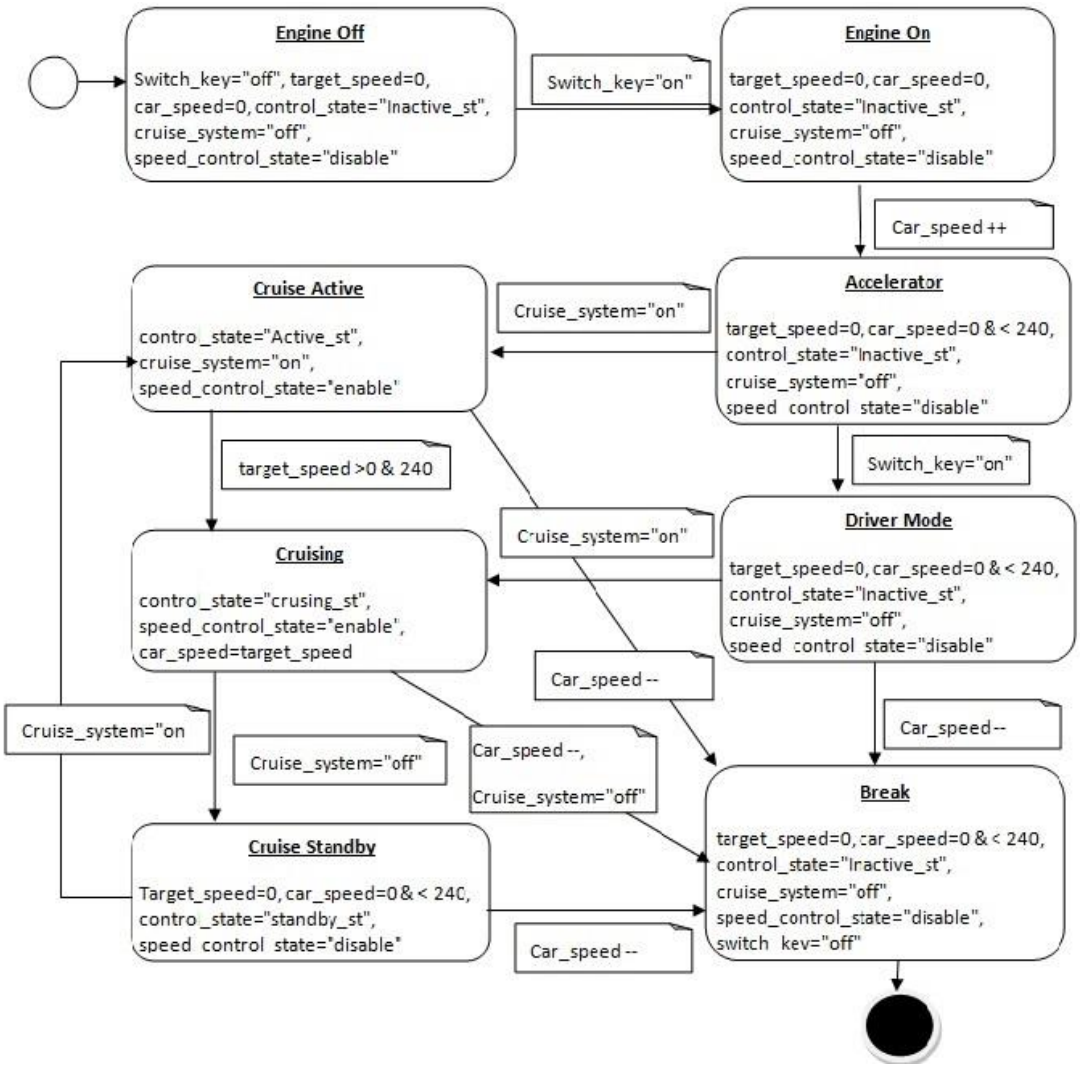

Figure 2. Cruise control system finite state machine diagram.

4.2 CCS Formal Model Using Perfect Language

In the second phase of our methodology, we build the CCS formal model from the informal specifications of the CCS using Perfect language. The formal specification consists of two main classes; the first one is the speed control class and the second is the controller class. The speed control class describes the system-related speed variables and schemas (functions). The controller class describes the related CCS variables and schemas. Due to space limitation, Table 1 shows the CCS formal model of the control class only.

4.3 Formal Model Verification Using Perfect Developer Toolset

In the third phase, the Perfect CC specification that is described in subsection 2.2 is verified by Perfect developer toolset in order to check the syntax, the semantic correctness and the validity of the model. The verifier in Perfect Developer is static analysis and automated theorem proving that collects and attempts to discharge proof obligations for the software with which it is presented.

"Using Formal Methods for Test Case Generation According to Transition-Based Coverage Criteria", Ahmad A. Saifan and Wafa Bani Mustafa.

4.4 FSM Adjacency Matrix for CCS Formal Model

The fourth phase involves the process of adjacency matrix extraction from the verified formal CCS model, which is shown in Table 2. The adjacency matrix reflects the system's states and what the adjacent state to each state in the system is. In the adjacency matrix, 'one' indicates what other states each state can go to. For example: "Engine Off" state can go to "Engine On"' state only, while "Engine On" can go to "Accelerator" state only. Zero indicates that there is no transition between the two states.

Table 1. Part of CCS Perfect formal model

```
class CONTROLLER ^=
abstract
const Inactive_st : int ^= 0;
const Active_st   : int ^= 1;
const Cruising_st : int ^= 2;
const Standby_st  : int ^= 3;
var   ControlState: int ;
var sp_con: SPEED_CONTROL ;
var getten_target_speed: int ;
var engin : bool ;
var cruise : bool;
build{!sp_con: SPEED_CONTROL }
post
ControlState != Inactive_st ,
engin != true ,cruise != false ,
getten_target_speed !sp_con.TargetSpeed;
schema !Break
pre
 sp_con.TargetSpeed <sp_con.CarSpeed ,
 engin = true ,cruise = true ,
 ControlState = Cruising_st
post
 sp_con!DisableControl ,
 ControlState != Standby_st ;
  schema !Accelerator
 pre
 engin = true ,cruise = true ,
 sp_con.TargetSpeed > sp_con.CarSpeed ,
 ControlState = Cruising_st
 post
 sp_con!EnableControl ,
 ControlState != Cruising_st ;
 schema !EnginOff
 pre
 ControlState = Active_st |ControlState
= Cruising_st  | ControlState =
Standby_st | ControlState = Inactive_st
 post
 ([ControlState = Cruising_st]:
(ControlState != Inactive_st ,
sp_con!DisableControl , engin != false)
, []: engin != false ) ,
 ([ControlState =  Active_st]:
(ControlState != Inactive_st ,
sp_con!DisableControl , engin != false)
, []: engin != false ),
 ([ControlState = Standby_st]:
(ControlState != Inactive_st ,
sp_con!DisableControl , engin != false)
, []: engin != false ) ,
 ([ControlState = Inactive_st ]:
(ControlState != Inactive_st ,
sp_con!DisableControl , engin != false)
, []: engin != false );
schema !EnginOn
pre
 ControlState = Inactive_st
post
 sp_con!ClearSpeed,
 ControlState != Inactive_st ;
  schema !CruiseOn
 pre
 ControlState = Inactive_st
st
 getten_target_speed != sp_con.TargetSpeed
 ,
 sp_con!EnableControl ,
 ControlState != Active_st ;
 schema !Cruise_Crusing
 pre
 engin = true ,
 ControlState = Active_st,
 sp_con.CheckSpeed = true
 post
 ControlState != Cruising_st ;
 schema !Cruise_Active
 pre
 engin = true ,cruise = true,
 sp_con.TargetSpeed > 0 ,
 sp_con.CarSpeed > 0
 post
 ControlState != Active_st ;
 schema !Cruise_Inactive
 pre
 engin = true ,
 cruise = false,
 sp_con.TargetSpeed = 0 ,
 sp_con.CarSpeed > 0
 post
 ControlState != Inactive_st ;
 schema !Cruise_Standby
 pre
 engin = true ,
 cruise = true,
 sp_con.TargetSpeed > 0 ,
 sp_con.CarSpeed > 0
 post
 sp_con!DisableControl ,
 ControlState != Standby_st ;
   schema !CruiseOff
  pre
  ControlState = Cruising_st | engin =
 false
   post
 sp_con!DisableControl ,
 ControlState != Standby_st ;
  schema !CruiseResume
  pre
  engin = true,
  cruise = true ,
  ControlState = Standby_st
  post
  sp_con!EnableControl,
  ControlState != Cruising_st ;
       end;  // the end of class CONTROLLER
```

Table 2. CCS adjacency matrix.

State	Engine Off	Engine On	Accelerator	Driver Mode	Cruise Active	Cursing	Cruise Standby	Break
Engine Off	0	1	0	0	0	0	0	0
Engine On	0	0	1	0	0	0	0	0
Accelerator	0	0	0	1	1	0	0	0
Driver Mode	0	0	0	0	1	0	0	1
Cruise Active	0	0	0	0	0	1	0	1
Cursing	0	0	0	1	0	0	1	1
Cruise Standby	0	0	0	0	1	0	0	1
Break	0	0	0	0	0	0	0	0

4.5 Extraction CC Formal Model Paths, States and Edges

The testing C# tool develops an algorithm called “extractPath” in order to extract the CCS finite state machine paths, states and edges. The “extractPath” algorithm depends on the CCS adjacency matrix and the pseudo code shown in Figure 3. In this phase, the verified formal Perfect specification is put into our C# testing tool and the structure of the cruise control system is prepared using the adjacency matrix that is shown in the previous phase. From the matrix, the algorithm in Figure 3 is used to extract the different system states, paths between system states and edges between states.

The extraction process depends on transition-based coverage criteria that focus on the transition sequence between the system states. The transition-based coverage criteria are represented by 1. all system states, 2. all pair-transitions where each state can go and 3. all system paths.

The algorithm shown in Figure 3 starts by identifying a list of strings (P) that contains all system state paths extracted from the adjacent matrix for a given state. Each state is given a number; for example, Engine Off =1, Engine On=2 … and so on. Then, we find all the adjacent states (by checking the adjacent matrix) for the current state, calling the function find_adjacent (). This function will add the adjacent state numbers to the paths in list P. For example, when list P contains an item (1,2), it means that there is a path from state 1 to state 2. Then, the algorithm continues by finding the adjacent state to the previous state in the path, in this example state 2. Adjacent to state 2 is state 3 (Accelerator). So, state 3 is added to the path (1,2) and the new path (1,2,3) is added to P ; P=[(1,2), (1,2,3)]. In this case, P has two paths. Next, the algorithm finds the adjacent states for state 3 which are states 4 and 5, which are both added to the current path. List P is now equal to [(1,2), (1,2,3),(1,2,3,4), (1,2,3,5)]. The algorithm continues until all paths that each state can reach are found.

Finally, the algorithm extracts the test paths (TP) from list P. A test path is a path that starts from the initial state which is state 1 and ends with the final state which is state 8.

```
For each state in the adjacent matrix Do
        define P as a list of strings contains all paths from the current state
        P= find_adjacent(currentstate)
        IF P.length === 0 then
                there is no path from the current state
        Else
                count=0
                While counter < = P.length DO
                        String currentPath = P.getitem [counter ]
                        //get the last index of the current item in the list P
                        I= currentPath[currentPath.length - 1].tostring()
                        P= find_adjacent(I)
                        counter ++
                End DO
        End IF

From P get all test paths TP that starts with state 1 and ends with state 8


Function list <String> find_adjacent (i)
        J=1
        String S=P[i]
        For state =1 to the last state DO
                IF  adj_Matrix [i,state]== 1 then
                        // add the state # to the path P[i]
                        S= P[i] + state
                        add the pathe S to the list P
                End IF
        return P
        End For //list filled with the adjacent states
```

Figure 3. The algorithm of path extraction.

4.6 Automatic Test Case Generation

After the system paths are extracted and system states counted, we automatically generate test cases from the verified cruise control system formal specification through the developed C# testing tool. Test cases will be generated from the test paths generated in the previous phase. For the process of test case generation, we use three algorithms:

Algorithm (1): random test case generation process that generates test cases without any restrictions. So, some of the test cases are considered to be redundant test cases. Algorithm 1 is presented in Figure 4. In the algorithm, TCR1 is a list that contains a set of test cases that are randomly generated from the test path (TP).

```
Algorithm 1
define TCR1 as a list of string that contains test cases generated using Alg 1
For I=1 to N // where N is the number ot test cases to be generated
        //get a random number
        item = Random (1, TP.length)
        TCR1.add( TP.ElementAt(item))
End For
```

Figure 4. Algorithm1.

Algorithm (2): random test case generation with pure restrictions. This algorithm depends on a random generation process with partial restrictions on the generated test cases. This algorithm restricts the results by which a set of randomly unique system paths must be generated for the results each time. In Figure 5, the algorithm randomly generates N test cases from the test path (TP) in such a way that M of them must be unique paths; where M is less than N. The others (N-M) could be redundant.

```
Algorithm 2
define TCR2 as a list of string that contains test cases generated using Alg 2
countDis=0 //represents the number of unique test cases
countAll=0 //to count the number of the generated test cases
// M is the number of unique test cases, M should be less than N
While (countAll <= N)  // where N is the number of test cases to be generated
        //get a random number
        item = Random (1, TP.length)
        IF (countDis <= M  )
                IF( TP.ElementAt(item) is not in TCR2 list )
                        TCR2.add( TP.ElementAt(item))
                        countDis++
                        countAll++
                End IF

        else
                TCR2.add( TP.ElementAt(item))
                countAll++
        End IF
End While
```

Figure 5. Algorithm 2.

Algorithm (3): random test generation with full and optimal restrictions. The algorithm restricts the selected paths by which all system paths must be chosen in the algorithm random process. Moreover, the algorithm forces the generation process to uniquely generate a number of test cases. In other words, if we need N test cases, then we have to generate them randomly and each one should be unique (redundancy in test cases is not allowed). Figure 6 shows algorithm 3.

```
Algorithm 3
define TCR3 as a list of string that contains test cases generated using Alg 3
countDis=0 //count represents the number of unique test case
 // where N is the number of test cases to be generated
While (countDis <= N && countDis < Tp.length)
        //get a random number
        item = Random (1, TP.length)
        IF ( TP.ElementAt(item) is not in TCR2 list )
                TCR3.add( TP.ElementAt(item))
                countDis++
        End IF
End While
```

Figure 6. Algorithm 3.

4.7 Coverage Evaluation for the Generated Test Cases

Finally, the test cases generated in the previous phase are evaluated to determine the system path coverage, state coverage (node coverage) and transition coverage (edge coverage). A set of coverage measurements is used here to evaluate path, state and transition coverage.

5. EXPERIMENTS AND EVALUATION

In our experiments, we use our framework to automatically generate the test cases using the three algorithms for the CCS. Subsection 5.1 discusses the coverage evaluation measures used in our framework. Subsection 5.2 makes a comparison between the three developed test case generation algorithms in terms of coverage and performance evaluation used in this framework.

5.1 Evaluation Measures

The evaluation process of our C# testing tool depends on three matrices in terms of coverage evaluation measurement. The three matrices shown in Figure 7 are state (node) coverage matrix, path coverage matrix and edge coverage matrix. The coverage value for each of the three types depends on the related value of executed state, executed paths and executed edges, respectively, in which the smaller execution value type achieves a smaller coverage value. The number of extracted states, paths and edges represents the number of states, paths and edges, respectively,

from the formal model. The number of executed states, executed paths and executed edges represents the number of states, paths and edges, respectively, that will be processed according to a specific number of test cases. For example, if we have eight states extracted from the system but the test cases that we have used only executed six of the states, then the coverage will be 6/8=75%.

Coverage Type	Coverage Matrix
State (node) coverage =	# Of executed states / # Of extracted states
Path coverage =	# Of executed paths / # Of extracted paths
Edge coverage =	# Of executed edges / # Of extracted edges

Figure 7. Coverage matrix measurements.

5.2 Comparisons and Evaluation Results

5.2.1 CCS Test Case Evaluation

The process of test case generation from the CCS model depends on three algorithms, as described in the previous section. The developed algorithms depend on a random generation process and are evaluated to five numbers of fixed test cases. Moreover, the three algorithms are compared with each other to determine their effectiveness.

As we have seen from Figure 2, the CCS extracted states were eight, the extracted test paths were nine and the extracted edges were twelve. The three random test case generation algorithms were evaluated to five numbers of test cases with 3, 5, 9, 12 and 15 test cases. The evaluation of state coverage results is shown in Table 3.

Table 3. CCS State coverage algorithm results.

T.C#/Algo.#	Algo.#1	Algo.#2	Algo.#3
3 Test Cases	75%	87%	100%
5 Test Cases	100%	100%	100%
9 Test Cases	87.5%	100%	100%
12 Test Cases	100%	100%	100%
15 Test Cases	100%	100%	100%
Average	92.5%	97.4%	100%

Table 3 shows that, for example, when we generate nine test cases by algorithm #1, the CCS state coverage is 87.5%. This means that the nine test cases execute seven system states from all eight extracted system states. When the nine test cases are generated using algorithm #2 (as well as algorithm #3), the state coverage is 100% which means that the nine test cases pass all system states. The averages of the state coverage for algorithm #1, algorithm #2 and algorithm #3 are 92.5%, 97.4% and 100%, respectively, which represents the average from generating 3, 5, 9, 12 and 15 test cases by each algorithm.

Table 4 shows the evaluation results for path coverage using the three algorithms.

Table 4. CCS path coverage algorithm results.

T.C#/Algo.#	Algo.#1	Algo.#2	Algo.#3
3 Test Cases	11.12%	33.34%	33.34%
5 Test Cases	33.34%	55.55%	55.55%
9 Test Cases	33.34%	55.55%	100%
12 Test Cases	44.45%	66.66%	100%
15 Test Cases	55.56%	77.77%	100%
Average	35.558%	57.774%	77.778%

Table 4 shows that, for example, when we generate nine test cases by algorithm #1, the CCS path coverage is 33.34%. This means that the nine test cases execute only three test paths from all nine extracted test paths. With the nine test cases generated using algorithm #2, the path coverage is 55.55% which mean that only five test paths from all extracted test paths were executed. For algorithm #3, the path coverage with nine test cases is 100%. This means that those nine test cases execute all nine test paths in the system. The averages of the path coverage for algorithm #1, algorithm #2 and algorithm #3 are 35.558%, 57.774% and 77.778%, respectively. Table 5 shows the evaluation results for edge coverage using the three algorithms.

Table 5. CCS edge coverage algorithm results.

T.C#/Algo.#	Algo.#1	Algo.#2	Algo.#3
3 Test Cases	41.66%	66.67%	75%
5 Test Cases	83.33%	91.67%	100%
9 Test Cases	66.67%	100%	100%
12 Test Cases	83.33%	100%	100%
15 Test Cases	83.33%	100%	100%
Average	71.66%	91.7%	95%

Table 5 shows that, for example, when we generate nine test cases by algorithm #1, the CCS edge coverage is 66.67%. This means that eight edges of the 12 extracted system edges are passed or executed. With the nine test cases generated using algorithm #2 and algorithm #3, the edge coverage was 100% which means that all the 12 extracted system edges are executed. The averages of the edge coverage for algorithm #1, algorithm #2 and algorithm #3 are 71.66%, 91.7% and 95%, respectively.

5.2.2 Test Case Generation Algorithm Results

In this section, we compare the three test case algorithm results. Figure 8 shows the coverage averages obtained from the three algorithms.

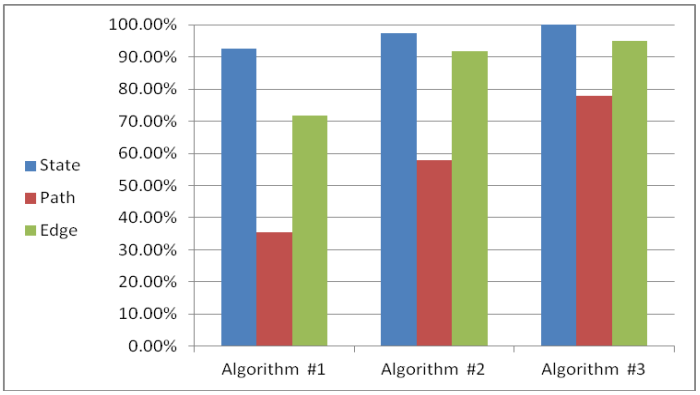

Figure 8. A comparison between the three test case algorithms.

From the results, we can see that algorithm #3 is the best, achieving the most effective coverage values in terms of state, path and edge coverage. Algorithm #2 is better than algorithm #1 in its average results, from which we can conclude that more restriction in the process of test case generation provides more effective coverage results.

6. LIMITATIONS AND FUTURE WORK

Our framework suggests there are benefits in the use of the Perfect formal model for efficiently testing a safety-critical system. However, it is important to note the limitations of our evaluation experiments and framework. First, our framework accepts only the CCS Perfect model and no other safety-critical systems. Moreover, more experimentation is necessary to strengthen the evaluation of our framework, ideally using a safety-critical system used in industry. Second, the finite state machine adjacency matrix was built manually. However, the automation of this process should be possible.

7. CONCLUSIONS

In this paper, we have reflected the importance and role of formal methods in developing safety-critical system formal models. The cruise control system was chosen for this study as a safety-critical system and its state machine diagram was built to reflect the system's states, transitions and variables.

Perfect formal specification language was used to develop the CCS formal model due to its reliability and effectiveness in presenting transition state systems' formal models, which is important in reducing software development costs. We built a consistent and reliable formal model that will play a role in increasing system quality and reducing system testing cost and effort.

We proposed three algorithms to generate test cases from the CCS Perfect formal model. The generated test cases were evaluated according to three coverage matrices; state coverage matrix, path coverage matrix and edge coverage matrix. We proved that using formal methods through the safety-critical software development life cycle plays a significant role in improving the testing stage, making it more effective in terms of both effort and cost.

REFERENCES

[1] J. R. Abrial, Modeling in Event-B: System and Software Engineering, 1st Edition, Cambridge University Press, New York, NY, USA, 2010.

[2] P. Ammann and J. Offutt, "Introduction to Software Testing," 2008, Available at: http://www.cs.gmu.edu/~offutt/softwaretest/.

[3] J. Atlee and J. Gannon, "State-Based Model Checking of Event-Driven System Requirements," IEEE Transactions on Software Engineering, vol. 19, issue 1, pp. 24-40, Jan. 1993.

[4] T. Bultan and C. L. Heitmeyer, "Applying Infinite State Model Checking and Other Analysis Techniques to Tabular Requirements Specifications of Safety-Critical Systems," Design Automation for Embedded Systems, vol. 12, issue 1, pp. 97-137, June 2008.
URL http://dx.doi.org/10.1007/s10617-008-9014-2.

[5] G. Carter and R. Monahan, "Software Refinement with Perfect Developer," 3rd IEEE International Conference on Software Engineering and Formal Methods (SEFM'05), pp. 363-373, 2005.

[6] Y. Chen, "Generation of Test Cases for Concurrent Software Systems Based on Data-Flow-Oriented Specifications," IEEE 2011 First ACIS/JNU International Conference on Computers, Networks, Systems and Industrial Engineering (CNSI), pp. 170-177, 23-25 May.

[7] D. Crocker, "Teaching Formal Methods with Perfect Developer," 2003, http://www.eschertech.com/papers/teaching_formal_methods.pdf.

[8] D. Crocker and J. Carlton, "Verification of C Programs Using Automated Reasoning," in: SEFM '07: Proceedings of the 5th IEEE International Conference on Software Engineering and Formal Methods, 2007 IEEE Computer Society, Washington, DC, USA, pp. 7-14.

[9] G. Fraser and A. Gargantini, "An Evaluation of Model Checkers for Specification Based Test Case Generation," 2013 IEEE 6th International Conference on Software Testing, Verification and Validation, pp. 41-50, Denver, Colorado, 1-4 April 2009.

[10] C. Heitmeyer, J. Kirby and B. Labaw, "Tools for Formal Specification, Verification and Validation of Requirements," Proceedings of the IEEE 12th Annual Conference on Computer Assurance (COMPASS '97), pp. 35-47, 16-19 June 1997.

[11] A. Iliasov, A. Romanovsky and F. Dotti, "Structuring Specifications with Modes," 4th IEEE Latin-American Symposium on Dependable Computing (LADC '09), PP. 81-88, 1-4 Sept. 2009.

[12] S. Kanwal and N. Zafar, "Formal Model of Automated Teller Machine System Using Z Notation," IEEE International Conference on Emerging Technologies (ICET 2007), pp. 131-136, 12-13 Nov. 2007.

[13] A. Krupp, O. Lundkvist, T. Schattkowsky and C. Snook, "The Adaptive Cruise Controller Case Study Visualization, Validation and Temporal Verification," in UML-B System Specification for Proven Electronic Design, 9 Dec. 2004, Kluwer Academic Publishers 2005.

[14] S. Liu, "Utilizing Test Case Generation to Inspect Formal Specifications for Completeness and Feasibility," 9th IEEE International Symposium on High-Assurance Systems Engineering (HASE'05), pp. 349-356, 2005.

[15] S. Liu and S. A. Nakajima, "A Decompositional Approach to Automatic Test Case Generation Based on Formal Specifications," IEEE 2010 4th International Conference on Secure Software Integration and Reliability Improvement (SSIRI), pp. 147-155, Singapore, 9-11 June 2010.

[16] Q. Malik, J. Lilius and L. Laibinis, "Scenario-Based Test Case Generation Using Event-B Models," IEEE 1st International Conference of Advances in System Testing and Validation Lifecycle (VALID '09), pp. 31-37, 20-25 Sept. 2009.

[17] D. Mery and N. K. Singh, "Critical Systems Development Methodology Using Formal Techniques," in: Proceedings of the 3rd Symposium on Information and Communication Technology (SoICT '12), pp. 3-12, Viet Nam, 23 – 24 August 2012. URL http://doi.acm.org/10.1145/2350716.2350720.

[18] A. Mishra, M. Rao, C. Cu, V. Rao, Y. Jeppu and N. Murthy, "An Auto-Review Tool for Model-Based Testing of Safety-Critical Systems," in: Proceedings of the 2013 International Workshop on Joining AcadeMiA and Industry Contributions to Testing Automation, JAMAICA 2013, pp. 47-52, ACM, New York, NY, USA, 2013.

[19] Y. Nakatsugawa, P. Kurita and K. Araki, "A Framework for Formal Specification Considering Review and Specification-Based Testing," 2010 IEEE Region 10 Conference-TENCON 2010, pp. 2444 – 2448, ISBN: 978-1-4244-6889-8, Fukuoka, 21-24 Nov. 2010.

[20] J. Offutt, Y. Xiong and S. Liu, "Criteria for Generating Specification-Based Tests," 5th IEEE International Conference on Engineering of Complex Computer Systems (ICECCS'99), pp. 119-131, Las Vegas, Nevada, USA, 18-21 October 1999.

[21] I. Sommerville, Software Engineering, 9th Edition. Addison-Wesley, Haelow, England, 2010.

[22] C. Tian, S. Liu and S. Nakajima, "Utilizing Model Checking for Automatic Test Case Generation from Conjunctions of Predicates," Proceedings of the 2011 IEEE 4th International Conference on Software Testing, Verification and Validation Workshops (ICSTW 2011), pp. 304-309.

[23] G. Tim, "Object-Z to Perfect Developer", 2007, Available at: http://www.doc.ic.ac.uk/~tk106/ObjectZ_project.pdf.

[24] A. Yasmeen, K. M. Feigh, G. Gelman and E. L. Gunter, "Formal Analysis of Safety-Critical System Simulations," in: Proceedings of the 2nd International Conference on Application and Theory of Automation in Command and Control Systems (ATACCS '12), pp.71-81, London, UK, 29-31 May 2012.

[25] D. You and S. Rayadurgam, "Practical Aspects of Building a Constrained Random Test Framework for Safety Critical Embedded Systems," in: Proceedings of the 1st International Workshop on Modern Software Engineering Methods for Industrial Automation (MoSEMInA 2014), pp. 17-25, ACM, New York, NY, USA, 2014.

[26] P. Nilsson, O. Hussien, Y. Chen, A. Balkan, M. Rungger, A. D. Ames, J. Grizzle, N. Ozay, H. Peng and P. Tabuada, "Preliminary Results on Correct-by-Construction Control Software Synthesis for Adaptive Cruise Control," Proc. 53rd IEEE Conference on Decision and Control (CDC), Dec. 2014.

[27] Y. Zhao, "Intuitive Representations for Temporal Logic Formulas," in Proc. of Forum on Specification and Design Language (FDL'03), pp. 405–413, Frankfurt, Germany, September 2003.

[28] A. Gotlieb, B. Botella and M. Rueher, "Automatic Test Data Generation Using Constraint Solving Techniques," in Proceedings of the 1998 ACM SIGSOFT International Symposium on Software Testing and Analysis (ISSTA '98), Will Tracz (Ed.), pp. 53-62, FL, USA, 02 – 04 March 1998.

[29] J. Yan, Z. Li, Y. Yuan, W. Sun and J. Zhang, "BPEL4WS Unit Testing: Test Case Generation Using a Concurrent Path Analysis Approach," IEEE 17th International Symposium on Software Reliability Engineering (ISSRE '06), pp. 75 – 84, 7-10 Nov. 2006.

[30] S. Jehan, I. Pill and F. Wotawa, "BPEL Integration Testing," 18th International Conference on Fundamental Approaches to Software Engineering (FASE), pp. 69-83, London, UK, 11-18 April 2015.

[31] M. Utting and B. Legeard, Practical Model-Based Testing: A Tools Approach, Morgan Kaufman Publishers Inc. San Francisco, CA, USA, 2007, ISBN:0123725011 9780080466484.

ملخص البحث:

تلعب الطرق الرسمية دوراً مهمّاً في زيادة جودة البرمجيات و إعتماديتها و متانتها وفعاليتها. أضف إلى ذلك أن استخدام الطرق الرسمية، وبخاصة في أنظمة السلامة الحرجة، من شأنه أن يساعد في الكشف المبكر عن أخطاء البرمجيات و عيوبها، الأمر الذي يؤدي إلى إختصار الكلفة و الجهد و الوقت التي يتطلبها اختبار البرمجيات.

يهدف هذا البحث إلى إثبات دور المواصفات الرسمية و فاعليتها في دراسة حالة لنظام من أنظمة قيادة السيارات و التحكم بها. و قد تم بناء نموذج رسمي لهذا النظام باستخدام لغة بيرفكت للمواصفات الرسمية، والتحقق من صحته باستخدام أدوات تطوير لغة بيرفكت. كذلك، تم بناء أداة لفحص البرمجيات جرى استخدامها لإنتاج حالات فحص عن طريق ثلاث خوارزميات مختلفة. وتمّ تقييم حالات الفحص تلك من أجل تحسين تغطيتها وفعاليتها.

أشارت النتائج الى أن خوارزمية التوليد العشوائي لحالات الفحص مع وجود المحدّدات كانت الأفضل من حيث النتائج الخاصة بالتغطية؛ فقد كانت نسبة تغطية المسار ٧٧,٧٨%، في حين بلغت نسبة تغطية الحالة ١٠٠%.

و أخيراً، فقد بينت النتائج التجريبية التي تم الحصول عليها أنّ لغة بيرفكت للمواصفات الرسمية ملائمة للاستخدام في نظام قيادة السيارات و التحكم بها، الذي يعّد من أهم برمجيات أنظمة السلامة الحرجة. كما مكّن ذلك الاستخدام من أن تصبح عملية الكشف عن جميع الحالات المستقبلية أكثر يسراً و سهولة.

Jordanian Journal of Computers and Information Technology (JJCIT), Vol. 1, No. 1, December 2015.

OPTIMIZING AND THINNING PLANAR ARRAY USING CHEBYSHEV DISTRIBUTION AND IMPROVED PARTICLE SWARM OPTIMIZATION

Noor Salem Alshdaifat[1] and Mohammed Hussein Bataineh[2]

Communications Engineering Department, Hijjawi Faculty of Engineering Technology, Yarmouk University, Irbid, Jordan
noor_88m99@yahoo.com[1], mohbat@yu.edu.jo[2]

(Received: 08-Aug.-2015, Revised: 13-Sep.-2015, Accepted: 10-Dec.-2015)

ABSTRACT

In this paper, a new approach to the optimum solution based on the Chebyshev distribution for planar array and an improved particle swarm optimization (IPSO) will be considered. The current excitation of each element is used as the optimization factor with an aim to suppress the side lobe level (SLL) and reduce the half power beam width (HPBW) with prescribed nulls. Chebyshev distribution is used to define IPSO search space. The same array is then thinned to find the best distribution of the active, or on, elements in order to obtain the desired requirements.

KEYWORDS

Planar array, Chebyshev distribution, Improved particle swarm optimization, Side lobe level suppression, Half power beam width.

1. INTRODUCTION

Wireless communication demands for high gain or directional antennas to decrease interference from other applications [1] necessitate a high gain and precise directional antenna to concentrate the energy in the desired direction. The obvious solution to these demandsis to reduce the HPBW of the radiation pattern. This can be achieved by replacing the antenna elements in a certain geometry and improving its performance by proper current and/or phase excitation. Recently, the optimization for solving antenna synthesis has revived with the evolutionary and nature inspired algorithms [2]-[3]. This has vividly improved wireless communication systems by using smart antennas [4]. Smart antennas have the ability to automatically direct the main lobe towards the desired user while directing the nulls in the direction of interference so that side lobes towards other users are minimized. In recent studies, researchers focused on various types of optimization to synthesize different array geometries [5]-[7].

Recent studies for planar array focus on new optimization techniques [8] in order to find their efficiency in finding the optimum solution for an array antenna to achieve the desired goal. Other researchers concentrate on the concept of array thinning. Thinned array means that some of uniformly spaced or periodic array elements are turned on while some of them are turned off where the element positions are fixed. This will lead to reduce the cost while maintaining the same characteristics of the radiation pattern when the filled array of the same size is on.

Planar array with uniform current excitation can be thinned to shape the radiation pattern in order to have a lower SLL and reduced HPBW. It is also possible to place nulls in certain directions. Linear and planar thinned arrays have become of interest to researchers in recent years [9]-[10],

because they can shape the radiation pattern without changing the current excitation. Keizer [11] has used the concept of array thinning and applied it on tapered planar arrays using Fourier transform. The same concept will be used in our treatment of IPSO. The algorithm will first find the optimum current for the desired requirements, then the algorithm will find the best distribution of the active (on) elements to maintain the desired requirements of the filled array with tapered current excitation.

In this paper, a new approach to the optimum solution for planar array based on Chebyshev distribution will be considered. Here, Chebyshev distribution defines IPSO search space as the upper and the lower limit based on the desired SLL. The algorithm seeks optimum excitation for the given objective function to obtain the desired radiation pattern in the new defined search space. This will enable the algorithm to search for the optimum solution and exclude the initial randomness of defining the search space; hence leading to reduce the search time and enhance the obtained results. After finding the optimum current, the algorithm will randomly apply thinning to the optimized array.

2. CHEBYSHEV DISTRIBUTIONS FOR PLANAR ANTENNA ARRAY SYNTHESIS

2.1 Planar Arrays

A planar array gives more degree of freedom to control the radiation pattern. Here, the radiation pattern is more flexible so that a planer array has some advantages over a linear array and encompasses more applications such as remote sensing, tracking radar, search radar and communications, to name just a few.

Planar arrays can be considered as an extension to linear arrays. A planer array consists of *N* elements in the *y*-axis and *M* elements in the *x*-axis spread over a rectangular grid as shown in Figure 1, where it can be seen as an *M* linear array of *N* elements or as an *N* linear array of *M* elements.

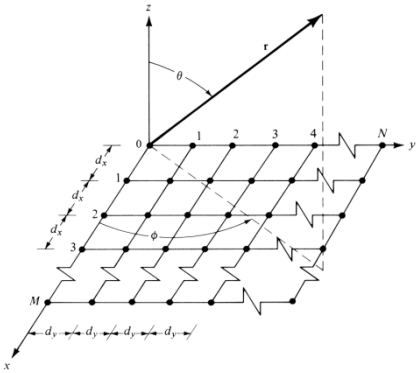

Figure 1. M×N planar array geometry with equal spacing in the *x* and *y* directions [12].

To formulate an equation of the array factor for planar arrays, there are two methods. The first is to use the principle of pattern multiplication; i.e., multiplying the array factor of the *M* linear array at the *x*-axis by the *N* linear array at the *y*-axis, which takes the form [12]:

$$AF = AF_x . AF_y \tag{1}$$

$$AF_x = \sum_{m=0}^{M-1} w_m e^{jm\Psi_x} \tag{1.a}$$

$$AF_y = \sum_{n=0}^{N-1} w_n e^{jn\Psi_y} \tag{1.b}$$

Jordanian Journal of Computers and Information Technology (JJCIT), Vol. 1, No. 1, December 2015.

Here, $\Psi_x = kd_x\hat{a}_x.\hat{a}_r = kd_x \sin\theta\cos\phi + \beta_x$, $\Psi_y = kd_y\hat{a}_y.\hat{a}_r = kd_y \sin\theta\sin\phi + \beta_y$, w_m and w_n is the current excitation of the m^{th} element and the n^{th} element at the *x*-axis and the *y*-axis, respectively, d_x and d_y are the uniform spacing between the elements in the *x*-axis and *y*-axis respectively, β_x and β_y are the phase excitation (relative to the array center) of the m^{th} element and the phase excitation (relative to the array center) of the n^{th} element, respectively.

The other method, that is adopted in this paper, is the same as Eq. (1), but it differs only in considering the mn^{th} current to be independent and not restricted to the value of the multiplication [8]. The array factor of the planar array will be given in the form:

$$AF = \sum_{m=0}^{M-1}\sum_{n=0}^{N-1} w_{mn} e^{jm\Psi_x} e^{jn\Psi_y} \quad (2)$$

In Eq. (2), the variables are increased, increasing the complexity of the optimization process, but at the same time additional control is given over the shape of the radiation pattern.

In order to steer the main beam to (θ_o, ϕ_o) direction, the phase excitations (β_x and β_y) need to be changed to:

$$\beta_x = -kd_x \sin\theta_o \cos\phi_o \quad (3.a)$$

$$\beta_y = -kd_y \sin\theta_o \sin\phi_o \quad (3.b)$$

To simplify the calculation and reduce the time consumed when taking all the azimuth angels into account (approximately 13.48 hours), one can take a single angle ($\phi = 0^{\circ}$) to simplify the radiation pattern of Eq. (2). The approximated far field array factor will be in the form:

$$AF = \sum_{m=0}^{M-1}\sum_{n=0}^{N-1} w_{mn} e^{j(m-1)(kd_x \sin\theta)} \quad (4)$$

The next step in the design process is to formulate the objective function. The fitness function is formulated such that the maximum peaks of the SLL of the obtained array factor are restricted not to exceed a predefined level (ζ). This fitness function may provide the solution to have the desired SLL, but it may affect the desired HPBW, so the difference between the desired beamwidth (BW_d) and the obtained one (BW) is calculated, and it sets nulls at the interference angles θ_n and make them equal to (q); i.e., a desired null depth.

$$\text{Costfunction} = \sum_m (AF(\theta_{msl}) - \zeta)^2 + (BW - BW_d)^2 + \sum_n (AF(\theta_n) - q)^2; \quad (5)$$

where m is the number of the SLL peaks and θ_{msl} represents the angles at these local maxima of the AF, BW_d is calculated using a formula given by [13].

2.2 Chebyshev Distribution

Chebyshev array was first introduced by Dolph [14], then it was examined by other researchers [15]-[16]. Chebyshev array has proven to produce the smallest HPBW for a given side lobe level or the lowest SLL for a given HPBW. Hence, it is usually referred to as an optimal array. The side lobes in Chebyshev array are equal in level. The idea of Chebyshev array is based on the relation between the cosine functions and the Chebyshev polynomials, where a symmetric amplitude excitation is usually assumed. To design a Chebyshev array, one needs the number of array elements and the desired side lobe level. Barbiere [16] analyzes the procedure to find the excitations for Chebyshev array and present a formula to directly calculate them.

3. PARTICLE SWARM OPTIMIZATION AND IMPROVED PARTICLE SWARM OPTIMIZATION

Particle swarm optimization (PSO) [17] is a robust heuristic multi-dimensional global optimization method, which is based on swarm intelligence. PSO starts by randomly distributing the agents within the search space, then evaluating the fitness of each agent using the fitness function, where each particle knows its best value (p_{best}) and each particle knows the best value

so far in the entire group (g_{best}) among all p_{best}. After that, each particle tries to modify its position based on the distance between the current position and p_{best} and the distance between the current position and g_{best}. The velocity and position of each particle (element) are changed according to:

Speed update:

$$v_{in}^{k+1} = wv_{in}^{k} + c_1 r_1^k \left(p_{best_{in}}^{k} - x_{in}^{k}\right) + c_2 r_2^k \left(g_{best_{in}}^{k} - x_{in}^{k}\right); \quad (6)$$

Position update:

$$x_{in}^{k+1} = x_{in}^{k} + v_{in}^{k+1}; \quad (7)$$

where v_{in}^{k} is the speed and x_{in}^{k} is the position of the i^{th} particle in the d^{th} dimension at its k^{th} iteration, the parameter w is a number in the range [0,1] called the "inertia weight", which controls the current speed of the particle depending on its previous speed, r_1^k and r_2^k are two uniformly distributed random numbers in the interval [0,1], w indicates the weight by which the particle's current velocity depends on its previous velocity. It was experimentally found in [17] that if the value of w is linearly damped with iterations, it will converge faster. $p_{best_{in}}^{k}$ and $g_{best_{in}}^{k}$ are the personal best position of the i^{th} particle and the global best position of the swarm, respectively.

The two coefficients c_1 and c_2 represent the relative weights of the personal best position *versus* the global best position, which regulate the length when flying to the most optimal particle of the whole swarm and to the most optimal individual particle, c_1 and c_2 are set to be 2. Figure 2 is a flow chart that illustrates the process of PSO algorithm.

3.1 Improved Particle Swarm Optimization

Improved particle swarm optimization [18] is a modification to the original PSO with the aim to enhance its searching ability. It has the same strong features of PSO, but has a better searching procedure which consequently makes the algorithm converge faster; the only change here is made on how to calculate velocity.

In Eq. (6), r_1 and r_2 are two uniformly distributed random numbers in the interval [0,1] which are independent of each other. There will be a problem in searching for the optimal solution if both of them were large. In this case, the agent will be taken far from the local optimum. If both of them were small, the personal and social experiences are not fully used and the convergence speed of the technique is reduced.

Instead of having two independent random numbers, one random number, say r_1, is used [18]. r_2 in Eq. (6) is set as $(1\text{-}r_1)$. When r_1 is large, $(1\text{-}r_1)$ will be small and *vice versa*. Another random number r_2 is added to have more control of the balance between the local and global search. The new formula to calculate the particle velocity is [18]:

$$v_{in}^{k+1} = r_2^k v_{in}^{k} + (1 - r_2^k) c_1 r_1^k \left(p_{best_{in}}^{k} - x_{in}^{k}\right) + (1 - r_2^k) c_2 (1 - r_1^k) \left(g_{best_{in}}^{k} - x_{in}^{k}\right); \quad (8)$$

where the position is calculated as in Eq. (7). Figure 2 summarizes the steps used in PSO and IPSO algorithms.

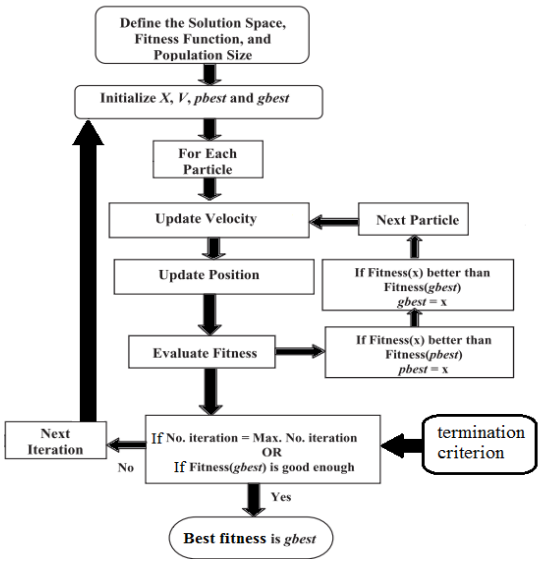

Figure 2. Flow chart of PSO and IPSO algorithm.

4. SIMULATION RESULTS

4.1 Planar Antenna Array Design Using IPSO

In this section, the current for optimizing 10×10 planar array will be demonstrated. The algorithm is implemented using MATLAB. The design parameters are illustrated in Table 1. The search space has changed, the new values are based on the current distribution of Chebyshev planar array [19].

Table 1. IPSO design parameters for a symmetric planar array.

Symbol	*Quantity*	*Value*
N	Number of elements	100
c_1 and c_2	Speeding figure	2
P_{size}	Number of particles	100
$iter_{max}$	Number of iterations	250
X_{space}	Define the search space	[1,64]

Example 1: Planar array with M×N=10×10 elements with the aim to produce a radiation pattern that has a -40 dB SLL and an HPBW of 14.4° with two nulls; one at $(\theta_{n1}, \phi_{n1}) = (30^{\circ}, 0^{\circ})$ and the second one at $(\theta_{n2}, \phi_{n2}) = (-30^{\circ}, 0^{\circ})$ with the maximum radiation pattern directed at $(\theta_d, \phi_d) = (0^{\circ}, 0^{\circ})$. The fitness function of Eq. (5) is the cost function and the array factor of Eq. (4) is used to compute the radiation pattern. The new current values of the elements are illustrated in Table 2.

Table 2. Optimized asymmetric current excitation of 10×10 planar antenna array synthesized using IPSO.

SLL	**Null Angle**	**Null Depth**	**HPBW**	**Directivity**
-40 dB ($\boldsymbol{\phi = 0^{\circ}}$) -26 dB ($\boldsymbol{\phi = 90^{\circ}}$)	$(-30^{\circ}, 0^{\circ})$ $(30^{\circ}, 0^{\circ})$	-80 dB -80 dB	14.9 ($\phi = 0^{\circ}$) 13.7 ($\phi = 90^{\circ}$)	22 dB

Magnitude of current excitation

w_{mn}	$n1$	$n2$	$n3$	$n4$	$n5$	$n6$	$n7$	$n8$	$n9$	$n10$
$m1$	1	3.14	12.34	7.22	7.68	9.73	4.41	14.47	2.82	1
$m2$	1	6.78	5.83	20.07	29.10	26.97	18.07	4.20	4.88	2.60
$m3$	7.02	10.52	20.85	35.11	38.39	30.65	34.17	21.53	11.22	4.17
$m4$	6.18	17.56	29.61	44.78	51.77	55.74	43.75	32.22	15.52	5.98
$m5$	7.20	20.64	36.52	53.37	63.50	63.55	54.05	36.30	18.60	7.39
$m6$	6.58	20.28	37.41	54.48	63.83	63.90	50.32	36.19	15.16	5.43
$m7$	5.11	17.33	29.56	38.44	52.45	54.50	44.10	31.69	16.91	4.69
$m8$	5.73	12.04	22.34	32.99	36.50	37.40	31.57	22.77	10.62	5.75
$m9$	2.38	8.45	4.52	26.47	16.49	20.92	18.42	8.06	4.16	1.18
$m10$	1	4.26	24.68	14.51	28.19	13.32	10.99	3.04	1.02	1

Table 2 shows the results of current excitation after the array has been optimized using IPSO, where it can be seen that the current magnitude gets higher as we move from the edges to the center.

Figure 3 shows the resulting radiation pattern after optimizing the current excitation at $\phi = 0^{\circ}$, while Figure 4 shows the resulting radiation pattern at $\phi = 90^{\circ}$. Since the current being optimized is asymmetric, the radiation pattern of these two planes ($\phi = 0^{\circ}, \phi = 90^{\circ}$) may and may not be identical. In this example, they are not.

It can be seen from Figure 3 that the radiation pattern at $\phi = 0^{\circ}$ achieves the desired SLL of -40 dB and places the nulls at the desired angle with a very good depth of -80 dB, where the HPBW achieved is 14.9° which is 0.4° higher than desired. In the other plane in Figure 4, the maximum SLL near the main beam is -31 dB, while the SLL at the edges is about -26.2 dB. This is considered a good result, since the fitness function does not evaluate the fitness of the algorithm at this plane, it yields an HPBW of 13.7° which is better than desired by 0.8°.

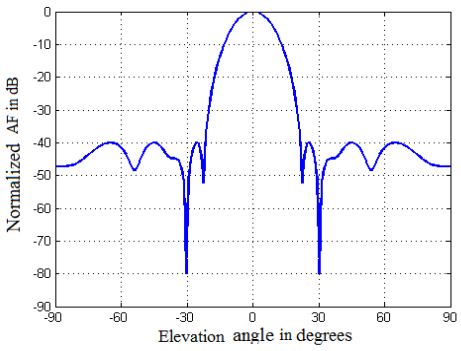

Figure 3. Synthesized radiation pattern of a 10×10 planar array antenna using IPSO for asymmetric current excitation at $\phi = 0^{\circ}$.

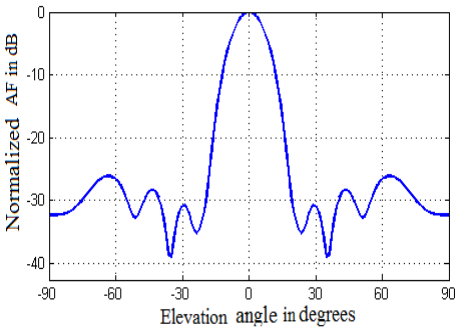

Figure 4. Synthesized radiation pattern of a 10×10 planar array antenna using IPSO for asymmetric current excitation at $\phi = 90^{\circ}$.

The average fitness (mean value of p_{best} in red line) and the fitness (g_{best} in blue line) of each iteration for IPSO are illustrated in Figure 5, which shows that the IPSO algorithm reaches its steady state and converges after 60 iterations.

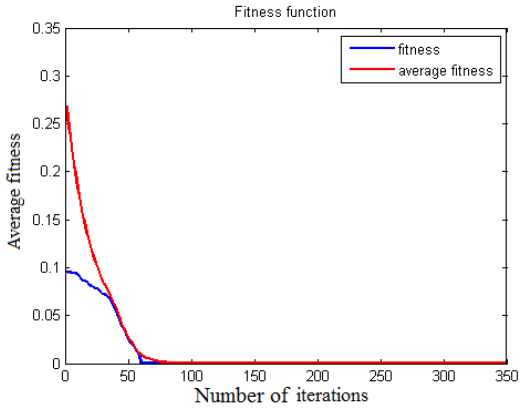

Figure 5. The average fitness of the global best value for each iteration using IPSO.

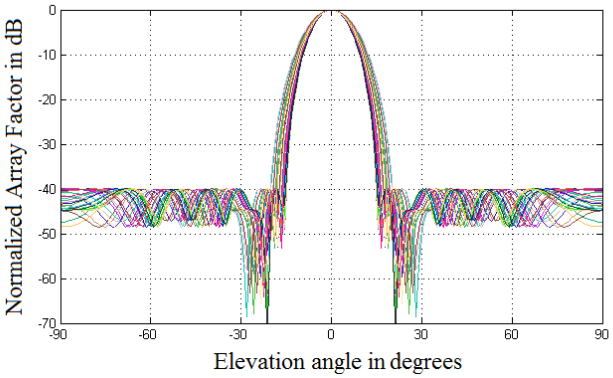

Figure 6. 2-D normalized AF of a 10×10 planar array antenna using IPSO for asymmetric current excitation at different angles ϕ.

Figure 6 exhibits the 2-D normalized radiation pattern of the optimized planar array at different angles ϕ, where it is obvious that the SLL being suppressed as desired.

4.2 Thinned Planar Array Design

The aim here is to find the best distribution of the active (on) elements to maintain the desired requirements of the filled array in example 1 with tapered current excitation. Here, the algorithm randomly turns on and off the elements, then evaluates the fitness of the resulting array factor. The goal is to maintain the same array factor characteristics of the filled array with tapered current.

Example 2: A 10×10 planar array with optimized current excitation using IPSO and uniform spacing with d=0.5λ is considered to be thinned. The current values are in Table 2 and the desired array factor is shown in Figure 3; a maximum SLL of -40 dB with an HPBW of 14.9° at $(\phi = 0^{\circ})$, a maximum SLL of -26.2 dB with an HPBW of 13.7° at $(\phi = 90^{\circ})$ and two nulls at $(\theta, \phi) = (-30^{\circ}, 0^{\circ}), (\theta, \phi) = (30^{\circ}, 0^{\circ})$. The fitness function of Eq. (5) is the cost function, and the array factor of Eq. (4) is used to compute the radiation pattern.

The new distribution of the active elements in the 10×10 thinned planar array is illustrated in Table 3. Figure 7 shows the resulting radiation pattern of the thinned array at $\phi = 0^{\circ}$, while Figure 8 shows the resulting radiation pattern at $\phi = 90^{\circ}$.

After thinning, 10 elements have been turned off, and the resulting radiation pattern has minor changes far from the main lobe, which is considered a very good result. In this paper, thinning is

limited to only 10% of the array elements, because the thinned array elements have a different (tapered) current excitation to achieve the desired array factor. Therefore, eliminating any elements will have greater impact on the array factor than the usual thinning which is applied to uniform current arrays. However, it is shown that when using uniform current distribution, 42% of the elements can be turned off [4].

In the given example, turning off more than 10 elements will cause undesired characteristics in the resulting array factor, such as higher SLL or higher HPBW. So, the maximum number of elements that can be turned off while maintaining the desired array factor is 10 elements.

Table 3. Thinned array of a 10×10 planar array with optimized current excitation synthesized using IPSO.

SLL			**Null Angle**		**Null Depth**		**HPBW**		**Directivity**
-35 dB ($\phi = 0^\circ$) -27 dB ($\phi = 90^\circ$)			$(-30^\circ, 0^\circ)$ $(30^\circ, 0^\circ)$		-64 dB -64 dB		14.9° ($\phi = 0^\circ$) 14° ($\phi = 90^\circ$)		21.9 dB
Magnitude of current excitation									
w_{mn}	***n1***	***n2***	***n3***	***n4***	***n5***	***n6***	***n7***	***n8***	***n9***	***n10***
m1	1	3.14	12.34	7.22	7.68	9.73	4.41	0	2.82	1
m2	0	0	5.83	20.07	29.10	26.97	18.07	4.20	0	2.60
m3	7.02	10.52	20.85	35.11	38.39	30.65	0	21.53	11.22	4.17
m4	0	17.56	29.61	44.78	51.77	55.74	43.75	32.22	15.52	5.98
m5	7.20	20.64	36.52	53.37	63.50	63.55	54.05	36.30	18.60	7.39
m6	6.58	20.28	37.41	54.48	63.83	63.90	50.32	36.19	15.16	5.43
m7	5.11	17.33	29.56	38.44	52.45	54.50	44.10	31.69	16.91	4.69
m8	0	12.04	22.34	32.99	36.50	37.40	31.57	22.77	10.62	5.75
m9	2.38	8.45	4.52	26.47	0	20.92	18.42	8.06	4.16	1.18
m10	1	4.26	24.68	14.51	28.19	0	10.99	0	1.02	1

It can be seen from Figure 7 that the radiation pattern at $\phi = 0^\circ$ achieves the desired SLL of -40 dB near the main lobe, where at the edges the SLL increases to -35 dB, placing the nulls at the desired angles with a good depth of -64 dB, where the HPBW achieved is as desired. In the other plane as shown in Figure 8, the maximum SLL near the main beam is -32 dB, while the SLL at the edges is about -27 dB which is better than desired. This is considered a good result, since the fitness function does not evaluate the fitness of the algorithm at this plane.

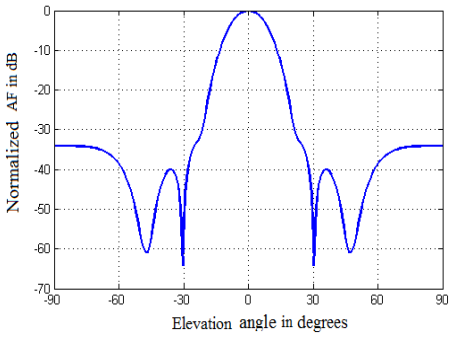

Figure 7. Synthesized radiation pattern of a 10×10 tapered tinned planar array antenna using IPSO at $\phi = 0^\circ$.

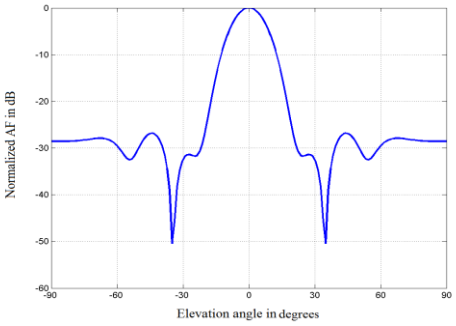

Figure 8. Synthesized radiation pattern of a 10×10 tapered thinned planar array antenna using IPSO at $\phi = 90^\circ$.

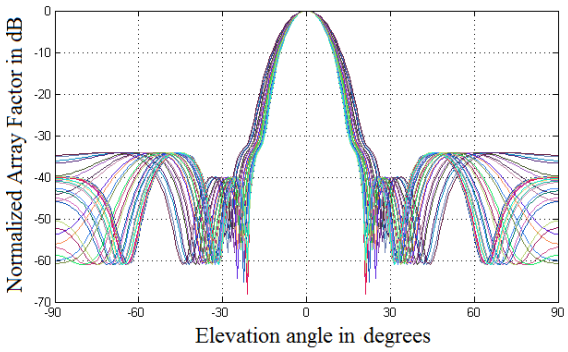

Figure 9. 2-D normalized AF of a 10×10 tapered thinned planar array antenna using IPSO for asymmetric current excitation at different angles ϕ.

Figure 9 exhibits the 2-D normalized radiation pattern of the optimized thinned planar array at different angles ϕ, it is obvious that the SLL are suppressed as desired.

5. CONCLUSIONS

In this paper, IPSO has been successfully used to optimize a planar array antenna. The efficiency of the algorithm especially in multi-objective optimization has been shown. By adjusting the current excitation, the algorithm was able to find the optimum value for the desired properties with fast convergence. The designed array has achieved the desired requirements for the filled array. Moreover, these requirements have been maintained for the thinned planar array. Thinning was limited to only 10% of the array elements, because the thinned array elements have different (tapered) current excitation to achieve the desired array factor. Therefore, eliminating any element will have greater impact on the array factor than usual thinning which is applied to uniform current arrays.

As the examples have been illustrated, turning off more than 10 elements will cause undesired characteristics in the resulting array factor, such as higher SLL or higher HPBW. So, the maximum number of elements that can be turned off while maintaining the desired array factor amount to 10 elements.

REFERENCES

[1] R. Gaokar and A. Cheeran, "Performance Analysis of Beamforming Algorithms," IJECT, vol. 2, pp. 43-48, 2011.

[2] S. Chatterjee, S. Chatterjee and D. Poddar, "Synthesis of Linear Array Using Taylor Distribution and Particle Swarm Optimization," International Journal of Electronics, v. 102, issue 3, pp. 514-528, 2014.

[3] C. H. Hsu, C. H. Chen, W. J. Shyr, K. H. Kuo, Y. C. Chung and T. C. Lin, "Optimizing Beam Pattern of Linear Adaptive Phase Array Antenna Based on Particle Swarm Optimization," IEEE 4th International Conference on Genetic and Evolutionary Computing (ICGEC), pp: 586-589, Shenzhen, China, 13-15 Dec. 2010.

[4] N. Alshdaifat, Design and Optimization of Beamforming Antenna Array, M. Sc. Thesis, Dept. Comm. Eng., Yarmouk Univ., Irbid, Jordan, 2015.

[5] G. Ram, D. Mandal, R. Kar and S. P. Ghosal, "Optimized Hyper Beamforming of Linear Antenna Arrays Using Cat Swarm Optimization," Scientific World Journal, 22 Jul. 2013.

[6] G. Ram, D. Mandal, R. Kar and S. P. Ghosal, "Design of Non-Uniform Circular Antenna Arrays Using Firefly Algorithm for Side Lobe Level Reduction," International Journal of Electrical, Electronic Science and Engineering, vol. 8, no. 1, pp. 40-45, 2014.

[7] S. Jayaprakasam, S. Rahim, C. Leow and K. Ramanathan, "Genetic Algorithm Based Weight Optimization for Minimizing Sidelobes in Distributed Random Array Beamforming," International Conference on Parallel and Distributed Systems (ICPADS), pp. 623-627, 2013.

[8] A. Charan, N. K. Manasa and N. V. Sarma, "Uniformly Spaced Planar Antenna Array Optimization Using Cuckoo Search Algorithm," International Journal of Computer Science and Information Technology, vol. 6, no. 4, pp. 157–167, 2014.

[9] Li Zhang, Y-C. Jiao, B. Chen and H. Li, "Orthogonal Genetic Algorithm for Planar Thinned Array Designs," International Journal of Antennas and Propagation, Vol. 2012 , 7 pages, 2012.

[10] P. Brahma, P. Nandi, A. Senapati and J. S. Roy, "Reduction of Side Lobe Level of Thinned Phased Array Antenna Using Genetic Algorithm," International Journal of Computer Applications, vol. 112, no. 8, pp. 13-15, 2015.

[11] W. P. M. N. Keizer, "Synthesis of Thinned Planar Circular and Square Arrays Using Density Tapering," IEEE Transactions on Antennas and Propagation, vol. 62, no. 4, pp. 1555-1563, 2014.

[12] C. Balanis, Antenna Theory-Analysis and Design, John Wiley and Sons, New York, 2005.

[13] A. Safaai-Jazi, "A New Formulation for the Design of Chebyshev Arrays," IEEE Transactions on Antennas and Propagation, vol. 42, no. 3, pp. 439-443, 1994.

[14] C. L. Dolph, "A Current Distribution for Broadside Arrays which Optimizes the Relationship Between Beam Width and Side-Lobe Level," Proceedings of the IRE , vol. 34, no. 6, pp. 335-348, 1946.

[15] C. J. Drane, Jr., "Useful Approximations for the Directivity and Beamwidth of Large Scanning Dolph-Chebyshev Arrays," Proceedings of the IEEE, vol. 56, no. 11, pp. 1779–1787, Nov. 1968.

[16] D. Barbiere, "A Method for Calculating the Current Distribution of Tschebyscheff Arrays," Proceedings of the IRE, pp. 78–82, 1952.

[17] J. Robinson and Y. Rahmat-Samii, "Particle Swarm Optimization in Electromagnetics", Proceeding of the IEEE Transactions on Antennas and Propagation, vol. 52, no. 2, pp. 397-407, 2004.

[18] S. Ho, S. Yang, G. Ni, E. Lo and H. Wong, "A Particle Swarm Optimization-Based Method for Multiobjective Design Optimizations," Proc. Of the IEEE Transactions on Magnetics, vol. 41, no. 5, pp. 1756-1759, 2005

[19] F. I. Tseng and D. K. Cheng, "Optimum Scannable Planar Arrays with an Invariant Sidelobe Level," Proceedings of the IEEE , vol. 56, no. 11, pp. 1771-1778, 1968.

ملخص البحث:

تـمّ فـي هـذا البحـث، إتّبـاع نهـج جديـد للوصـول إلـى الحـلّ الأمثـل للمصـفوفة الهوائيـة السـطحية باسـتخدام توزيـع Chebyshev و تحسـين الاسـتفادة المثلـى لسـرب الجسـيمات. اسـتخدم تيـار الإثـارة لكـل عنصـر عامـل اسـتفادة مثلـى بهـدف تقليـل مسـتوى الإشـعاع مـن عـرض شـعاع منتصـف القـدرة مـع الكـبح المسـبق للإشـعاع فـي اتجاهـات معينـة. و الجـدير بالإشـارة أن توزيـع Chebyshev يسـتخدم لتحديـد فضـاء البحـث لسـرب الجسـيمات المحسّـن. و قـد تـم ترقيـق المصـفوفة نفسـها لإيجـاد أفضـل توزيـع للعناصـر النشـطة، أو العاملـة؛ مـن أجـل الحصول على المتطلبات المطلوبة.

Jordanian Journal of Computers and Information Technology (JJCIT), Vol. 1, No. 1, December 2015.

A HYBRID APPROACH FOR INDEXING AND SEARCHING THE HOLY QURAN

Monther Tarawneh[1] and Emad Al-Shawakfa[2]

Department of Computer Information Systems, Yarmouk University, Irbid, Jordan.
monther.t@yu.edu.jo[1], shawakfa@yu.edu.jo[2]

(Received: 27-Oct.-2015, Revised: 19-Nov.-2015, Accepted: 21-Dec.-2015)

ABSTRACT

Searching and retrieving information from the Holy Quran have recently received special attention by Muslim and Arab researchers. Many applications and websites offered to perform search through the Quran using keywords, semantic search or even both. Arabic; as the language of the Quran, is having a complex structure and thus the searching process of Arabic scripts is rather more difficult than English. In this paper, we propose a hybrid approach; using a combination of syntactic (keyword) and word semantics, to search through the Quran text. The Quran text was pre-processed and represented in a XML format. A system was implemented using Python, where the concept of regular expressions is used to test the approach with a Graphical User Interface used to manipulate user requests. Good and promising results from the approach were obtained.

KEYWORDS

Arabic NLP, IR, Quran, Keyword search, Semantic search.

1. INTRODUCTION

Information has mostly been stored in digital formats, so that it can be accessed from anywhere at any time [1]. In such a world, the information storage and retrieval has become one of the top research areas, particularly over the period of the past few years [2]. Despite a number of research approaches conducted to customize and improve information retrieval techniques, there is still room for improvements in these techniques [3]. The major aim is to make query processing as natural as possible, so that the users can enter a query into the search engine in any language and the system should be able to respond and retrieve the information within the minimum possible delay.

An information retrieval system should be able to serve the users of all levels of expertise; occasional or experts [4]. In return of a user's query, a Search Engine explores all the possible reachable resources [5] considering entered keywords. The high quality retrieval algorithms within a search engine should, however, be able to narrow down the scope of the retrieved documents and return only those documents which are closely related to the query; a problem that becomes more serious when it comes to languages other than English. This is because most of the searching algorithms for retrieving information were developed to serve Latin-based languages such as English. Therefore, applying these algorithms to other languages poses a clear challenge, due to the fundamental underlying differences in the nature of these languages. So, the performance of any algorithm or application is based on the nature and complexity of the language [6], mainly on the characteristics of the language itself.

Islam is one of the fastest growing religions in the world, where Muslims receive their inspirations and beliefs from two major sources: the Quran; the word of the Almighty Allah (God) and the Hadith; the sayings of the prophet Mohammad (peace be upon him). Nowadays,

both Quran and Hadith can be stored digitally and thus offer a better and efficient way to process them using text analytic techniques. These techniques have the potential to summarize, search, analyze and effectively present different concepts from these resources. There is a need for building intelligent tools that could help Quran readers to search for most relevant and effective results related to a given concept.

In this paper, an initial effort was made to introduce and build an approach that can help in processing and understanding the Quran text. This approach can be further used in other works and could be extended to serve other search processes for Islamic knowledge such as searching the Hadith, Fiqh and even through Islamic History.

2. RELATED WORK

There has been some work on Arabic Natural Language Processing related to the field of search and retrieval of Information from the Holy Quran. Most of the implemented Quran information retrieval systems were based on keyword search [7]. Such implemented systems can be further improved and extended to give more close and accurate results, which has formulated the major objective behind this research.

Many websites and/or online search engines or tools were established to deal with searching through the Quran. Some of these were SearchTruth, Allah.pk, the Islamic Search tools, IntoIslam, … and many others.

The SearchTruth system [8], for instance, searches on the basis of keyword substring matching. No exact word matching is performed, but rather searches are performed for a word that is part of any other word in the Quran. For instance, if you search for the word "حم", all verses that contain a word with the substring "حم" will come up as part of the result page such as "رحم", "حم" , "لحم", … etc.

The guided way technology [9], however, offers searching the Quran using different languages. It searches for exact words in the Quran; thus eliminating all other possibilities of word forms, which may lead to less related results. Chatbot [10] tries to find the most considerable words in the query and performs keyword based search to find the relevant verse in the Quran.

The search engine Islamic Search tools [11] performs search using Google web search Engine to find an exact word match (or partial) based on some Islamic related keywords, such as "Quran", "Islam" and other words. Allah.pk [12] is a search engine that looks for an exact keyword match and provides results in both English translation and Arabic. IslamiCity [13] gives results based on the exact string matching in the translation of the Quran. It gives the Arabic verse, its translation and the phonetic verse. IntoIslam [14] is similar to the search engine Islamic Search Tools and searches using the Google API. IntoIslam provides searching in the form of audio, video, translation or text files.

In most of the used approaches to Arabic IR, light stemming is performed [15]-[16]. To search for Arabic words, three methods are usually applied: full-word-based, stem-based and word synonyms-based. The above mentioned tools search on the basis of keywords by different translations using the syntactic approach. However, a semantic search approach is, on the other hand, beyond the syntactic level of matching keywords [17]-[18]. For example, a search for the word "جنة" using the syntactic approach would give only those verses that has the word "جنة" itself in them. However, using the semantic (*or conceptual*) approach, then using the synonyms of the word "جنة" we could find the word to be reflected in other words such as "فردوس", "عدن" or "دار", thus leading to more verses that are related to the concept of "جنة". Unfortunately, the conceptual search approach has not been fully explored and need more attention.

Many of the available hybrid searches today [19] can be used to combine keyword search and ontology-based search. However, such approaches still force the user to choose either keyword-based or ontology-based search without the ability to merge them. A hybrid approach for

extracting information based on keyword and semantic search was proposed by [20], but deals mainly with the English language and uses Resource Description Framework (RDF) for representing data and SPARQL for querying data.

The concept of XML has been introduced widely to be used in fulfilling a semantic search using semantic rules [21]-[22]. Using this concept, all chapters of the Holy Quran could be easily represented in an XML document, thus making it easier to represent, exchange and process data on the web or within any system that supports the usage and manipulation of XML documents. In addition, a structured database can be easily manipulated when stored in XML format. An XML parser is available in most programming languages of today such as the Document Object Module (DOM) parser built in Java.

The concept of regular expressions (regex) was initially introduced in the Unix operating system and then was further adopted to be used in programming languages and is not related to a specific language by itself. So, regex could be found in languages like C++, C#, Python, … etc. to help in searching for text using patterns [23]. By combining XML parsers with regular expressions, we can build a great searching tool, such as that of [24].

With the existence of different approaches to deal with concepts in the Holy Quran, a unified approach was suggested by [27]. In their proposed approach, the authors have started to identify different formats to map different linguistic annotations into SketchEngine format. According to the authors, their approach can be easily reused to unify the alternative concept tagsets; thus making it easier to provide an accessible Quran resource for linguistic research.

A bilingual (Arabic/English) web-based search tool for searching for around 1100 concepts and/or topics of the Holy Quran was introduced by [28]. In this research, the authors used the Mushaf Al Tajweed from which semantic conceptual information were annotated to each verse. To search for any concept, the user navigates through the ontology tree to the requested concept, from which he/she can obtain a list of tagged verses.

A survey on different projects dealing with searching and Information Extraction from the Holy Quran was studied by [29]. In their study, 11 different projects were studied using an 8-criteria comparison approach for projects that were using ontologies as a means of representation and encapsulation of the knowledge in the Holy Quran. According to the authors, an authentic framework, suitable for ontology applications, was used for the purposes of comparison. Different shortcomings of existing projects were mentioned.

A cloud-based integrated Quran portal was introduced in the work of [30]. In their work, the authors have used the Drupal platform technology to build the portal which can be used to search the Qur'an in more than one language. According to the authors, their work can be reused through a set of APIs accessible through the cloud.

A very good survey of existing ontology projects applied to the Holy Quran was made by [31]. In their paper, the authors have surveyed 12 different projects using a 9-criteria comparison process and found out that most of the existing ontologies are incomplete focusing on some specific domains each with no agreement on the type of formats, technologies to use and how to verify their approaches.

3. METHODOLOGY

Following is the methodology that was used to conduct this research, including data collection, pre-processing and the methods used for storage, searching and ranking of the result.

3.1 Data Collection

The text of the Holy Quran was downloaded from [21] in the format of an XML file with fully vocalized text. The file has only attributes for Chapter number, Verse Number and Verse vocalized Text. This website represents a Quranic project that was launched in early 2007 with a mission of producing a standard Quran text that could serve as a reliable source to be used in different Quran related studies.

As part of the research effort, we had to build the full corpora and add to the XML file other attributes and values that refer to the non-vocalized version of the verses, translation of each verse into English, list of synonyms for Quran words as per the context and the explanation (tafsir) of the Quran words and verses. The translation of the meanings of the Quran words was also added from [25], the explanation was added by authors from [26] and based on the word context and Quranic commentaries on each verse from the tafsir in [26] and the list of synonyms was manually added to the attributes of the XML file. To produce the non-vocalized version of the Holy Quran, a simple program was written to strip the verses' words from diacritic symbols. This effort, which took quite some time, has resulted in the final Quran text database that could be used for the purposes of this, as well as other, research on the Holy Quran.

3.2 Regular Expressions

A Regular Expression is a sequence of characters that define a search pattern using some special characters like (^…, […], $, *…) that can be used to help in searching for text. Regular expressions are found in several search engines, search and replace dialogs of several word processors and text editors. Many programming languages provide regular expression capabilities, some are built-in, such as Perl, JavaScript, Ruby, AWK and TCL, while others offers regular expressions via a standard library, like the .NET languages, Java, Python and C++. Using a regular expression to search for a word that starts at the beginning of a string we use the caret (^), where if the search was for a word that is located at the end of a string, we use the dollar sign ($). For instance, to search for any string that starts with the word "hello", we use the pattern: ^hello; which could produce strings like "hello world", "hello there", … etc., where a search like "world$" would give resulting strings like "hello world", "in the world", … etc.

Patterns are constructed to search through the Quran or specific verses. The search is extended to search using the synonyms of the words to reach meaning levels of words; for example, if a query contains the word "جنة", one may get a result that contains synonym words of "جنة" like ['فردوس', 'نعيم', 'يمين']. Patterns are built based on regular expression rules. An example of a pattern could be given as [20]:

^([a-zA-Z0-9._-])+@([a-zA-Z0-9.-])+\.([a-zA-Z.]){2,5}$

which is mainly used to match with texts that represent email addresses of the form email_address@organization.toplvl

In this research, we have built a set of patterns based on regular expressions to help in simplifying the search process of Quranic text. We used the Python programming language that has a module which provides regular expression matching operations similar to those found in Perl with powerful functions to conduct matching, replacing, filtering and validating of text operations. Having in mind the right to left property of the Arabic language, the following is an example of a Regular Expression Pattern to search for the word "الله" with its all variations in the Quran like "اللهم", "والله", "تالله", … etc.

(ء|ا|ا|و|ف|ل|ب|ت|ي) الله (م|$)

3.3 Holy Quran Data Set

In this research, we have used the concept of XML to represent the different chapters of the Holy Quran. The 114 chapters (Sura) of the Quran are grouped by the tag <SURA> and ended with the tag </SURA>. Each chapter has a number of verses (Aya) which are represented by the tag <AYA> and ended with </AYA>. Chapter tags has a number of attributes: the kind of the chapter; either a value of "مكية" or "مدنية", an index; holding the order number of the Chapter in Quran, the name of the Chapter, the total number of words in each chapter and the part (Juz'o) number. The AYA tag has an attribute "index" which holds the verse number in the Chapter and the Hizb. AYA has subtag(s) named "word", which stores values related to the word such as its English translation, the explanation (Tafseer) of the word and any existing Synonyms; words in the Quran that have the same meaning, to serve for semantic search.

The XML document of the Quran is stored in a file that is read by the Dom parser. DOM parses the file and builds a tree structure of the XML document called Document Object Model (DOM) tree. DOM3 is a standard for creating and manipulating in memory representation of XML content. Figure 1 gives a sample XML representation of Chapter 108 (Al-Kawthar).

Figure 1. XML representation of Chapter 108 (*Al-Kawther*).

The size of the Quran text is fixed and hence, the complete tree of the Quran is built from the XML document representation as shown in Figure 1. A user may be interested in finding additional relevant information from the search; this includes details about the Chapter, Part, page number, explanation and any other related information; something that can be easily determined from the built tree.

3.4 Searching the Quranic Text

The Quran in its original form has the text fully vocalized; with diacritics on different characters. To search through a fully vocalized text is a tedious process and thus, a non-vocalized version was inserted within the XML document. To search for a given string in the Holy Quran, a system was built supported with a graphical user interface with two inputs: the string to search for and the search region style, which can be either the whole Quran text or a specific Chapter.

A Tokenization process is performed on the string being searched and then stored into an array of Tokens. If the "Chapter" search style was chosen, the given Chapter is then selected and the search is performed in that specific chapter; otherwise, the search will cover all chapters of the Holy Quran. Initially, the search starts by storing the synonyms for every word in the Quran into an array of synonyms. Then, using regular expressions, a word match of every word in the query with the synonyms array for every verse is performed. If a match is found, the index of the verse in a search index array is stored. Once the search is done, the index array is sorted and

the term weight representing the count, or the number of times each index in the array has occurred, is calculated. The verse with the highest term weight is chosen as the most relevant verse to the query. The main purpose behind searching a word by word is to consider the different sequences of words and then apply words conceptual search to improve the efficiency of the search. The algorithm used for our approach to build Al-Baheth Searcher is given in Figure 2.

1. *Input the user query to search for.*
2. *Perform Tokenization of query words.*
3. *Check for the chosen search region,*
   If (Chapter Search) then
   Get synonyms of Chapter words from the XML Document
   Else
   Get Synonyms of the Whole Quran from the XML Document
   End if
4. *For each Token in the query perform the following:*
   a. *Word match between the token and the Synonym array.*
   b. *If a match is found then*
   Store the chapter and verse indexes of the matching synonym.
5. *Once search is done, sort the found index array*
6. *Perform a match of the chapter index with the top sort from the Quran document.*
7. *Display the Verse that matches the index of the searched Token.*

Figure 2. Algorithm used for searching the Quran in Al-Baheth.

Of course, before we could do any search, the Holy Quran text was pre-processed to build the XML document, and this was performed only once. The pre-processing involved removing diacritic symbols to obtain the non-vocalized version of the Quran and applying light stemming on the Quran words to obtain different word forms as part of the Synonyms. Additional synonyms were added to fill the different values of the XML document attributes. While Figure 3 shows the logical flow of the methodology, Figure 4 shows the GUI interface of the built system.

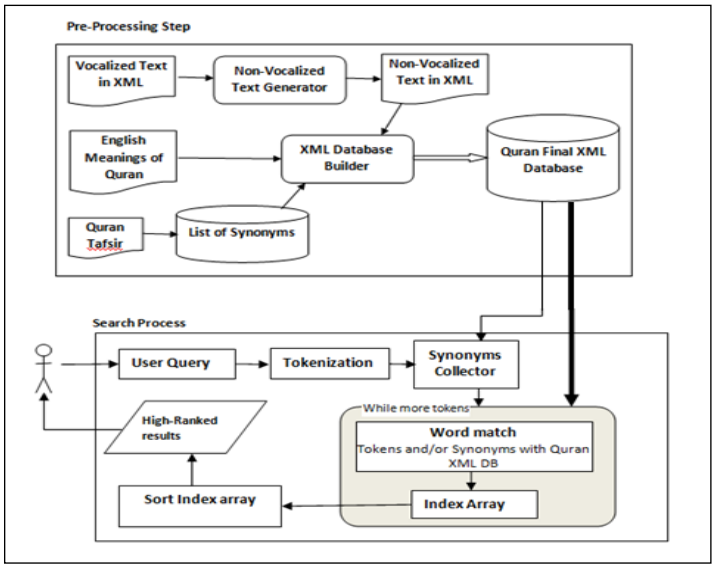

Figure 3. Logical flow of methodology.

Figure 4. Graphical user interface of Al-Baheth searcher of Quran text.

4. EXPERIMENTAL RESULTS

In this research, and for comparison purposes, we have conducted a thorough search with different systems that are known to be used to retrieve text from the Holy Quran and compared their results with the results obtained from our built system; Al-Baheth. Table 1 gives such comparison.

Looking at the results obtained by our approach, in comparison with others, we can say that our approach resulted in obtaining excellent results. For instance, when retrieving the verses that contain the word "الله", the total number of occurrences in the Holy Quran is 2707 and Al-Baheth found 2697 of them with a recall accuracy of 99.6%. Similarly, a recall accuracy of 100% was obtained for the word "الشهر", a 93.2% for the word "الملائكة", a 89.7% for the word "الشياطين", a 98.3% for the word "الدنيا" and a 96.5% recall accuracy for the word "الآخرة".

Table 1. A Comparison of retrieved words between Al-Baheth and other systems.

Al-Baheth	IntoIslam	برنامج القران الكريم جامعة الملك سعود	إحصاء القران الكريم، الإصدار ٣	SearchTruth	Guidedways	Allah.Pk	العدد الفعلي	
2697	0	1745	2557	1746	6212	0	2707	الله
12	0	5	6	7	6212	0	12	الشهر
82	0	53	0	53	6212	0	88	الملائكة
79	0	14	0	17	6212	0	88	الشياطين
113	0	111	115	111	6212	0	115	الدنيا
111	0	110	112	115	6212	0	115	الآخرة

From the above results, we can notice that both Allah.pk and IntoIslam did not retrieve any words. The main reason for that is the fact that they are not suitable for searching the Holy Quran in Arabic. Furthermore, "Guidedways" is not suitable as well to search the Holy Quran in Arabic, and that is why the total number of verses in the Quran instead was retrieved as the result. However, when performing search on Guidedways in English, it has outperformed Allah.pk engine which has the capability to search in English.

When searching the Holy Quran using Al-Baheth, both semantic and syntactic information of the words in the query are being used for the purposes of the search using the concept of regular expression patterns. This approach has enhanced the probability of finding our answers via

searching the non-vocalized attribute of each verse combined with the list of synonyms that might be attached to the non-vocalized version of the words of the verse, which has resulted in obtaining better results than other compared approaches.

5. CONCLUSION AND FUTURE RESEARCH

Despite the number of research approaches that have been taken to customize and improve the information retrieval techniques, especially when dealing with Arabic language, there is still room for improvement to these techniques. In this research, we proposed and implemented a hybrid approach; a combination of syntactic- and semantic-based approach to index and search through the Holy Quran. The proposed algorithm efficiently identifies the required part from the Holy Quran that best matches a user's query. We used XML to index the Holy Quran text in a specific structure, which has proven to be an efficient way of representation. The concept of regular expressions was helpful in identifying the requested words because of the flexibility it offers. Results of this work have shown the efficient performance of the proposed algorithm in the retrieval of information from the Quran text. According to the authors' knowledge, no work at this level has been completed for the Arabic language, which could provide the user with the searching capabilities at the level of words. This could refer our approach as the first of its kind on Arabic.

Due to the obtained good results of this approach, and as a future research, it would be helpful to use the approach to search for other topics and concepts in different parts of the Holy Quran. Using this approach, we are planning to conduct a future research for extracting information from different sacred documents like Hadith, Fiqh and even other Islamic historical documents.

REFERENCES

[1] O. Alonso, J. Strötgen, R. A. Baeza-Yates and M. Gertz, "Temporal Information Retrieval: Challenges and Opportunities," TWAW 11, pp. 1-8, 2011.

[2] N. Mitton, S. Papavassiliou, A. Puliafito and K. S. Trivedi, "Combining Cloud and Sensors in a Smart City Environment," EURASIP Journal on Wireless Communications and Networking, pp. 1-10, 2012.

[3] W. Hu, N. Xie, L. Li, X. Zeng and S. Maybank, "A Survey on Visual Content-Based Video Indexing and Retrieval Systems," IEEE Transactions on Man and Cybernetics, Part C: Applications and Reviews, vol. 41, no. 6, pp. 797-819, 2011.

[4] Smirnova and K. Balog, "A User-Oriented Model for Expert Finding," Advances in Information Retrieval, Springer, pp. 580-592, 2011.

[5] T. Sari and A. Kefali, "A Search Engine for Arabic Documents," Colloque International Francophone sur l'Ecrit et le Document, Groupe de Recherche en Communication Ecrite, France, Oct. 2008.

[6] A. El Salam Al Hajjar, M. Hajjar and K. Zreik, "A System for Evaluation of Arabic Root Extraction Methods," Proc. on IEEE 5th International Conference on Internet and Web Applications and Services (ICIW), pp. 506 - 512, Barcelona, Spain, 9-15 May 2010.

[7] S. A. Raza, M. Rehan, A. Farooq, S. M. Ahsan and M. S. Khan, "An Essential Framework for Concept-Based Evolutionary Quranic Search Engine (CEQSE)," Science International, vol. 26, no. 1, 2014.

[8] Search Truth, "Online Quran and Hadith Search Web Portal," last accessed September 1st, 2015 from: www.searchtruth.com.

[9] Guided Ways Technologies, "Online Quran and Hadith Search Web Portal," last accessed July 30th, 2015 from: http://www.guidedways.com/search.php.

[10] B. Abu Shawar and E. Atwell, "An Arabic Chatbot Giving Answers from the Qur'an," Proc. TALN04: XI Conference sur le Traitement Automatique des Langues Naturelles, vol. 2, pp. 197-202, 2004.

[11] IslamicSearch.com, "Islamic Search Powered by Google," last accessed July 12th, 2015 from: http://IslamicSearch.com.

[12] Allah.pk, "The Multilingual Quran and Hadith Search Engine," last accessed August 25th, 2015 from: http://Allah.pk.

[13] IslamiCity.com, "Islam and the Global Muslim eCommunity," last accessed on August 15th, 2015 from: www.quran4theworld.com.

[14] IntoIslam.com, "Islamic Search Engine," last accessed June 10th, 2015 from: http://IntoIslam.com.

[15] K. Darwish and D. W. Oard, "CLIR Experiments at Maryland for TREC-2002: Evidence Combination for Arabic-English Retrieval," DTIC Document, issue LAMP-TR-101, Maryland Univ. College Park Inst. for Advanced Computer Studies, Feb. 2003.

[16] L. S. Larkey and M. E. Connell, "Arabic Information Retrieval at UMass in TREC-10," DTIC Document, Massachusetts Univ. Amherst Center for Intelligent Information Retrieval, 2006.

[17] C. Rocha, D. Schwabe and M. P. Aragao, "A Hybrid Approach for Searching in the Semantic Web," Proc. of the 13th International Conference on World Wide Web, pp. 374-383, New York, NY, USA, 17 – 22 May 2004.

[18] R. Bhagdev, S. Chapman, F. Ciravegna, V. Lanfranchi and D. Petrelli, "Hybrid Search: Effectively Combining Keywords and Semantic Searches," Proc. of the ESWC, Springer, Berlin, Heidelberg, pp. 554-568, 2008.

[19] A. Kiryakov, B. Popov, I. Terziev, D. Manov and D. Ognyanoff, "Semantic Annotation, Indexing, and Retrieval," Web Semantics: Science, Services and Agents on the World Wide Web, vol. 2, no. 1, 2011.

[20] F. Alkhateeb, A. Alzubi, I. A. Doush, S. Aljawarneh and Al E. Maghayreh, "Extracting Authoring Information Based on Keywords and Semantic Search," Proc. of the 1st International Conference on Intelligent Semantic Web-Services and Applications, pp. 1-6, 2010.

[21] Y. Kotb, K. Gondow and T. Katayama, "The SLXS Specification Language for Describing Consistency of XML Documents," Proc. of the 4th International Workshop on Information Computer Science (WICS2002), IEEE Computer Society, 17-18 March 2002.

[22] Y. Kotb, K. Gondow and T. Katayama, "The XML Semantics Checker Model," in: Proc. of the 3rd International Conference on Parallel and Distributed Computing, Applications and Technologies (PDCAT'02), 2002.

[23] elebda3.net, "Regular Expression e-book," downloaded from: http://files.books.elebda3.net/elebda3.net-5647.pdf, on September 2nd, 2015.

[24] A. Arara, A. Smeda and I. Ellabib, "Searching and Analyzing Arabic Text Using Regular Expressions: e–Quran Case Study," International Journal of Computer Science and Electronics Engineering, vol. 1, no. 5, pp. 627-631, 2013.

[25] QuranComplex, "Al-Madinah Mushaf Website," last accessed September 25th, 2015 from: http://publications-img.qurancomplex.gov.sa/?p=44.

[26] Altafsir.com, "Tafsir Website," last accessed on September 28th, 2015 from: http://www.altafsir.com.

[27] N. Abbas, L. Aldhubai, H. Al-Khalifa, Z. Alqassem, E. Atwell, K. Dukes, M. Sawalha and A. Sharaf, "Unifying Linguistic Annotations and Ontologies for the Arabic Quran," in: Proc. of WACL'2 2nd Workshop on Arabic Corpus Linguistics, Lancaster University, UK, 22 July 2013.

[28] N. Abbas and E. Atwell, "Annotating the Arabic Quran with a Classical Semantic Ontology," in: Proc. of WACL'2 2nd Workshop on Arabic Corpus Linguistics, Lancaster University, UK, 22 July 2013.

[29] O. Ahmad, I. Hyder, R. Iqbal, M. Murad, A. Mustapha, N. Sharef and M. Mansoor, "A Survey of Searching and Information Extraction on a Classical Text Using Ontology-Based Semantics Modelling: A Case of Quran," Life Science Journal, vol. 10, no. 4, pp 1370-1377, 2013.

[30] Z. Adhoni and H. Al Hamad, "A Cloud Qur'an Application Using Drupal Technology," International Journal of Web Applications, vol. 6, no. 1, pp 23-38, 2014.

[31] S. M. Alrehaili and E. Atwell, "Computational Ontologies for Semantic Tagging of the Quran: A Survey of Past Approaches," in: Proc. of the 9th International Conference on Language Resources and Evaluations (LREC'14), Reykjavik, Iceland, 26-31 May 2014.

ملخص البحث:

إستحوذت عملية البحث في نصوص القرآن الكريم واسترجاع المعلومات منه على إهتمام العديد من الباحثين العرب والمسلمين في الآونة الأخيرة. و تزخر شبكة الإنترنت بالكثير من التطبيقات والمواقع الإلكترونية التي تفسح المجال للباحث ليقوم بالبحث في القرآن الكريم؛ إما باستخدام الكلمات المفتاحية أو عن طريق معاني الكلمات، أو بالطريقتين معاً.

و الجدير بالذكر أن اللغة العربية، لغة القرآن الكريم، تتميز بتراكيب معقدة تجعل البحث في النصوص العربية أصعب من البحث في النصوص الإنجليزية.

في هذا العمل البحثي، تم اقترح منحى هجين للبحث في القرآن الكريم يجمع بين البحث باستخدام الكلمات المفتاحية والبحث باستخدام معاني الكلمات. ولتحقيق هذه الغاية، تمت معالجة نصوص القرآن الكريم مسبقاً و تجهيزها بنسيق XML لتكون ملائمة لعملية البحث. و للتحقق من صلاحية المنحى المقترح و ملائمته لعملية البحث و استرجاع المعلومات من القرآن الكريم، تمّ بناء نظام باستخدام لغة بايثون؛ إذ يستخدم مفهوم التعابير المنتظمة لاختبار المنحى المقترح مع توفير واجهة برمجية لمعالجة طلبات المستخدمين. و قد تم الحصول من المنحى المقترح على نتائج جيّدة و واعدة.

Jordanian Journal of Computers and Information Technology (JJCIT), Vol. 1, No. 1, December 2015.

COMPREHENSIVE INVESTIGATION MODELING FOR SEMICONDUCTOR OPTICAL AMPLIFIER (SOA)

Esra A. Alquda[1] and Aser M. Matarneh[2]

Department of Electrical Engineering, Mutah University, Jordan.
aser_m2002@yahoo.com[1], aser.matarneh@mutah.edu.jo[2]

(Received: 03-Oct.-2015, Revised: 22-Dec.-2015, Accepted: 28-Dec.-2015)

ABSTRACT

This paper presents the effects of the input signal on the gain and carrier density response of a semiconductor optical amplifier (SOA). The SOA is modeled using a segmentation method. The input bias current input power, wavelength and the length of SOA required for amplification and switching functions are investigated. Moreover, the effect of temperature on SOA operation is investigated, as well as the thermo-optical effect. The operation principle is simulated, and the results show the input boundary conditions and requirements in which the SOA can be used as an amplifier and as a switch.

KEYWORDS

Semiconductor optical amplifier (SOA), Carrier density, Stimulated emission, Gain response, Thermo-optical effect, Dynamic range, Phase shift, Linear region.

1. INTRODUCTION

As the demand for network capacity is rising due to the rapid increase in the Internet traffic volume, there is a growing need for all-optical based systems. The all-optical based system should offer much greater bandwidth and higher reliability than the traditional copper cables and the optoelectronic based communication technologies.

In the beginning, optical fiber network started as a simple connection with no routing capability. The use of wavelength division multiplexing (WDM) and optical time division multiplexing (OTDM) increased the overall capacity of the point-to-point optical fiber transmission systems.

The development of second-generation high speed systems, such as the synchronous optical network and the synchronous digital hierarchy, offered supplementary switching and routing capabilities to the network [1]-[2]. Optical add/drop multiplexers and optical cross connectors were further introduced to the network in order to offer wavelength routing capabilities [3]-[4]. However, in such systems, the switching process is still performed in the electrical domain requiring optical-electrical-optical (O-E-O) conversion modules [5]-[6]. To meet the network speed and capacity demands and to overcome the bottlenecks of O-E-O conversion, ultra-fast photonic networks that rely on photonic signal processing are required. The next generation optical network is aimed to carry out all the processing in the optical domain, operating at speeds (hundreds of gigabits per second) well beyond the existing electronic devices [7]-[12]. It is important to note that an all-optical processing technology is not a replacement, but is a complementary alternative, to electrical processing, particularly at the backbone optical layer. Both circuit and packet switching could be adopted in all- optical networks.

However, packet switching is more flexible than circuit switching in throughput and switching speed [13]. An all-optical network offers transparency, implying that data can be carried at a range of bit rates and protocols and can also support different higher layers.

The development of high capacity optical networks increased the demand for new optical devices that are able to perform in almost all-optical functions. The key processes in all-optical switching are regeneration and wavelength conversion, where SOA is the key building block. Among all-optical switches [14], ultra-fast all-optical switches based on the SOA, such as Mach-Zehnder interferometers (MZI) [15]-[21] are the most promising candidates for the realization of all-optical switching and processing applications compared to other switches, such as ultra-fast non-linear interferometers (UNIs) [22]-[23] and terahertz optical asymmetric demultiplexers (TOADs) [24]-[26].

The use of SOA-based Mach-Zehnder interferometer (SOA-MZI) schemes will allow the processing of packets 'on-the-fly' in future photonic routers. The SOA-MZI is used in almost all functions inside a photonic router, such as clock extraction circuits, header/payload separation, optical flip-flops, wavelength converters, all-optical gates and switching [27]-[34]. The performance of SOA, in terms of the gain temporal behavior, the carrier density and stimulation emission, is affected by several factors, including the dimensions of the waveguide and input parameters, such as the external bias current and the power and wavelength of the propagating input signal. Controlling these factors will lead to improving and optimizing the SOA amplification and/or switching characteristics, as well as the uniformity of the generated output signal that is necessary to reduce the system power penalty.

This paper proposes a segmentation model of the SOA based on numerical and mathematical equations. The model is used to analyze the impact of the input parameters and propagating signals on the SOA carrier density and its gain response to further understand the SOA operation. The segmentation model has been introduced in modeling the semiconductor devices [35]. However, the segmentation model used in this paper takes into account the differential gain effect and the temperature effect of the semiconductor optical amplifier. It also investigates switching operation in more details. Moreover, the dynamic behavior of SOA, including optical-thermo-effect and dynamic range will be thoroughly investigated.

Next stage will be dealing with optimization of SOA parameters to maximize the output gain for amplification and optimization of SOA non-linear characteristics when used in optical switching. The boundaries and conditions necessary for the input parameters to achieve the 180º induced phase shift are managed for switching function in SOA-based optical switches.

The paper is organized as follows; in the next section, the principle of SOA is presented. Section three introduces the mathematical model used, including segmentation model and rate equations of SOA with phase shift equations. Section four presents the results and discussion. The conclusion is then drawn.

2. PRINCIPLE OF SOA

SOAs amplify incident light through stimulated emission. An electrical pump current is used to excite the electrons in the active region of the SOA. When the optical signal travels through the active region, it causes these electrons to lose energy in the form of photons and get back to the ground state. The stimulated photons have the same wavelength as the optical signal, thus amplifying the optical signal as shown in Figure 1. The basic working principle of a SOA is the same as a semiconductor laser, but without feedback.

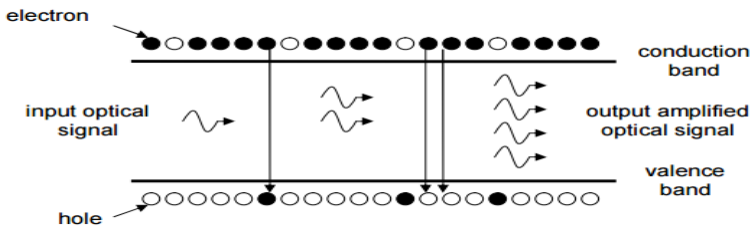

Figure 1. SOA amplifications due to stimulation emission process [36].

3. METHOD

3.1 Segmentation Model

In order to understand the factors affecting the SOA gain and the emerging output signals, a segmentation model of the SOA is introduced, where the SOA is divided into ten equal segments of length l=L/10 each. The model helps in identifying the small changes that occur within the short length of each segment. Ten segments were chosen for a sufficient accurate investigation on the change in the carrier density and the signal gain along the SOA.

3.2 Mathematical Model

The rate equations in small segments in an SOA are iteratively calculated while taking the carrier density change and the SOA length into account [37].

3.2.1 Rate Equations

When light is injected into the SOA, changes occur in the carrier and photon densities within the active region of the SOA. These changes can be described using the rate equations. The gain medium of the amplifier is described by the material gain coefficient, g (per unit length) which is dependent on the carrier density N and is given by [38]:

$$g = a_1 (N - N_0); \quad (1)$$

where N_0 is the carrier density at transparency point and a_1 is the differential gain parameter. The net gain coefficient g_t is defined by:

$$g_t = \Gamma . g - a_s \quad (2)$$

where a_s is the internal waveguide scattering loss and Γ is the confinement factor, which is the ratio of the light intensity within the active region to the sum of light intensity [39]. The total gain G of an optical wave experienced at the location z of an SOA can be calculated according to:

$$G = e^{gt.z} \quad (3)$$

assuming a constant carrier density at any given location z within the active region of the SOA. Therefore, the average output power P_{av} over the length of the SOA becomes:

$$P_{av} = P_{in} \frac{(e^{gt.L} - 1)}{g_t . L} \quad (4)$$

where L is the length of the SOA and P_{in} is the input signal power. The carrier density rate equation expresses the conservation of carriers inside the active layer. It takes into account the current density and the net rate of carrier generation and recombination averaged over the active layer. The recombination rate consists of spontaneous and stimulated recombination. The spontaneous recombination rate includes the radiative and non-radiative components. The non-radiative recombination takes into account the Auger recombination, which is generally the

dominant non-radiative process in long wavelength lasers. The dynamic equation for the change in the carrier density within the active region of the device is given by:

$$\frac{dN}{dt} = \frac{I_{dc}}{q.V} - R(N) - \frac{\Gamma . g. P_{av} . L}{V. h. f} \tag{5}$$

where I_{dc} is the DC bias current injected to the SOA, q is the electron charge and V is the active volume of the SOA:

$$V = L. H. W \tag{6}$$

where W and H denote the width and the thickness of the active region, respectively. $R(N)$ is the recombination rate, h is the Planck constant and h is the light frequency. The definition for R (N) used in this model is given by:

$$R\ (N) = A. N + B. N^2 + C. N^3 \tag{7}$$

where A is the non-radiative coefficient recombination at defects and traps, B is the spontaneous radiative recombination coefficient and C is the Auger recombination coefficient. The cubic equation is the best to fit the real gain coefficient g. The material gain coefficient depends on both the carrier density N and the input signal wavelength λ and can be rewritten as [40]:

$$g = \frac{a_1(N - No) - a_2(\lambda - \lambda_N)^2 + a_3(\lambda - \lambda_N)^3}{1 + \in . P_{av}} \tag{8}$$

where a_2 and a_3 are empirically determined constants that are chosen to fit an experimentally measured SOA gain curve. λ_N is the peak gain wavelength and ∈ is the gain compression factor. The peak gain wavelength is given by:

$$\lambda_N = \lambda_0 - a_4\ (N - N_0\ ) \tag{9}$$

where λ_0 is the peak gain wavelength at transparency and a_4 denotes the empirical constant that shows the shift of the gain peak.

3.2.2 Phase Shift Equations

Changes in the carrier density take place with the propagation of the input signal pulse through the SOA, hence affecting its propagation coefficient (via the non-linear refractive index variations in the SOA active region). Because of the finite carrier lifetime, the leading edge of the input pulse experiences a different phase shift relative to the lagging edge. This process is (SPM). Let Δn represent the effective refractive index variation within the active region [39]:

$$\Delta n = \Gamma . \frac{\mathrm{dn}}{\mathrm{dN}} . (N - N_{ss}\ ) \tag{10}$$

where dn/dN is the refractive index shift coefficient and N_{ss} is the carrier density at steady state (i.e., with no input signal launched to the biased SOA). The total phase shift experienced by the propagating input signal is [40]:

$$\Delta\ \emptyset = \int_0^L \left(\frac{2\pi}{\lambda}\ . \Delta n \right) . dz \tag{11}$$

A thermo-optical effect is a change in the optical properties of a material in response to temperature. The thermo-optical effect may eventually lead to unstable operation of the SOA, since the effective refractive index changes as a function of temperature. A linear approximation for the effective refractive index as a function of temperature is given as shown below [41]:

$$n\ (T) = n_0 + \frac{\Delta n}{\Delta T}\ (T - T_0\ ) \tag{12}$$

Jordanian Journal of Computers and Information Technology (JJCIT), Vol. 1, No. 1, December 2015.

where n_0 is the refractive index at room temperature, T_0. n_0 for silicon device is 3.48314 [42]. $(\frac{\Delta n}{\Delta T})$ is the index variation with temperature (thermo-optical coefficient).
The total phase shift experienced by the propagating input signal is [40]:

$$\Delta \emptyset = \int_0^L \left(\frac{2\pi}{\lambda} \ .n\,(T) \right).dz \tag{13}$$

4. RESULTS AND DISCUSSION

The rate equations shown in the previous section are derived via Matlab to investigate the gain response of the SOA model while employing the segmentation method. The standard SOA parameters used are given in Table 1. The segmentation method involves dividing the SOA into ten equal segments of length l=L/10 each. The carrier density is assumed to be constant within a segment. However, the carrier density changes from one segment to another depending on its input power and the carrier density of the previous segment using equation (5). In all of the equations, the segment length *l* will replace the SOA length L for segment total gain and carrier density calculations.

Figure 2 shows the dynamic range of a semiconductor optical amplifier (SOA); that is the input power range within which an SOA can be operated error free. It is among the most important parameters describing the usability range of an SOA in an access network. Figure 3 shows the normalized gain response of the SOA using the physical parameters in Table 1. As it can be seen, the gain of the SOA increases rapidly up to a steady state value, where it becomes almost constant. This increase is due to the injection of the bias current to the SOA, hence resulting in a large number of electrons to overcome the energy gap to reach the conduction band.

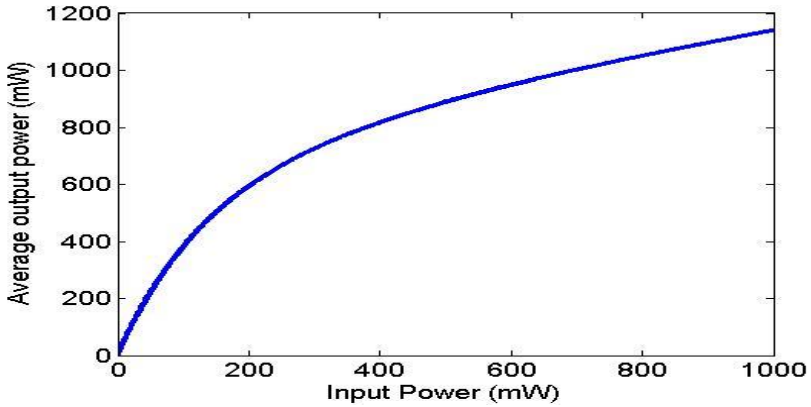

Figure 2. Dynamic range of SOA.

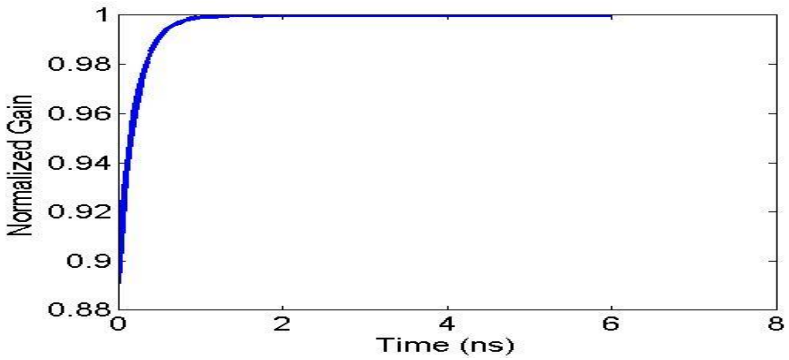

Figure 3. The Normalized gain response of the SOA with no input signal.

Table 1. Physical parameters of the SOA.

Parameter	**Value**
Carrier density at transparency (N_0)	$1.4 \times 10^{24}/m^3$
Initial carrier density (N_i)	$3 \times 10^{24}/m^3$
Wavelength at transparency (λ_0)	$1605nm$
Initial waveguide scattering loss (a_s)	$40 \times 10^2/m$
Differential gain (a_1)	$2.78 \times 10^{-20}\ m^2$
Gain constant (a_2)	$7.4 \times 10^{18}/m^3$
Gain constant (a_3)	$3.155 \times 10^{25}/m^4$
Gain peak shift coefficient (a_4)	$3 \times 10^{-32}\ m^4$
SOA length (L)	500 µm
SOA width (W)	3 µm
SOA height (H)	80 nm
Confinement factor (Γ)	0.3
Surface and defect recombination coefficient (A)	$3.6 \times 10^8/s$
Radiative recombination coefficient (B)	$5.6 \times 10^{-16}m^3/s$
Auger recombination coefficient (C)	$3 \times 10^{-41}m^6/s$
Gain compression factor (ε)	$0.2/W$
Equivalent refractive index (n_{eq})	3.5
Differential of equivalent refractive index with respect to carrier density (dn/dN)	$-1.2 \times 10^{-26}/m^3$
Index variation with temperature ($\frac{\Delta n}{\Delta T}$)	$10^{-4}/K$

4.1 Amplification

In order to use the SOA as an amplifier, it is necessary to ensure that the signal will not be affected by the SOA non-linear response that occurs when the SOA gain reaches its saturation value as shown in Figure 4, where the SOA decreases sharply to the saturation level. The reason for such response is that a depletion of the carrier density happens due to the continuous

stimulation emission process. A range of input pulse signals with optical power values from 1 mW to 10 mW were applied to the SOA, and the signal output gains are illustrated in Figure 5.

As it can be seen from Figure 5, the simulated result is in clear agreement with the measured result. As expected, the figure shows that, for both curves, at a fixed wavelength, the gain gradually decreases with increasing the input power level. This effect is because a signal with higher power will interact with a larger number of excited electrons in the conduction band, thus resulting in increased depletion in the carrier density and the SOA gain. This process is applied for 1550 nm wavelength. As it can be noted from 1 mW input power at measured and simulated curves, the gain values obtained are 100 and 98 respectively; where it should be noted that the small discrepancy between the measured and simulated curves is due to simulation accuracy.

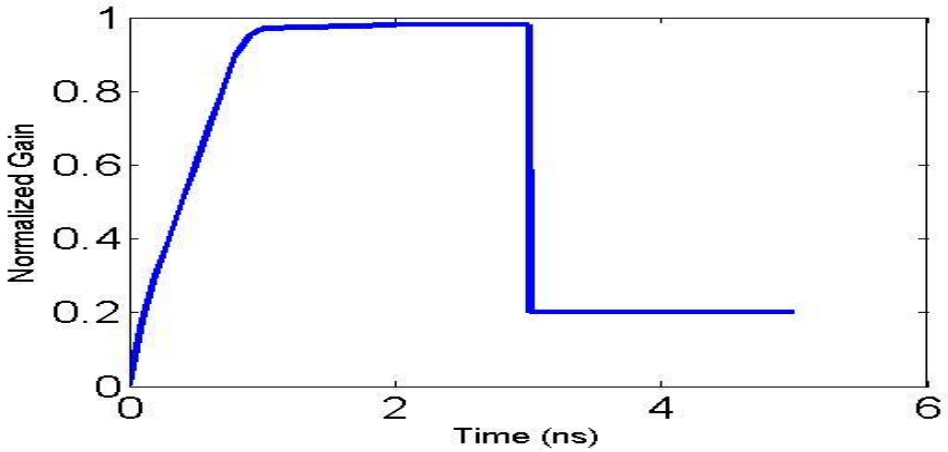

Figure 4. Normalized gain response of the SOA due to continuous wave (CW) probe.

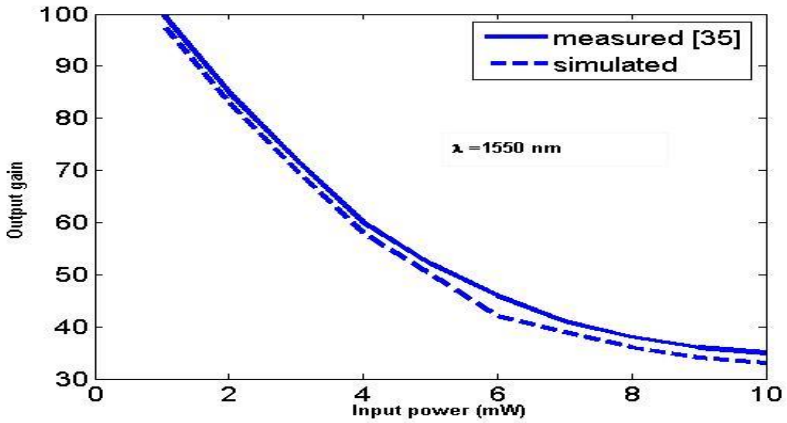

Figure 5. Signal output gain corresponding to the input power at a wavelength of 1550 nm.

4.2 Input Signal Wavelength Investigation

The wavelength of the input signal has a direct impact on the SOA gain as can be seen from the third order gain coefficient equation. The depletion of the SOA gain that occurs due to the injection of input signal is directly related to the input power. Therefore, in order to understand these effects, the SOA gain as a function of the input power, for a range of wavelengths in the C-band (1530 to 1565 nm), is illustrated in Figure 6. As expected, the SOA gain reduces with increasing the input signal power at all wavelengths. This gain reduction is because a signal

with higher power level will interact with a larger number of excited electrons in the conduction band, thus resulting in higher depletion of the carrier density and the SOA gain. From the figure, it is observed that at lower wavelengths, lower gains are achieved.

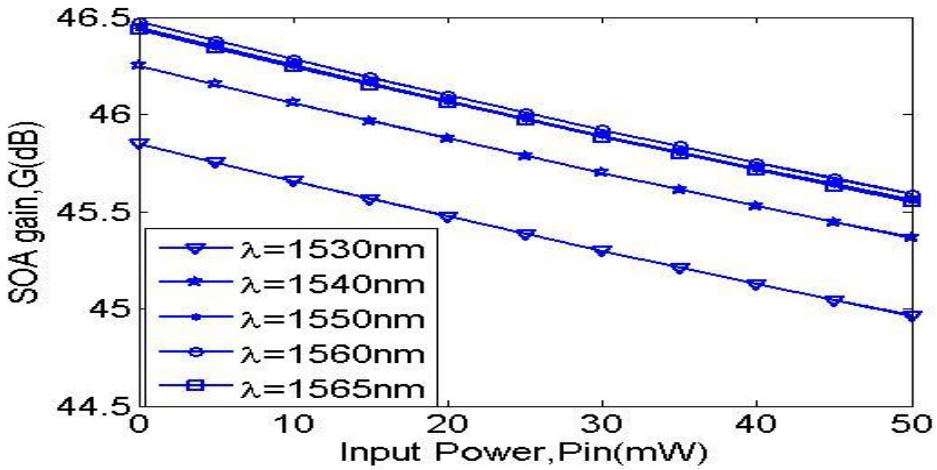

Figure 6. SOA gain as a function of input signal power when operated in the C- band.

4.3 Applied Bias Current Investigation

The applied current that is used for biasing the SOA has also a direct impact on the SOA carrier density and gain. At higher bias current, the larger number of electrons that overcome the energy gap will lead to an increase the carrier density, thus leading to an increased SOA total gain. In Figure 7, the SOA gain reduces with increasing the input signal power and this response appears at all bias current values at 1550 nm wavelength. On the other hand, higher biasing current values result in higher SOA gain achievement. The highest gain achieved is 48 dB with a 40% drop from the steady state value at a bias current of 200 mA and a power of 1 mW. For lower values of bias current, the gain profile is almost flat. For example, injecting the same 1 mW input at 100 mA current, 46.4 dB gain is achieved with just 0.6% drop from steady state. These results correspond to the number of electrons available for amplification in the conduction band.

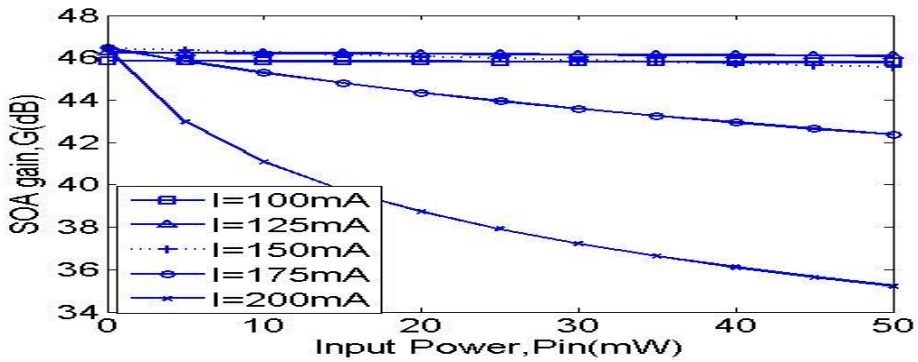

Figure 7. SOA gain *versus* input signal power for a range of bias currents at a wavelength of 1550 nm.

4.4 SOA Length Investigation

The length of the SOA is an important physical parameter that affects the total gain. The dependence of the gain on the SOA length is plotted in Figure 8 for a range of input power values at 150 mA bias current. For short lengths (< 100 µm), where the depletion of N is negligible, the gain is the same for all values of P_{in} . On the other hand, for longer lengths (< 700 µm), the gain is increasing, peaking at L of ~500 µm beyond which the gain drops. The result confirms that the gain is higher for lower values of P_{in} . For longer length (800 µm – 1.5 mm) SOAs, maintaining a stable applied bias current, the number of electrons per unit length is smaller because of lower current density. Therefore, in order to achieve high gain at longer length SOAs, the applied bias current needs to be increased in order to maintain the number of electrons per unit length.

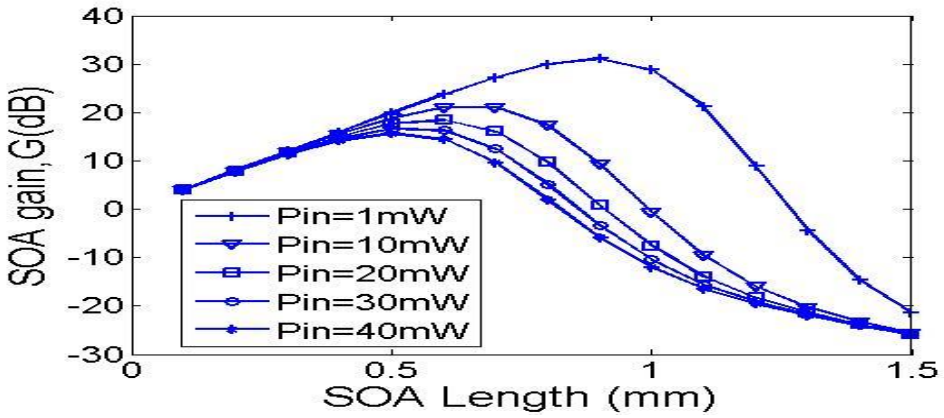

Figure 8. SOA gain responses as a function of SOA length for a range of input power levels with 150 mA bias current.

4.5 Switching

On the contrary to amplification, in order to use cross phase modulation (XPM) and self phase modulation (SPM) characteristics of SOA for the switching function, the signal should experience a phase shift of 180º for the complete deconstructive interference [43]. Therefore, phase shift calculation employing Equations (10), (11), (12) and (13) is crucial for setting the boundaries for the SOA switching function. The phase shift could be induced by the input signal injected to the active region of the SOA.

4.6 Input Signal Wavelength Investigation

The phase shift experienced by the input signal is directly proportional to the depletion of N as defined in (10) and (11). As a result of changes in the refractive index Δn, change is induced in phase shift. Figure 9 shows the phase shift as a function of the input power for a range of wavelengths in the C-band. To achieve an induced phase shift of 180º at 1550 nm wavelength, the input signal power is 60 mW, where the induced phase shift increases with increasing the input power.

4.7 Applied Bias Current Investigation

To explain the effect of bias current on the induced phase shift of the input signal, Figure 10 explains the induced phase shift of the input signal achieved at a range of input power at different biasing current values. From Figure 10, it can be observed that at higher bias current

values, the input signal propagating along the SOA induces more phase shift. Higher biasing results in higher SOA gain. From the third term in (5), which shows the depletion of the carrier density, one can observe that higher gain results in more N depletion. Therefore, the phase shift increases accordingly.

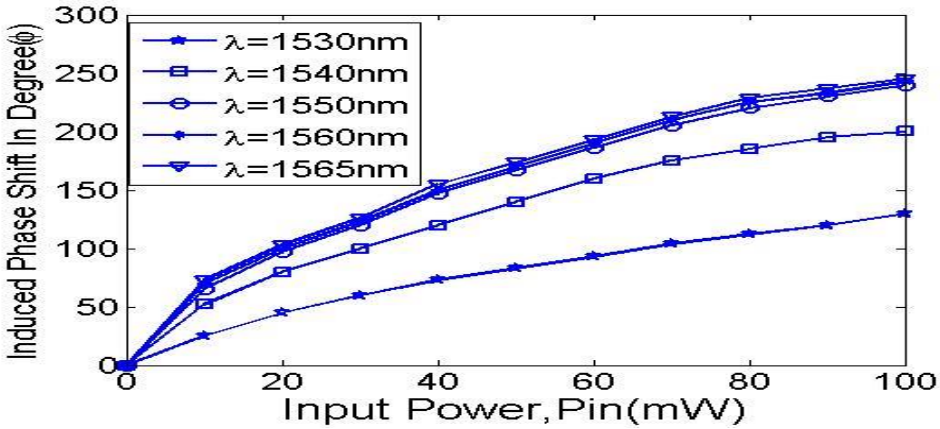

Figure 9. Induced phase shift experienced by the input signal power for a range of wavelengths.

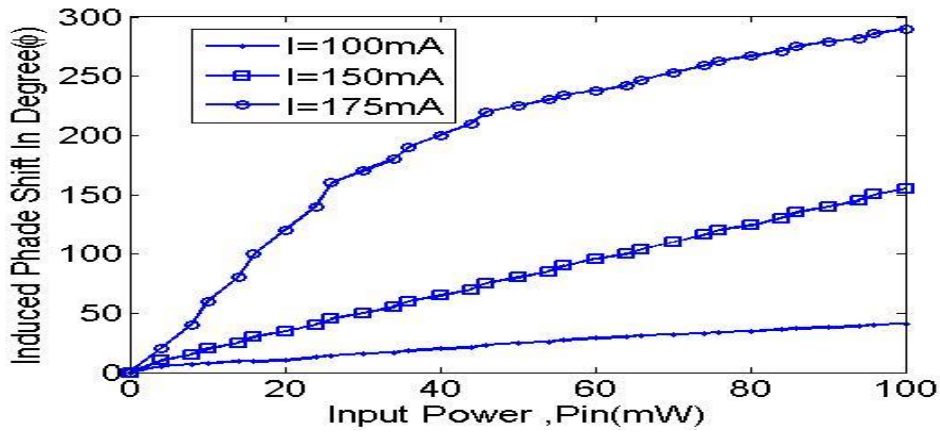

Figure 10. Induced phase shift of the input signal achieved *versus* the input signal power for a range of biasing current values.

4.8 SOA Length Investigation

It is important to explain the dependence of the phase shift of the input signal on the SOA length. It is known that lower gains are achieved at short (< 100 μm) and long (> 700 μm) SOA lengths. It was shown in Figure 10 that higher input power induces more phase shift, which explains the response in Figure 11. The figure shows the induced phase shift corresponding to the input power at different SOA lengths at 150 mA bias current. It can be concluded that the maximum phase shift is achieved at 500 μm.

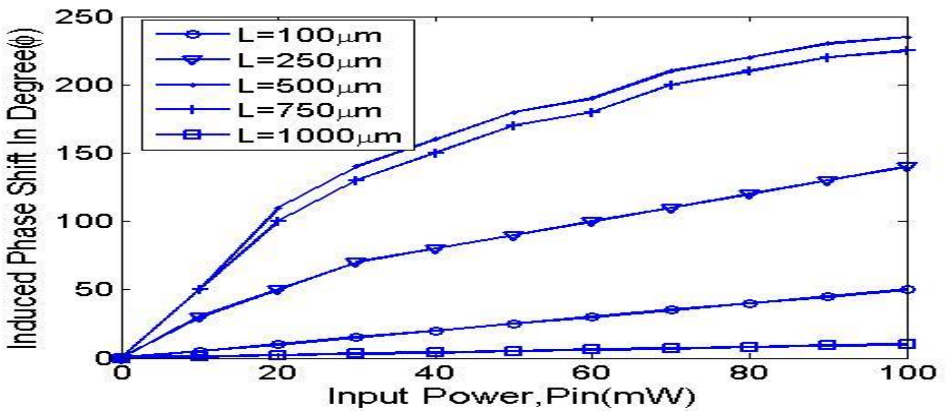

Figure 11. Induced phase shift of the input signal achieved as a function of the input signal power for a range of SOA lengths at 150 mA bias current.

4.9 SOA Temperature Investigation

The temperature of the SOA is an important parameter that affects the total gain and phase shift. The dependence of the gain on the SOA temperature at a wavelength of 1550 nm is shown in Figure 12. It can be noticed that the input signal propagating along the SOA induces the temperature dependence of SOA. The temperature dependence of the peak signal gain is approximately (-0.2) dB/K.

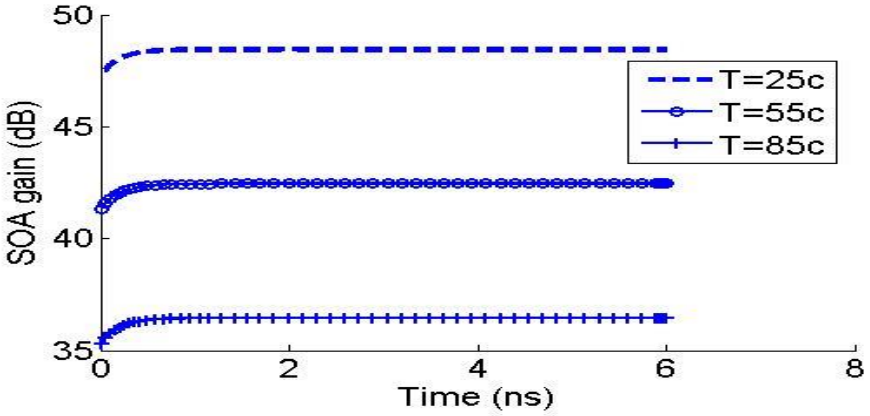

Figure 12. SOA gain corresponding to temperature.

Figure 13 shows that, due to temperature effect on medium gain, the SOA gain decreases with increasing temperature. Such investigation is carried out by using Equations 10, 12 and 13. Temperature can be controlled to obtain a certain phase shift that will become a function of temperature.

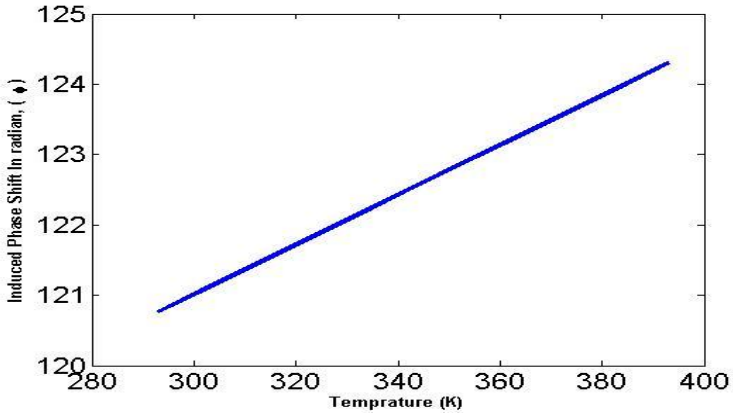

Figure 13. Temperature effect on phase shift.

4.10 Differential Gain Effect

To calculate the saturation power, the following relationship can be used [44]:

$$P_{in\,(sat)} = \frac{hf\ 2\ln(2)}{Go-2}\ \frac{A}{\Gamma}\frac{1}{a_1}\frac{1}{t_c} \tag{14}$$

$$Go = \exp(\ \Gamma a_1\ (N - N_o)\ L \tag{15}$$

where Go is the reasonable unsaturated gain, t_c is the effective carrier lifetime.

Figure 14 shows the effect of differential gain on the linearity of the device. Moreover, increasing the differential gain leads to a decrease in the linear region, in terms of 3 dB bandwidth, meaning a decrease in saturation power. On the other hand, decreasing the differential gain leads to an increase in the linear region, meaning an increase in saturation power.

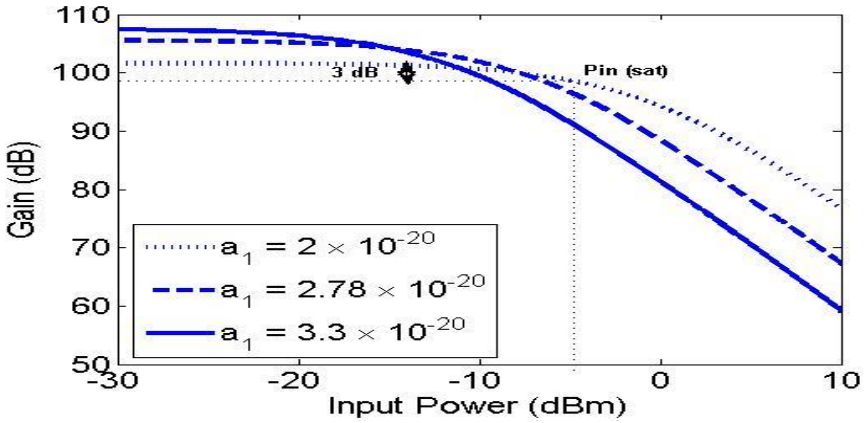

Figure 14. SOA gain as a function of the input power; the 3-dB saturation input power is marked.

5. CONCLUSION

The total gain response of an SOA model using the segmentation method has been simulated. CW probe and pump signals have been applied to the proposed segmentation of SOA model in order to investigate the corresponding gain response. The results have been discussed to achieve amplification and all-optical switching. The optimum performance conditions regarding the input signal power, the bias current and the signal wavelengths have been investigated for the SOA, to function as an amplifier and a switch. Furthermore, thermos-optical effect on total gain and phase shift has been introduced. Moreover, the effect of differential gain on the linear region has been investigated. The model can be extended to investigate vertical cavity SOA.

REFERENCES

[1] R. Ramaswami and N. Sivarajan, Optical Network – a Practical Perspective, 2nd Edition, USA: Morgan Kaufmann, 2002.

[2] N. S. Bergano, "Wavelength Division Multiplexing in Long-Haul Transoceanic Transmission Systems," IEEE Journal of Lightwave Technology, vol. 23, pp. 4125-4139, 2005.

[3] G. P. Agrawal, Lightwave Technology - Telecommunication System, New Jersey, USA: John Wiley and Son, Inc., 2005.

[4] R. Medina, "Photons vs. Electrons [All-Optical Network]," Proc. Of the IEEE Potentials, vol. 21, issue 2, pp. 9-11, May 2002.

[5] D. Adami, S. Giordano, M. Pagano and L. Gustavo Zuliani, "MCP-RWA: A Novel Algorithm for QOT-Guaranteed Online Provisioning in Photonic Networks," 2010 International Congress on Ultra-Modern Telecommunications and Control Systems and Workshops (ICUMT), pp. 141-147, Moscow, Russia, 18-20 Oct. 2010.

[6] C. Schubert, J. Berger, S. Diez, H. J. Ehrke, R. Ludwig, U. Feiste, C. Schmidt, H. G. Weber, G. Toptchiyski, S. Randel, Bakopoulos, D. Petrantonakis, G. T. Kanellos, G. Maxwell and H. Avramopoulos, "Optical Signal Processing Using Integrated Multi-Element SOA-MZI Switch Arrays for Packet Switching," Proc. Of the IET Optoelectronics, vol. 1, pp. 120-126, 2007.

[7] E. Kehayas, J. Seoane, Y. Liu, J. M. Martinez, J. Herrera, P. V. Holm Nielsen, S. Zhang, R. McDougall, G. Maxwell, F. Ramos, J. Marti, H. J. S. Dorren, P. Jeppesen and H. Avramopoulos, "All-Optical Network Subsystems Using Integrated SOA-Based Optical Gates and Flip-Flops for Label-Swapped Networks," Proc. of the IEEE Photonics Technology Letters, vol. 18, pp. 1750-1752, 2006.

[8] S. L. Jansen, S. Spalter, G. D. Khoe, W. Huug de, H. E. Escobar, L. Marshall and M. Sher, "16×40 gb/s over 800 km of SSMF Using Midlink Spectral Inversion," Proc. of the IEEE Photonics Technology Letters, vol. 16, pp. 1763-1765, 2004.

[9] A. Barbieri, G. Colavolpe, T. Foggi, E. Forestieri and G. Prati, "OFDM *versus* Single-Carrier Transmission for 100 Gbps Optical Communication," Proc. of the IEEE, Journal of Lightwave Technology, vol. 28, pp. 2537-2551, 2010.

[10] A. Paraskevopoulos, S. H. Voss, M. Talmi and G. Walf, "High Speed (>100 Gbps) Key Components for a Scalable Optical Data Link, to be Implemented in Future Maskless Lithography Applications," Proc. of the 25th European Mask and Lithography Conference (EMLC), pp. 1-8, 2009.

[11] H. Uemura, H. Hamasaki, H. Furuyama, H. Numata, C. Takubo and H. Shibata, "Extremely-Compact and High-Performance (160Gbps = 20GB/s) Optical Semiconductor Module Using Lead Frame Embedded Optoelectronic Ferrule", Proc. of the 58th Conference on Electronic Components and Technology (ECTC 2008), pp. 1936-1940, 2008.

[12] A. V. Nguyen, H. P. Nguyen, N. B. Le and V. L. Dang, "Digital Lightwave Receiver Employing Parallel-DSP-Based Equalization Technique for 100 Gbps 1000-km RZ-DQPSK Optical

Communication System," Proc. of International Conference on Advanced Technologies for Communications (ATC), pp. 152-155, 2011.

[13] J. M. Martinez, J. Herrera, F. Ramos and J. Marti, "All-Optical Correlation Using Cascaded Logic XOR Gates Based on Active Mach-Zehnder Interferometers," Proc. of the 31st European Conference on Optical Communication (ECOC 2005), vol. 1, pp. 103-104, 2005.

[14] J. Leuthold, P. A. Besse, J. Eckner, E. Gamper, M. Dulk and H. Melchior, "All-Optical Space Switches with Gain and Principally Ideal Extinction Ratios," Proc. of the IEEE, Journal of Quantum Electronics, vol. 34, pp. 622-633, 1998.

[15] K. Morito, J. Leuthold and H. Melchior, "Dynamic Analysis of MZI-SOA All-Optical Switches for Balanced Switching," Proc. of the 11th International Conference on Integrated Optics and Optical Fiber Communications, and 23rd European Conference on Optical Communications (Conf. Publ. No.: 448), vol. 2, pp. 81-84, 1997.

[16] N. Pleros, P. Zakynthinos, A. Poustie, D. Tsiokos, P. Bakopoulos, D. Petrantonakis, G. T. Kanellos, G. Maxwell and H. Avramopoulos, "Optical Signal Processing Using Integrated Multi-Element SOA-MZI Switch Arrays for Packet Switching," Proc. of the IET Optoelectronics, vol. 1, pp. 120-126, 2007.

[17] A. Maziotis, B. Schrenk, M. Bougioukos and H. Avramopoulos, "Cognitive Routing in Converged Access-Metro Environment via Selective SOA-MZI Switch," Proc. of the IEEE Photonics Technology Letters, pp. 1-1, 2011.

[18] D. Petrantonakis, D. Apostolopoulos, M. Spyropoulou, N. Pleros, K. Vyrsokinos and H. Avramopoulos, "40 Gb/s NRZ Wavelength Conversion with Enhanced 2R Regeneration Characteristics Using a Differentially-Biased SOA-MZI Switch," LEOS Annual Meeting Conference Proceedings of IEEE (LEOS '09), pp. 781-782, 2009.

[19] J. Kurumida, Y. Tatara, H. Uenohara and K. Kobayashi, "All-Optical Header Recognition Sub-System Based on SOA-MZI Switches," Proc. of Conference on Lasers and Electro-Optics Pacific Rim (CLEO/Pacific Rim), pp. 1790- 1791, 2005.

[20] S. Gupta, M. Presi, N. Calabretta, G. Contestabile and E. Ciaramella, "Operational Equivalence of Self-Switching Effect in SOA-Based Nonlinear Polarization and MZI Switches," Proc. in: Lasers and Electro-Optics Society, LEOS, 20th Annual Meeting of IEEE, pp. 810-811, 2007.

[21] S. Nakamura, K. Tajima and Y. Sugimoto, "Experimental Investigation on High-speed Switching Characteristics of A Novel Symmetric Mach-Zehnder All-Optical Switch," Applied Physics Letter, vol. 65, pp. 283-385.

[22] G. P. Agrawal, "Population Pulsations and Non-degenerate Four-Wave Mixing in Semiconductor Lasers and Amplifiers," J. Opt. Soc. Am. B, vol. 5, no. 1, pp. 147– 159, 1988.

[23] C. Cheng, X. Zhang, Y. Zhang, L. Liu and D. Huang, "Measurement of the Carrier Recovery Time in SOA Based on Dual Pump FWM," Proc. in: Communications and Photonics Conference and Exhibition (ACP), Asia, pp. 1-2, 2009.

[24] H. Le Minh, Z. Ghassemlooy and N. Wai Pang, "Characterization and Performance Analysis of a TOAD Switch Employing a Dual Control Pulse Scheme in High-speed OTDM Demultiplexer," Proc. of the IEEE Communications Letters, vol. 12, pp. 316-318, 2008.

[25] J. M. Tang, P. S. Spencer, P. Rees and K. A. Shore, "Enhanced TOAD Performance by Negative Frequency-Detuned Signal and Control Picoseconds Optical Pulses," Proc. of the IEEE Journal of Quantum Electronics, vol. 36, pp. 574-582, 2000.

[26] J. Wei, Z. Min and P. Ye, "All-Optical-Packet Header and Payload Separation for Unslotted Optical-Packet-Switched Networks," Proc of the IEEE Journal of Lightwave Technology, vol. 25, pp. 703-709, 2007.

[27] E. S. Awad, C. J. K. Richardson, P. S. Cho, N. Moulton and J. Goldhar, "Optical Clock Recovery Using SOA for Relative Timing Extraction between Counterpropagating Short Picosecond Pulses," Proc. of the IEEE Photonics Technology Letters, vol. 14, pp. 396-398, 2002.

[28] R. Giller, R. J. Manning and D. Cotter, "Gain and Phase Recovery of Optically Excited Semiconductor Optical Amplifiers," Proc. of the IEEE Photonics Technology Letters, vol. 18, pp. 1061-1063, 2006.

[29] J. Moerk, M. Nielsen and T. Berg, "The Dynamics of Semiconductor Optical Amplifiers-Modeling and Applications," Proc. in: Optics and Photonics News, vol. 14, pp. 42-48, 2003.

[30] E. Tangdiongga, Y. Liu, H. Waardt, G. Khoe, A. Koonen and H. Dorren, "All-Optical Demultiplexing of 640 to 40 Gbits/s Using Filtered Chirp of a Semiconductor Optical Amplifier," Proc. of the Optics Letters, vol. 32, pp. 835-837, 2007.

[31] A. Perez-Pardo, T. T. Ng, P. Petropoulos, S. Sales and D. J. Richardson, "Analysis of the Dynamic Responses of SOA Wavelength Converters Using Linear Frequency Resolved Gating Technique," Proc. of the IEEE Photonics Technology Letters, vol. 20, pp. 1079-1081, 2008.

[32] M. Matsuura, N. Kishi and T. Miki, "All-Optical Wavelength Conversion with Large Wavelength Hopping by Utilizing Multistage Cascaded SOA-Based Wavelength Converters," Proc. of the IEEE Photonics Technology Letters, vol. 18, pp. 926-928, 2006.

[33] T. Kise, K. N. Nguyen, J. M. Garcia, H. N. Poulsen and D. J. Blumenthal, "Demonstration of Cascadability and Phase Regeneration of SOA-Based All-Optical DPSK Wavelength Converters," Proc. of the Optical Fiber Communication Conference and Exposition (OFC/NFOEC) and the National Fiber Optic Engineers Conference, pp. 1-3, 2011.

[34] L. Pei-Li, H. De-Xiu and Z. Xin-Liang, "SOA-Based Ultra-fast Multifunctional All-Optical Logic Gates with PolSK Modulated Signals," Proc. of the IEEE Journal of Quantum Electronics, vol. 45, pp. 1542-1550, 2009.

[35] J. Moerk, M. Nielsen and T. Berg, "The Dynamics of Semiconductor Optical Amplifiers-Modeling and Applications," Proc. of the Optics and Photonics News, vol. 14, pp. 42-48, 2003.

[36] E. S. Awad, C. J. K. Richardson, P. S. Cho, N. Moulton and J. Goldhar, "Optical Clock Recovery Using SOA for Relative Timing Extraction between Counterpropagating Short Picosecond Pulses," Proc. of the IEEE Photonics Technology Letters, vol. 14, pp. 396-398, 2002.

[37] H. Le Minh, "All-Optical Router with PPM Header Processing High-Speed Photonic Packet Switching Networks," North Umbria University, 2007.

[38] M. Y. Jeon, Y. A. Leem, D. C. Kim, E. Sin, S. B. Kim, H. Ko, D. S. Yee and K. H. Park, "40 Gbps All-Optical 3R Regeneration and Format Conversion with Related InP-Based Semiconductor Devices," Proc. of the ETRI Journal, vol. 29, no. 5, pp. 633-640, Oct. 2007.

[39] H. Wang, J. Wu and J. Lin, "Studies on the Material Transparent Light in Semiconductor Optical Amplifiers," Proc. of the Journal of Optics A: Pure and Applied Optics, vol. 7, pp. 479-492, 2005.

[40] F. Marino, G. Catalan, P. Sánchez, O. Piro and S. Balle, "Thermo-optical Canards and Excitable Limit Cycles," Physical Review Letter, vol. 92, 073901, Feb. 2004.

[41] Bradley J. Frey, Douglas B. Leviton and Timothy J. Madison, "Temperature-Dependent Refractive Index of Silicon and Germanium," NASA Goddard Space Flight Center, Greenbelt, MD 20771.

[42] A. Abd El Aziz, W. P. Ng, Z. Ghassemlooy, M. H. Aly, R. Ngah and M. F. Chaing, "Characterization of the Semiconductor Optical Amplifier for Amplification and Photonic Switching Employing the Segmentation Model," International Conference on Transparent Optical Networks "Mediterranean Winter" 2008 (ICTON-MW‘08), ISBN 978-1-4244-3485-5, Marrakech, Morocco, pp. Fr1A.1 (1-6), 11-13 Dec. 2008.

[43] G. P. Agrawal and N. A. Olsson, "Self-Phase Modulation and Spectral Broadening of Optical Pulses in Semiconductor Laser Amplifiers," Proc. of the IEEE Journal of Quantum Electronics, vol. 25, pp. 2297-2306, 1989.

[44] R. Bonk, T. Vallaitis, J. Guetlein, C. Meuer, H. Schmeckebier, D. Bimberg, C. Koos, W. Freude and J. Leuthold, "The Input Power Dynamic Range of a Semiconductor Optical Amplifier and Its Relevance for Access Network Applications," Proc. of the IEEE Photonics Journal, vol. 3, no. 6, December 2011.

ملخص البحث:

يعالج هذا البحث تأثيرات إشارة الدخل في مقدار الكسب و كثافة الناقل في المكبر الضوئي شبه الموصل. تمت نمذجة المكبر الضوئي شبه الموصل باستخدام طريقة التجزئة؛ و أخذ بعين الاعتبار كلٌّ من تيار انحياز الدخل، و قدرة الدخل، و الطول الموجي، وطول المكبر اللازمة لعمل المكبر الضوئي شبه الموصل في حالتي التكبير و التبديل. علاوة على ذلك، جرى استقصاء تأثير درجة الحرارة على عمل المكبر الضوئي شبه الموصل، كما تمت دراسة الأثر الحراري الضوئي.

و قد أظهرت محاكاة مبدأ التشغيل الشروط و المتطلبات الحدّية للدّخل التي يمكن عندها استخدام المكبر الضوئي شبه الموصل كمكبّر و مبدّل.

المجلة الاردنية للحاسوب و تكنولوجيا المعلومات

كانون الاول ٢٠١٥ المجلد ١ العدد ١ ISSN 2413-9351

JJCIT

www.jjcit.org jjcit@psut.edu.jo

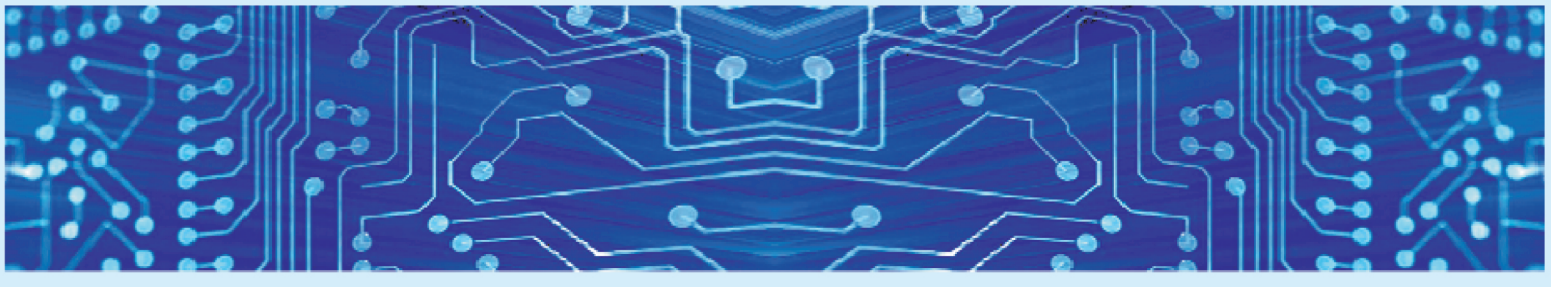

مجلة علمية عالمية متخصصة محكمة

تصدر بدعم من صندوق دعم البحث العلمي